

ETD Archive

2010

Human Prostate Cancer Cell Apoptosis Induced by Interferon- γ and Double-Stranded RNA and Studies on the Biological Roles of Transmembrane and Coiled-Coil Domains 1

Haiyan Tan
Cleveland State University

Follow this and additional works at: <https://engagedscholarship.csuohio.edu/etdarchive>

 Part of the [Chemistry Commons](#)

[How does access to this work benefit you? Let us know!](#)

Recommended Citation

Tan, Haiyan, "Human Prostate Cancer Cell Apoptosis Induced by Interferon- γ and Double-Stranded RNA and Studies on the Biological Roles of Transmembrane and Coiled-Coil Domains 1" (2010). *ETD Archive*. 289.

<https://engagedscholarship.csuohio.edu/etdarchive/289>

This Dissertation is brought to you for free and open access by EngagedScholarship@CSU. It has been accepted for inclusion in ETD Archive by an authorized administrator of EngagedScholarship@CSU. For more information, please contact library.es@csuohio.edu.

**HUMAN PROSTATE CANCER CELL APOPTOSIS
INDUCED BY INTERFERON- γ AND DOUBLE-STRANDED RNA
AND
STUDIES ON THE BIOLOGICAL ROLES OF TRANSMEMBRANE
AND COILED-COIL DOMAINS 1**

HAIYAN TAN

**Bachelor of Science in Medicine
Norman Bethune University of Medical Sciences, China
July, 1995**

**Submitted in partial fulfillment of the requirements for the degree
DOCTOR OF PHILOSOPHY IN
CLINICAL AND BIOANALYTICAL CHEMISTRY
at the
CLEVELAND STATE UNIVERSITY
August, 2010**

This dissertation has been approved for the Department
of Chemistry and the College of Graduate Studies by

Dissertation Committee Chairperson, Dr. Aimin Zhou

Department & Date

Dr. David Anderson

Department & Date

Dr. Xue-long Sun

Department & Date

Dr. Crystal M Weyman

Department & Date

Dr. Sihe Wang

Department & Date

ACKNOWLEDGEMENTS

First and foremost, I want to heartily thank my advisor, Dr. Aimin Zhou, for his exceptional mentorship and constant support throughout my Ph.D. work. He was always available to listen to and discuss my ideas and questions, and showed me different ways to research problems. Most importantly, he taught me the need to be persistent to accomplish any goal, and his optimistic attitude toward his career and life has deeply affected me. I would like to express my special appreciation to my advisory committee, Dr. David Anderson, Dr. Crystal M Weyman, Dr. Sihe Wang, and Dr. Xue-long Sun, for their advice, encouragement, and support. Dr. Anderson provided me with a lot of encouragement and support. His instruction for my first job interview in the United States really touched me. Dr. Weyman is a model of a successful woman scientist and her instruction is always helpful. Also, I appreciate the help from her lab members for sharing their scientific opinions and resources. Dr. Sun's dedication and persistence through his research have helped me understand how to be a good scientist. I appreciate Dr. Wang's guidance during my internship study in the Cleveland Clinic, and I thank him for sharing with me the successful experience of his career.

I am thankful to Dr. Michael Kalafatis, Dr. Girish Shukla, Dr. G. Valentin Börner, and Dr. Xiaoxia Li for allowing me to use their valuable instruments, and would also like to thank Aekam Barot for the training on the Hermes upright fluorescence microscope.

I would like to thank all my colleagues who are, or were, in Dr. Zhou's lab: Cun Zeng, Xin Yi, Lin Zhang, Booseok Yun, Stephen Moreton, Christopher P Lanigan, Drs. Hongli Liu and Xiaoli Chen for their support during my study; I will cherish our friendship.

I would like express my special thanks to Dr. Yan Xu for his guidance, encouragement, and support during my study. I also want to thank Richelle and Michelle for their administrative assistance and Janet for all her help and support.

I also appreciate the help from Abigail Cory and Stephen Moreton in proofreading this dissertation.

I would like to thank my husband Zhiping and our lovely children, Ray and Annie. Their patience, love, and encouragement have made me able to accomplish these projects.

I would especially like to thank my parents. It is hard to find the appropriate words to express their role in my education and life. Whatever I have achieved today is because of their love, guidance, and constant support, both emotionally and morally. I deeply appreciate the effort they put into taking care of Ray and Annie so that I had time to pursue my doctoral studies; this dissertation would certainly not have existed without them.

This dissertation research was supported by the Cellular and Molecular Medicine Specialization Fellowship (CSU and Cleveland Clinic) and the Doctoral Dissertation Research Expense Award (CSU).

**HUMAN PROSTATE CANCER CELL APOPTOSIS
INDUCED BY INTERFERON- γ AND DOUBLE-STRANDED RNA
AND
STUDIES ON THE BIOLOGICAL ROLES OF TRANSMEMBRANE
AND COILED-COIL DOMAINS 1**

HAIYAN TAN

ABSTRACT

Project I:

Currently, chemotherapy is the only treatment for metastatic prostate cancer. However, due to toxicity and resistance, the currently available chemotherapeutic drugs are not good enough to control this disease. To find a novel and effective method to treat this disease, we studied the effect of interferons (IFNs) and double-stranded RNA (dsRNA) on the apoptosis of prostate cancer cells. Interestingly, pretreatment of PC3 cells, a human prostate adenocarcinoma cell line, with IFNs significantly sensitized these cells to dsRNA induced apoptosis, and cell apoptosis was confirmed by a variety of assays such as Annexin V, TUNEL, DNA fragmentation and the activity of caspase 3. In comparison with IFN- α or β treatment, IFN- γ treatment remarkably augmented dsRNA-induced apoptosis in PC3 cells. By using mutant cell lines, we demonstrated that IFN-signaling is necessary for these effects. Silence of dsRNA-dependent protein kinase R (PKR) and RNase L by siRNA did not have any significant impact on

this event, suggesting that neither RNase L nor PKR is involved. Further investigation of the apoptotic pathway revealed that Bak, a pro-apoptotic member of the Bcl-2 family, is up-regulated by IFN- γ and dsRNA. Our findings may lead to the design of novel therapeutic strategies for prostate cancer.

Project II:

Transmembrane and coiled-coil domains 1 (TMCO1) is a membrane-associated protein with unknown function. Recently, a homozygous frame shift mutation, c.139_140delAG, has been identified in the TMCO1 gene in patients with TMCO1 defect syndrome (TDS). TDS is characterized by distinctive craniofacial dysmorphism, skeletal anomalies, and mental retardation. In order to study the biological function of this gene, human TMCO1 was expressed in both bacteria and mammalian cells. The recombinant TMCO1 expressed in bacteria was purified in order to prepare an antibody, and subcellular localization revealed that TMCO1 may be expressed in the mitochondria of cells. Further study showed that the lymphocytes isolated from peripheral blood of patients with TDS grew significantly faster than those from healthy individuals, suggesting that TMCO1 may be involved in the regulation of cell proliferation. In addition, we have generated a TMCO1 knock down cell line, which will be used to further study the molecular basis of TDS.

TABLE OF CONTENTS

ABSTRACT.....	v
LISTE OF FIGURES.....	ix
ABBREVIATION.....	xii
CHAPTER I: INTRODUCTION	
Project I	
1.1.1 Prostate cancer: epidemiology and treatment.....	1
1.1.2 Overview of the IFN system and their biological functions.....	4
1.1.3 IFNs and apoptosis.....	7
1.1.4 Clinical application of IFNs in cancer treatment.....	10
1.1.5 DsRNA and cell apoptosis.....	11
1.1.6 Our hypothesis.....	13
1.1.7 References.....	13
Project II	
1.2.1 Chromosome 1 and its related diseases.....	20
1.2.2 Introduction of the human TMCO1 gene.....	21
1.2.3 TMCO1 defect syndrome.....	25
1.2.4 Biological function of TMCO1.....	26
1.2.5 References.....	30

CHAPTER II: HUMAN PROSTATE CANCER CELL APOPTOSIS INDUCED BY INTERFERON- γ AND DOUBLE-STRANDED RNA

2.1 Abstract.....	36
2.2 Introduction.....	37
2.3 Materials and methods.....	39
Reagents and antibodies.....	39
Cell culture and treatments.....	40
Cell viability assay.....	40
Annexin V assay.....	41
Determination of DNA fragmentation.....	43
TUNEL assay.....	44
Caspase activity assay.....	44
Western blot analysis.....	46
Inhibition of the expression of PKR in PC3 cells by siRNA.....	47
Inhibition of the expression of RNase L in PC3 cells by siRNA.....	48
2.4 Results.....	49
IFN- γ and dsRNA synergistically decrease PC3 cells viability.....	49
IFN- γ /dsRNA induce apoptosis in PC3 cells.....	54
IFN- γ /dsRNA activate caspase 3.....	55
IFN- γ /dsRNA enhance the expression of Bak.....	55
JAK/SATA pathway is involved in IFN- γ /dsRNA induced PC3 cell apoptosis.....	56
PKR is not involved in the IFN- γ /dsRNA induced PC3 cell apoptosis	63
RNase L is not involved in the IFN- γ /dsRNA induced PC3 cell apoptosis.....	64

INF- γ has no effect on the expression of DAP3 and DAP5.....	75
2.5 Discussion.....	77
2.6 References.....	79

CHAPTER III: STUDIES ON THE BIOLOGICAL ROLES OF TMCO1

3.1 Abstract.....	83
3.2 Introduction.....	84
3.3 Materials and methods.....	85
Materials and reagents.....	85
Subcloning of TMCO1 to pET-21d.....	86
Subcloning of TMCO1 to pIRESHyg	87
Other subclonings.....	88
Immunofluorescence staining.....	88
TMCO1 protein expression in <i>E. coli</i> BL21 cells.....	94
Purification of TMCO1.....	95
Production of polyclonal anti-TMCO1 antibody.....	95
RNA isolation and RT-PCR.....	96
Western blot analysis.....	97
Knockdown of TMCO1's expression.....	98
Growth rate of lymphocytes from patients with TMCO1 defect.....	98
3.4 Results.....	99
TMCO1 was subcloned to the pET-21d and pIRESHyg vectors.....	99
Purification of the recombinant TMCO1 protein	99

Localization of TMCO1.....	105
TMCO1 mRNA, but not the protein, is expressed in the lymphocytes of patients with TMCO1 defect syndrome.....	105
TMCO1 is ubiquitously expressed in all cells examined.....	109
TMCO1 is knocked down by TMCO1 shRNA in U87 cells.....	109
TMCO1 may be involved in the regulation of cell proliferation.....	110
3.5 Discussion.....	116
3.6 References.....	118

LIST OF FIGURES

Figure 1.1.1 Prostate cancer.....	2
Figure 1.1.2 IFN signaling pathway.....	6
Figure 1.1.3 Mechanism of IFN-induced apoptosis	9
Figure 1.2.1 Ideograms of chromosome 1.....	22
Figure 1.2.2 Schematic protein structure of TMCO1.....	24
Figure 1.2.3 Clinical features of TMCO1 defect syndrome.....	27
Figure 1.2.4 Partial pedigree chart of the family with TMCO1 defect syndrome	28
Figure 2.3.1 Principle of the Annexin-V assay.....	42
Figure 2.3.2 Working principle of the TUNEL assay.....	45
Figure 2.4.1 IFN- γ and dsRNA synergistically decrease PC3 cell viability.....	50
Figure 2.4.2 Growth of PC3 cells are inhibited significantly by the IFN- γ /dsRNA treatment.....	51
Figure 2.4.3 Morphology of PC3 cells treated with IFN- γ /dsRNA.....	52
Figure 2.4.4 IFN- γ and dsRNA synergistically inhibit the growth of DU145 cells	53
Figure 2.4.5 Determination of PC3 cell apoptosis by Annexin-V analysis.....	57
Figure 2.4.6 Determination of PC3 cell apoptosis by TUNEL assay.....	58
Figure 2.4.7 IFN- γ and dsRNA induce DNA fragmentation in PC3 cells.....	59
Figure 2.4.8 Caspase 3 activity assay.....	60
Figure 2.4.9 A scheme of major apoptotic pathways in mammalian cells.....	61

Figure 2.4.10 Effect of IFN- γ and dsRNA on the expression of apoptotic proteins	62
Figure 2.4.11 Effect of IFN- γ /dsRNA on the viability of LNCap cells.....	65
Figure 2.4.12 Effect of IFN- γ /dsRNA on the viability of U3A cells.....	66
Figure 2.4.13 Effect of IFN- γ /dsRNA on the viability of 2FTGH cells.....	67
Figure 2.4.14 Role of PKR in IFNs' functions.....	68
Figure 2.4.15 Role of PKR in IFNs/dsRNA-induced PC3 cell apoptosis.....	69
Figure 2.4.16 Knockdown of PKR by siRNA in PC3 cells	70
Figure 2.4.17 The 2-5 A system.....	71
Figure 2.4.18 Knockdown of RNase L by siRNA in PC3 cells.....	72
Figure 2.4.19 Role of RNase L in IFN- γ /dsRNA induced PC3 cell apoptosis.....	73
Figure 2.4.20 Expression of RNase L in IFNs/dsRNA treated PC3 cells.....	74
Figure 2.4.21 Expression of DAPs in IFN- γ treated PC3 cells.....	76
Figure 3.3.1 pET-21d vector map.....	89
Figure 3.3.2 pEREShyg vector information.....	90
Figure 3.3.3 pFLAG-CMV-2 vector information.....	91
Figure 3.3.4 pCMV-Myc vector information.....	92
Figure 3.3.5 pCMV-HA vector map and MCS.....	93
Figure 3.4.1 Digestion of PCR products and vectors.....	100
Figure 3.4.2 TMCO1/pET-21d clone selection.....	101
Figure 3.4.3 TMCO1/pIREShyg clone selection.....	102
Figure 3.4.4 Purification of TMCO1 protein by nickel affinity chromatography.....	103

Figure 3.4.5 Purified TMCO1 protein.....	104
Figure 3.4.6 Subcellular localization of pFlag-CMV-2 conjugated TMCO1 in U87 cells.....	106
Figure 3.4.7 TMCO1 mRNA expression in human lymphocytes.....	107
Figure 3.4.8 TMCO1 protein expression in human lymphocytes.....	108
Figure 3.4.9 TMCO1 expression in different cell lines.....	111
Figure 3.4.10 TMCO1 knockdown clone selection.....	112
Figure 3.4.11 TMCO1 is knocked down by TMCO1 shRNA.....	113
Figure 3.4.12 Effect of TMCO1 on the growth of human lymphocytes.....	114
Figure 3.4.13 Medium color changes related to the growth of human lymphocytes.....	115

ABBREVIATIONS

2-5 A	2' to 5' linked oligo adenylate
CIP	calf intestinal alkaline phosphatase
DAP	death-associated protein
DEPC	diethyl pyrocarbonate
dsRNA	double-stranded RNA
GAS	gamma-activated sequence
HRPC	hormone-refractory prostate cancer
IAP	inhibitor of apoptotic protein
IFN	interferon
IRF	IFN regulatory factor
ISG	IFN-stimulated genes
ISGF3	interferon-stimulated gene factor 3
ISRE	IFN-stimulated regulatory element
JAK	Janus tyrosine kinase
MAPK	mitogen activated protein kinase
OAS	oligoadenylate synthetase
PARP	poly (ADP-ribose) polymerase
PKR	dsRNA dependent protein kinase R
PI	propidium iodine
PI3-K	phosphatidylinositol 3-kinase
Poly I:C	polyinosinic:polycytidylic acid
PS	phosphatidylserine

PSA	prostate specific antigen
RIDs	regulators of IFN-induced death
siRNA	small interference RNA
shRNA	short hairpin RNA
SNP	single nucleoid polymorphysim
STAT	signal transducers and activators of transcription
TDS	TMCO1 defect syndrome
TDT	terminal deoxynucleotidyl transferase
TMCO1	transmembrane and coiled-coil domains 1
TLR 3	toll-like receptor 3
TUNEL	terminal deoxynucleotidyl transferase dUTP nick end labeling

CHAPTER I

INTRODUCTION

Project I: Human prostate cancer cell apoptosis induced by interferon- γ (IFN- γ) and double-stranded RNA (dsRNA)

1.1.1 Prostate cancer: epidemiology and treatment

The prostate is a small gland situated just below the bladder and surrounding the urethra (Figure 1.1.1). Its size and shape are similar to a walnut [American cancer society, 2009]. The function of a prostate is to produce the seminal fluid through which sperm is transported. Usually prostate cancer arises if the prostate cells fail to grow in an organized and controlled manner, which eventually leads to the formation of a tumor.

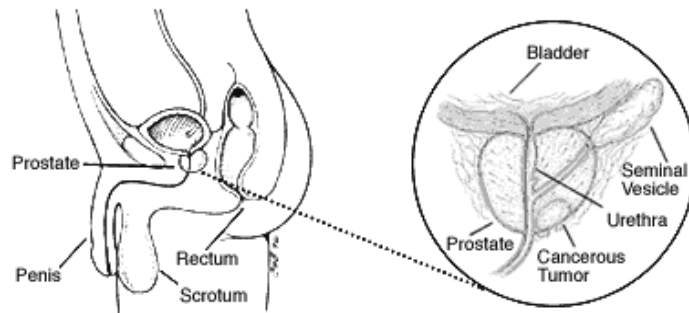


Figure 1.1.1 Prostate cancer [American cancer society, 2009]

In developed countries, prostate cancer is the second most frequently diagnosed cancer in men. Although prostate specific antigen (PSA) screening and early detection have been undertaken to reduce the mortality [Baade, *et al.*, 2004], prostate cancer is still the second leading cause of cancer death in men, affecting about one in six men in the United States [Damber, *et al.*, 2008]. The American Cancer Society estimates that there were about 192,280 new cases of prostate cancer in the United States in 2009 and that about 27,360 men died of the disease during that year.

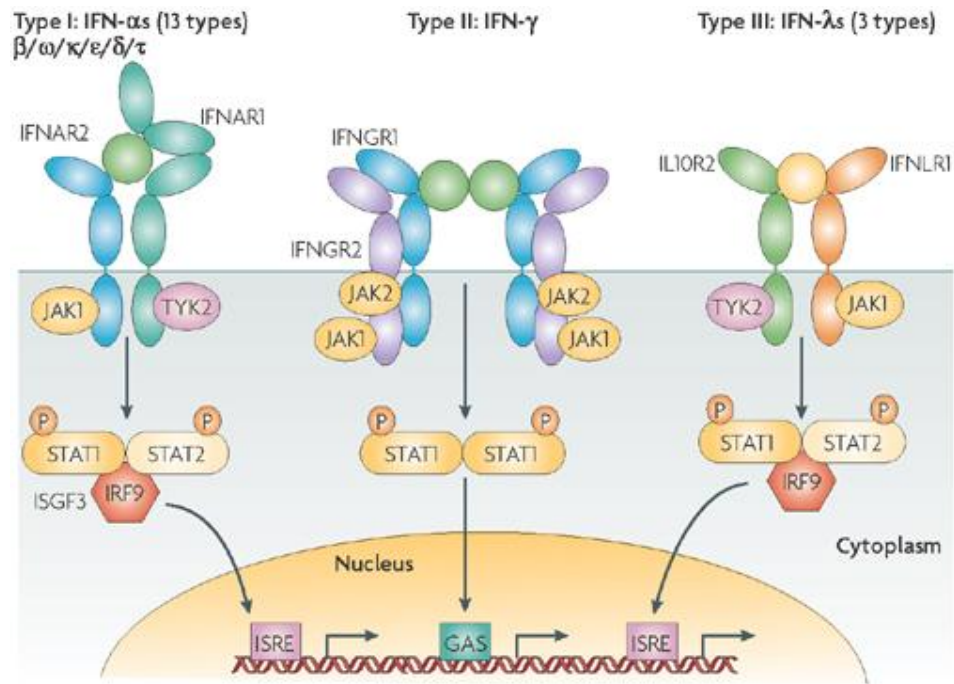
The treatment of prostate cancer depends on the cancerous stages of patients. Localized disease is curable. For aged patients, especially with slowly growing tumors, watchful waiting may be suggested. In the case of young patients and fast growing tumors, the most common treatments are radical prostatectomy and transurethral resection of the prostate [Chowdhury, *et al.*, 2007; Strief, *et al.*, 2007]. Radiation therapy, a treatment with radiation to kill and shrink cancer cells, is applied as the first treatment for low-grade cancer that has not spread outside the prostate gland or to local tissues. Cryosurgery, a technique using metal probes to freeze prostate cancer cells, can also be used for the treatment of prostate cancer that has not spread. For men who are diagnosed with a metastatic disease, there is only one choice: the androgen-ablation therapy, also called hormonal therapy. This treatment decreases the level of androgen, causing the prostate tumor to shrink or to grow more slowly. Unfortunately, hormonal therapy is effective for an average of only 2 years and most patients eventually become refractory to hormonal therapy. Hormone-

refractory prostate cancer (HRPC) is a common condition that causes considerable morbidity and mortality. To date, cytotoxic chemotherapy is thought to be the best way to control this situation. Recent studies have shown that docetaxel chemotherapy can achieve a remarkable improvement on the survival of HRPC patients. Thus docetaxel treatment has become the first-line chemotherapy treatment for HRPC and has been approved for use in the United States and Europe. However, lack of a response and development of resistance to docetaxel in a considerable number of patients limit its applications in prostate cancer therapy, requiring that most patients with HRPC undergo as much as third-line treatments [Chang and Kibel, 2008]. Therefore, development and discovery of new drugs capable of prolonging survival have become an urgent clinical need.

1.1.2 Overview of the IFN system and their biological functions

IFNs are a family of cytokines expressed in all eukaryotic cells as an early response to multiple stimuli, such as viral infection, dsRNA, and immune inducers [Stark, *et al.*, 1998]. There are two major classes of IFNs: type I and type II. Type I IFNs consist of several subtypes, mainly IFN- α and IFN- β , and are induced in most cell types by viruses and dsRNA; whereas type II IFN is induced potentially in T lymphocytes and natural killer cells in response to immune and inflammatory stimulation [Samuel, *et al.*, 2001]. Most recently, a new type of IFN-like protein was identified and classified as Type III IFN or IFN- λ [Kotenko, *et al.*, 2003].

Despite the differences in their amino acid sequences, all three types of IFNs display similar biological responses through inducing the expression of a series of IFN-stimulated genes (ISGs). The well-established IFN signaling pathways involve tyrosine phosphorylation, the activation of the Janus tyrosine kinases (JAKs), and the signal transducers and activators of transcription (STATs). Although the JAK/STAT signaling pathway is used by all three types of IFNs, the components and transducing mode in the pathways are distinctive (Figure 1.1.2). After binding with type I IFN, dimerization of type I IFN receptor subunits, IFNAR1 and IFNAR2, leads to the initiation of a tyrosine phosphorylation cascade (JAK1 and Tyk2), resulting in the association of STAT1 and STAT2. The phosphorylated STAT1/STAT2 heterodimer is associated with the DNA-binding protein p48 (in cytoplasm) to form a heterotrimer complex (ISGF3) which translocates into the nucleus, binding to the IFN-stimulated regulatory element (ISRE) of type I IFN responsive genes to initiate transcription. In type II IFN signaling, the activated type II receptor subunits IFNGR1 and IFNGR2 are associated with and activate JAK1 and JAK2, which subsequently phosphorylate STAT1. The phosphorylated STAT1 forms a homodimer, which translocates to



Nature Reviews | Drug Discovery

Figure 1.1.2 IFN signaling pathway [Kotenko, *et al.*, 2003]

the nucleus where it binds to the gamma-activated sequence (GAS) of IFN- γ -inducible genes to stimulate transcription. The type III IFN uses the same JAK/STAT pathway as type I IFN, but through different receptors. In recent years, studies have revealed that IFNs are able to activate other signaling pathways, such as the mitogen activated protein kinase (MAPK) and phosphatidylinositol 3-kinase (PI3-K) pathways [Platanias and Fish, 1999]. However, the biological significance of this cross-talk between IFN signaling and other signaling pathways remains to be fully understood.

1.1.3 IFNs and apoptosis

Apoptosis is a naturally occurring process by which a cell is directed to the programmed death. Apoptosis serves to eliminate undesired or superfluous cells in a targeted manner and plays an important role in tissue development, homeostasis, and differentiation. When cells go through apoptotic characteristics, changes take place in cell morphology, condensation of the chromatin, degradation of DNA, and cell shrinkage. Other commonly used biomarkers include cleavage of poly (ADP-ribose) polymerase (PARP), release of cytochrome C from mitochondria, and an increase of caspase activities. Additionally, apoptosis is involved in regulating the functions of the immune system and eliminating altered cells. Thus, abnormalities in the regulation of cell apoptosis can lead to various diseases, including cancer, autoimmunity, and degenerative disorders [Pommier, *et al.*, 2001; Schulze-Bergkamen and Krammer, 2004; Liu *et al.*, 2004; Tatton, *et al.*, 2003; Roth, 2001].

Type I and Type II IFNs are able to effectively induce apoptosis in a wide range of malignant cell types, such as herpes-associated lymphomas, acute promyelocytic leukemia (APL), non-small-cell lung cancer, non-melanoma skin cancer and glioma [Barber, 2003]. It is believed that IFNs induce cell apoptosis through activating the death receptor cascade (Figure 1.1.3) [Chawla-Sarkar, *et al.*, 2003]. The induction of TRAIL, and/or Fas/FasL, in response to IFNs leads to recruitment and activation of FADD. FADD activation in turn activates caspase-8, initiating the activation of the caspase cascade. On the other hand, IFNs also induce caspase-4 and caspase-8. Activated caspase-8 cleaves Bid, a proapoptotic member of Bcl-2 family, resulting in disruption of mitochondrial potential and the release of cytochrome C from the mitochondria into the cytoplasm where it acts as a cofactor to stimulate the complex of Apaf1 with caspase-9, subsequently activating proscaspase-3. A variety of ISGs, including the members of the IFN regulatory factor (IRF) family, dsRNA dependent protein kinase (PKR), 2-5A dependent RNase L (RNase L), TNF-related apoptosis-inducing ligand (TRAIL), promyelocytic leukemia gene (PML), and the death-associated proteins (DAPs), exert their tumor suppressing functions through inducing apoptosis in tumor cells [Chawla-Sarkar, *et al.*, 2003]. Interestingly, the involvements of different ISGs in IFN-induced apoptosis depend on cell types. For example, TRAIL and XIAP associated factor 1(XAF1) are believed to

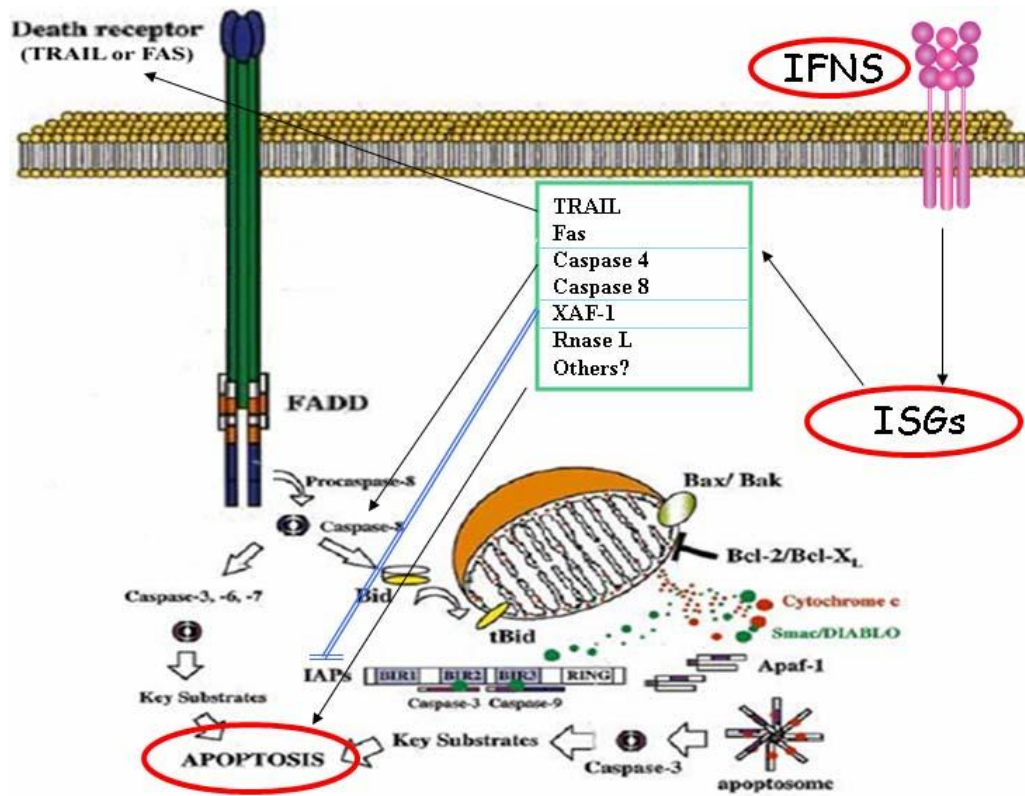


Figure 1.1.3 Mechanism of IFN-induced apoptosis [Zimmermann, 2001]

contribute to IFN-induced apoptosis in melanoma cells, whereas an induction of regulators of IFN-induced death (RIDs) is necessary in IFN-induced ovarian carcinoma cell apoptosis. The survival benefit may invoke a cancer cell to selectively inhibit one or more of the apoptotic ISGs, or acquire defects in IFN-signal transduction components.

1.1.4 Clinical application of IFNs in cancer treatment

The applications of IFNs in the treatment of cancer have been studied extensively. To a certain extent, success has been achieved in the treatment of several malignant hematological diseases and solid tumors by IFNs [Friedman, 2008]. Treatment with IFN- α , the first IFN used in the treatment of cancer, results in significant clinical responses and prolongs survival in patients with hairy cell leukemia, chronic myelogenous leukemia, renal cell carcinoma, ovarian cancer, hepatocellular carcinoma, and melanoma [Walter, *et al.*, 1998; Wadler and Schwartz, 1997; Borden and Parkinson, 1998; Baker, *et al.*, 2002; Borden, *et al.*, 2002, Borden, *et al.*, 2007 and Hastie, *et al.*, 2008]. Furthermore, clinical trials have revealed that IFN- α also exerts its therapeutic activity on other types of tumors including renal cell carcinoma, Kaposi's sarcoma, and melanoma. Pre-clinical studies have shown that IFNs are able to inhibit the growth of prostate cancer cells. For example, IFN- β increases the expression of the androgen receptor, improving adhesion potential of androgen-insensitive prostate cancer cells [Angelucci, 2007]. Forced expression of human IFN- β in human prostate cancer cells can significantly inhibit the prostatic growth which has been

correlated with down regulation of angiogenic molecules [Lee, 2006]. Adenovirus-mediated delivery of the IFN- γ gene can inhibit the growth of prostate cancer cells in vitro and xenografts *in vivo* [Zhao, *et al.*, 2007]. IFNs have also been used in clinical trials for prostate cancer patients [Van Haelst-Pisani, *et al.* 1992; Bulbul, *et al.* 1986]. However, the role of IFNs in the treatment of prostate cancer is under-studied, particularly in clinical applications. The limited application is due to high toxicity accompanied by limited beneficial effect [Kuratsukuri, *et al.*, 2000]. To solve these problems, IFNs have been used in combination with other cytotoxic agents for the treatment of prostate cancer in recent years. For example, IFN- α is combined with paclitaxel or 13-cis-retinoic acid in a phase I clinical trial to treat prostate cancer [Thalasila, *et al.*, 2003]; a phase II study indicates that IFN- γ as an adjuvant enhances antitumor effects in ¹³¹I-labeled high affinity CC49 monoclonal antibody therapy in patients with metastatic prostate cancer [Meredith, *et al.*, 1999]; the combination chemotherapy of 5-fluorouracil and a low dose of IFN- α in patients with HRPC proves feasible with acceptable toxicity [Shinohara, *et al.*, 1998]. Thus, a combination of IFN with other cytotoxic agents may be a novel approach for prostate cancer therapy.

1.1.5 DsRNA and cell apoptosis

The synthetic dsRNA, Polyinosinic:polycytidylic acid (Poly I:C), is a toll-like receptor 3 (TLR 3) ligand and a potent inducer of type I IFN. Poly I:C is active against a number of transplanted tumors, such as melanoma and leukemia [Bart

and Kopf, 1969; Zeleznick and Bhuyan, 1969]. It can also inhibit the growth of a variety of human tumor cells in culture, for example colon carcinoma cells and bladder carcinoma cells [Lin, *et al.*, 1982; Hubbel, *et al.*, 1984]. Poly I: C induces cell apoptosis through multiple pathways such as TLR3, NF-kappaB, interferon regulatory factors 3 (IRF3), and the IFN stimulated pathway [Chin, *et al.*, 2010; Huang, *et al.*, 2006]. Although the therapeutic efficacy and toxicity of dsRNA in the treatment of cancer patients have been evaluated in the past years, its striking side-effects have greatly blocked its clinical applications because the therapeutic responses are observed only at high doses [Friboulet, *et al.*, 2010]. Furthermore, several laboratories have reported that if dsRNA is delivered by cationic liposome to cancer cells, it can inhibit the growth of many cancer cells even at a low concentration, suggesting a possible clinical application of dsRNA [Okamoto, *et al.* 1998]. It has been observed that 25µg/mL poly I:C can inhibit LNCap cell (prostate cancer cell) proliferation through the IFN-independent pathway involving protein kinase C activation; however, 25ug/mL poly I:C only has slight inhibition effect on the PC3 cell proliferation [Paone, *et al.*, 2008]. Furthermore, it has been reported that human IFN and dsRNA can synergistically inhibit the growth of some human cancer cells, but studies about the mechanism are largely lacking [Chapekar and Glazer, 1985; Chapekar and Glazer, 1986]. Also, there are no reported studies on checking the effect of IFNs and dsRNA on prostate cancer cell apoptosis.

1.1.6 Our hypothesis

The effect of IFNs on prostate cancer has been studied for decades, but the limited application of IFNs on the treatment of prostate cancer is due to the cytotoxicity and lack of efficacy in prostate cancer patients. To solve these problems, IFNs have recently been used in combination with other cytotoxic agents for the treatment of prostate cancer. On the other hand, the antitumor function of the adjuvant molecule poly I:C has been studied extensively; however, the significantly inhibiting effect of poly I:C on human malignant cells has been performed with a very high concentration of 100µg/m. Recently, the combination of low dose of poly I:C with other factors such as the IAP (inhibitor of apoptotic protein) inhibitor RMT 5265 can produce a synergistic effect on apoptosis induction and/or inhibition of clonogenic growth [Friboulet, *et al.*, 2010]. Here, we hypothesis that a low dose of IFNs combined with a low dose of dsRNA may augment the inhibiting effect on the growth of prostate cancer cells.

1.1.7 References

- American cancer associaty. Overview: prostate cancer. 2008, http://www.cancer.org/docroot/CRI/content/CRI_2_2_1X_How_many_men_get_prostate_cancer_36.asp?rnav=cri
- Angelucci C, Iacopino F, Ferracuti S, Urbano R and Sica G. Recombinant human IFN-beta affects androgen receptor level, neuroendocrine differentiation, cell adhesion and motility in prostate cancer cells. *J Interferon Cytokine Res*, 2007, 27(8):643-652

- Baade PD, Coory MD, Aitken JF. International trends in prostate cancer mortality: the decrease is continuing and spreading. *Cancer Causes Control*, 2004, 15:237-241
- Baker PK, Pettitt AR, Slupsky JR, Chen HJ, Glenn MA, Zuzel M and Cawley JC. Response of hairy cells to IFN-alpha involves induction of apoptosis through autocrine TNF-alpha and protection by adhesion. *Blood*, 2002,100: 647-653
- Barber GN. The interferons and cell death: guardians of the cell or accomplices of apoptosis? *Semin Cancer Biol*, 2003,10(2):103-111
- Bart RS and Kopf AW. Inhibition of the growth of murine malignant melanoma with synthetic double-stranded ribonucleic acid. *Nature*, 1969,224:3-12
- Borden EC, Lindner D, Dreicer R, Hussein M and Peereboom D. Second-generation interferons for cancer: clinical targets. *Semin Cancer Biol*. 2000,10(2):125-144
- Borden EC and Parkinson D. A perspective on the clinical effectiveness and tolerance of interferon-alpha. *Semin Oncol*, 1998, 25(1 Suppl 1):3-8
- Borden EC, Sen GC, Uze G, Silverman RH, Ransohoff RM, Foster GR and Stark GR. Interferons at age 50: past, current and future impact on biomedicine. *Nat Rev Drug Discov*, 2007, 6:975-990
- Bulbul MA, Huben RP and Murphy GP. Interferon-beta treatment of metastatic prostate cancer. *J Surg Oncol*, 1986, 33:231-233
- Chapekar MS and Glazer RI. Synergistic effect of human immune interferon and double-stranded RNA against human colon carcinoma cells in vitro. *Cancer Res*, 1985, 45:2539-2544

- Chapekar MS and Glazer RI. Potentiation of the cytotoxic effect of human immune interferon by different synthetic double-stranded RNAs in the refractory human colon carcinoma cell line BE. *Cancer Res*, 1986, 46:1698-1702
- Chawla-Sarkar M, Lindner DJ, Liu YF, Williams BR and Sen GC, Silverman RH and Borden EC. Apoptosis and interferons: Role of interferon-stimulated genes as mediators of apoptosis. *Apoptosis*, 2003,8 (3):237-249
- Chin AI, Miyahira AK, Covarrubias A, Teague J, Guo B, Dempsey PW and Cheng G. Toll-like receptor 3-mediated suppression of TRAMP prostate cancer shows the critical role of type I interferons in tumor immune surveillance. *Cancer Res*, 2010, 70(7):2595-2603
- Chowdhury S, Burbridge S and Harper PG. Chemotherapy for the treatment of hormone-refractory prostate cancer. *Int J Clin Pract*, 2007,61(12): 2064-2070
- Damber JE and Aus G. Prostate Cancer, *Lancet*, 2008,371(9625): 1710-1721
- Friedman RM. Clinical uses of interferons. *Br J Clin Pharmacol*. 2008, 65(2):158-162
- Friboulet L, Gourzones C, Tsao SW, Morel Y, Paturel C, Temam S, Uzan C and Busson P. Poly(I:C) induces intense expression of c-IAP2 and cooperates with an IAP inhibitor in induction of apoptosis in cancer cells. *BMC Cancer*, 2010,10(1):327
- Hastie Claire. Interferon γ , a possible therapeutic approach for late-stage prostate cancer? *Anticancer Res*, 2008, 28:2843-2850

- Huang CC, Duffy KE, San Mateo LR, Amegadzie BY, Sarisky RT and Mbow ML. A pathway analysis of poly (I: C)-induced global gene expression change in human peripheral blood mononuclear cells. *Physiol Genomics*, 2006, 26(2):125-133
- Hubbel HR, Liu RS and Maxwell BL. Independent sensitivity of human tumor cell lines to interferon and double-stranded RNA. *Cancer Res*, 1984, 44:3252-3257
- Kotenko SV, Gallagher G, Baurin VV, Lewis-Antes A, Shen M, Shah NK, Langer JA, Sheikh F, Dickensheets H and Donnelly RP. IFN- λ s mediate antiviral protection through a distinct class II cytokine receptor complex. *Nature immunology*, 2003,4(1):69-77
- Kuratsukuri K, Nishisaka N, Jones RF, Wang CY and Haas GP. Clinical trials of immunotherapy for advanced prostate cancer. *Urol Oncol*, 2000,5:265-273
- Lee J, Wang A, Hu Q, Lu S and Dong Z. Adenovirus-mediated interferon-beta gene transfer inhibits angiogenesis in and progression of orthotopic tumors of human prostate cancer cells in nude mice. *Int J Oncol*, 2006, 29(6):1405-1412
- Lin SL, Greene JJ, Ts'o POP and Carter WA. Sensitivity and resistance of human tumor cells to interferon and rI_n·rC_n. *Nature*, 1982,297:417-419
- Liu CC, Navratil JS, Sabatine JM and Ahearn JM. Apoptosis, complement and systemic lupus erythematosus: a mechanistic view. *Curr Dir Autoimmun*, 2004,7:49-86

- Meredith RF, Khazaeli MB, Macey DJ, Grizzle WE, Mayo M, Schlom J, Russell CD and LoBuglio AF. Phase II study of interferon-enhanced in ¹³¹I-labeled high affinity CC49 monoclonal antibody therapy in patients with metastatic prostate cancer. *Clin Cancer Res*, 1999, 5(10 Suppl):3254s-3258s
- Okamoto S, Watanabe Y, Takakura Y and Hashida M. Cationic liposome-mediated efficient induction of type I interferons by a low dose of poly I:poly C in mouse cell lines. *J Biochem*, 1998,124(4):697-701
- Paone A, Starace D, Galli R, Padula F, De Cesaris P, Filippini A, Ziparo E and Riccioli A. Toll-like receptor 3 triggers apoptosis of human prostate cancer cells through a PKC- α -dependent mechanism. *Carcinogenesis*, 2008,29(7):1334-1342
- Platanias LC and Fish EN. Signaling pathways activated by interferons. *Exp Hematol*, 1999, 27(11):1583-1592
- Pommier Y, Sordet O, Antony S, Hayward RL and Kohn KW. Apoptosis defects and chemotherapy resistance: molecular interaction maps and networks. *Oncogene*, 2004,23(16):2934-2949
- Roth KA. Caspases, apoptosis, and Alzheimer disease: causation, correlation, and confusion. *J Neuropathol Exp Neurol*, 2001, 60(9):829-838
- Samuel CE. Antiviral actions of interferons. *Clinical Microbiology Rev*, 2001, 14(4): 778-809
- Schulze-Bergkamen H and Krammer PH. Apoptosis in cancer--implications for therapy. *Semin Oncol*, 2004, 31(1):90-119

- Shinohara N, Demura T, Matsumura K, Toyoda K, Kashiwagi A, Nagamori S, Ohmuro H, Ohzono S and Koyanagi T. 5-fluorouracil and low-dose recombinant interferon-alpha-2a in patients with hormone-refractory adenocarcinoma of the prostate. *Prostate*, 1998,35(1):56-62
- Stark GR, Kerr IM, Williams BR, Silverman RH and Schreiber RD. How cells respond to interferons. *Annu Rev Biochem*, 1998, 67:227-264
- Strief DM. An overview of prostate cancer: diagnosis and treatment. *Urol Nurs*, 2007, 27(6): 475-479
- Tatton WG, Chalmers-Redman R, Brown D and Tatton N. Apoptosis in Parkinson's disease: signals for neuronal degradation. *Ann Neurol*, 2003,53 Suppl 3:S61-70; discussion S70-72
- Van Haelst-Pisani CM, Richardson RL, Su J, Buckner JC, Hahn RG, Frytak S, Kvols LK and Burch PA. A phase II study of recombinant human alpha-interferon in advance hormone-refractory prostate cancer. *Cancer*,1992,70:2310-2312
- Thalasila A, Poplin E, Shih J, Dvorzhinski D, Capanna T, Doyle-Lindrud S, Beers S, Goodin S, Rubin E and DiPaola RS. A phase I trial of weekly paclitaxel, 13-cis-retinoic acid, and interferon alpha in patients with prostate cancer and othere advanced malignacncies. *Cancer Chemother Pharmacol*, 2003, 52(2): 119-124
- Wadler S and Schwartz EL. New advances in interferon therapy of cancer. *Oncologist*, 1997, 2(4):254-267

Walter MR, Bordens R, Nagabhushan TL, Williams BR, Herberman RB, Dinarello CA, Borden EC, Trotta PP, Pestka S and Pfeffer LM. Review of recent developments in the molecular characterization of recombinant alfa interferons on the 40th anniversary of the discovery of interferon. *Cancer Biother Radiopharm*, 1998, 13(3):143-154

Zeleznick LD and Bhuyan RK. Treatment of leukemia (L1210) mice with double-stranded polyribonucleotides. *Proc Soc Exp Biol Med*, 1969, 130:126-128

Zhao P, Zhu YH, Wu JX, Liu RY, Zhu XY, Xiao X, Li HL, Huang BJ, Xie FJ, Chen JM, Ke ML and Huang W. Adenovirus-mediated delivery of human IFN gamma gene inhibits prostate cancer growth. *Life Sci*, 2007, 81(9):695-701

Zimmermann KC and Gree DR. How cells die: Apoptosis pathways. *J Allergy Clin Immunol*, 2001, 108(4):S99-103

Project II: studies on the biological roles of TMCO1

1.2.1 Human chromosome 1 and its related diseases

Chromosome 1 is the largest of the human chromosomes, spanning about 260 million base pairs and containing 8% of the human genome [Gregory, *et al.*, 2006]. There are about 3,000 genes on chromosome 1 and due to this great number of genes, there are also a large number of diseases associated with chromosome 1. Over 350 human diseases have been linked to the disruption in the sequence of chromosome 1 including cancers, neurological, developmental disorders, distinctive facial features, birth defects, cardiovascular disease, and other medical problems [Ohya, *et al.*, 2006; Povey and Parrington, 1986]. A few examples include: Parkinson's disease, familial adenomatous polyposis, Alzheimer's disease, porphyria cutanea tarda, Chediak–Higashi syndrome, Diamond–Blackfan syndrome, factor V Leiden thrombophilia, hereditary antithrombin III deficiency, Gaucher disease, type 2 hemochromatosis, etc. [Caramazza, *et al.*, 2010]. Changes to chromosome 1 may include a missing segment of the short (p) or long arm (q) of the chromosome in each cell (partial monosomy 1p or 1q), an extra segment of the short or long arm of the chromosome, or a circular structure called ring chromosome 1 [<http://ghr.nlm.nih.gov/chromosome=1>]. For instance, the nonrandom duplication of the long arm material of chromosome 1, which tends to occur at a relatively late stage of cancer, may contribute to the progression of all forms of cancer [Atkin, 1986]. Impressively, chromosome 1 plays an important role in the

regulation of the development and growth of humans, which can be seen in several developmental disorders. One disorder, known as 1p36 deletion syndrome, is a disease characterized by typical craniofacial dysmorphism, developmental delay, and mental retardation. In individuals with 1p36 deletion syndrome, the genetic deletion on the outermost band of the short arm of chromosome 1 (1p36 chromosome region) occurs, which includes *de novo* terminal 1p36 deletion, interstitial deletion, complex chromosome rearrangements, 1p36 deletion with a 1p36 duplication, or a derivative chromosome 1 [Battaglia, *et al.*, 2008]. The clinical features of GLUT1 deficiency syndrome are mental and developmental delay, hypoglycorrhachia. This syndrome is caused by various *de novo* mutations in the facilitated human glucose transporter 1 gene (1p34.2) [Aktas, *et al.*, 2010]. Chromosome 1q syndrome is another developmental disorder related to Chromosome 1. The interstitial deletion of chromosome 1q (q23-q31) causes pre- and postnatal growth retardation, severe psychomotor retardation, microbrachycephaly and some other clinical syndromes [Schwemmler, *et al.*, 2006].

1.2.2 Introduction of the human TMCO1 gene

The human TMCO1 gene is located on chromosome 1q22-q25. TMCO1 is a plasma membrane-associated protein and belongs to the DUF841 superfamily of several eukaryotic proteins with unknown functions based on the predicted amino acid sequence [Zhang, *et al.*, 2010]. TMCO1 is also known as HP10122, PCIA3, PNAS-136, RP11-466F5.7 or TMCC4. An earlier study proved that HP10122, an alias for TMCO1, is

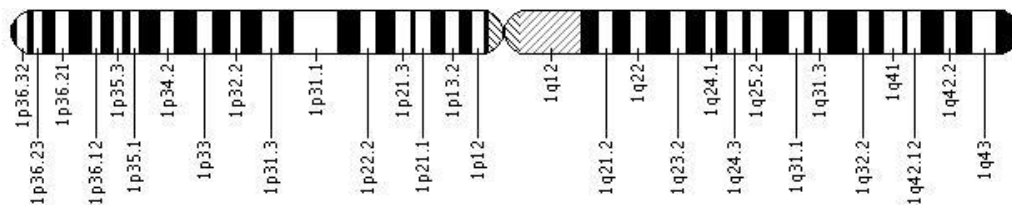


Figure 1.2.1 Ideograms of chromosome 1 (<http://ghr.nlm.nih.gov/chromosome=1>)

located in the endoplasmic reticulum and Golgi apparatus in COS7 cells (Monkey kidney cell line) by fusing TMCO1 with a green fluorescent protein tag [Iwamuro, *et al.*, 1999], whereas another recent study showed the porcine TMCO1 localizing in mitochondrion [Zhang, *et al.*, 2010]. A full-length cDNA clone HP10122, isolated from human HT-1080 cDNA library, contains a 5'-untranslated region of 138bp, an open reading frame of 567bp, and a 3'-untranslated region of 481bp [Iwamuro, *et al.*, 1999]. The TMCO1 gene consists of seven coding exons, and the 564-bp coding region encodes a predicted protein of 188 amino acids. Figure 1.2.2 shows the schematic structure of TMCO1 protein [Xin, *et al.*, 2010]. One coiled-coil domain (amino acids 32-89) and two transmembrane segments (amino acids 10-31 for TM1 and amino acids 90-109 for TM2) were predicted by SMART sequence analysis. Reversible phosphorylations of serine, threonine, and tyrosine residues are critical steps in the signal transduction pathways. Previous studies indicate that three phosphorylation sites (phosphoserines) involved in the signaling networks across the cell cycle are identified [Olsen, *et al.*, 2006; Nousiainen, *et al.*, 2006; Wang, *et al.*, 2008; Daub, *et al.*, 2008; Dephoure, *et al.*, 2008; Yachie, *et al.*, 2009]. There are two known isoforms of the human TMCO1 protein which are produced by alternative splicing. The expression of TMCO1 transcript is universal in different tissues; the EST profile of the NCBI database (UniGene Hs.31498) shows that the TMCO1 transcript was found to be expressed in 42 of 45 adult tissues examined. Furthermore, mRNA expression of TMCO1 was displayed at



Figure 1.2.2 Schematic protein structure of TMCO1 [Xin, *et al.*, 2010] One coiled-coil domain (amino acids 32-89) and two transmembrane segments (amino acids 10-31 for TM1 and amino acids 90-109 for TM2) were predicted by SMART sequence analysis. The red stars indicate three verified phosphoserine residues.

all developmental stages, including the embryoid body, blastocyst, fetus, neonate, infant, juvenile, and adult (<http://www.ncbi.nlm.nih.gov/UniGene/ESTProfileViewer.cgi?uglist=Hs.31498>).

The HP10122 mRNA was detected by Northern blot analysis as a single band of 1.5kb in various human tissues with different expression levels: highly expressed in the thymus, prostate, testis and small intestine and scarce in kidney, placenta, lung, and brain [Iwamuro, *et al.*, 1999]; while in swine, the quantitative PCR results indicated that the expression of TMCO1 mRNA was higher in the liver, heart and kidney, significant in doris, logngissimus, backfat, brain, lymph, lung, large intestine, small intestine and lower in stomach and spleen [Zhang, *et al.*, 2010]. From the amino acid sequence comparison, it has been known the entire sequence is highly conserved with 100% homology among eight mammalian TMCO1 proteins in GenBank [Xin, *et al.*, 2010]; analysis by a SOSUI software predicts the secondary structure of the TMCO1 protein as a membrane protein with a transmembrane helix [Zhang, *et al.*, 2010].

1.2.3 TMCO1 defect syndrome

A unique autosomal recessive condition characterized by distinctive craniofacial dysmorphism, skeletal anomalies, and mental retardation was described in Old Order Amish of Northeast Ohio. This condition was called TMCO1 defect syndrome [Xin, *et al.*, 2010]. The typical craniofacial dysmorphism includes highly arched bushy eyebrows, long eyelashes, brachycephaly,

synophrys, low-set ears, microdontism of primary teeth, and generalized gingival hyperplasia; whereas, skeletal anomalies are represented by Sprengel deformity of the scapula, rib abnormalities, pes planus, fusion of the spine and pectus excavatum (Figure 1.2.3). Depressed deep tendon reflexes, unstable gait, and intention tremor were found in some older patients through neurological examination.

Through genome-wide single nucleotide polymorphism (SNP) homozygosity mapping in affected individuals from a consanguineous pedigree (Figure 1.2.4), a single large, shared block of homozygous SNPs was identified on chromosome 1q23.3-q24.1, and 23 genes were revealed from the examination of the minimal shared region. From gene sequencing, homozygous 2-base pair deletion (c.139_140delAG) within exon 2 of the TMCO1 gene was identified as the pathogenic change in patients with TMCO1 defect syndrome. It is predicted that this homozygous frame shift mutation can result in premature truncation of translation at amino acid position 47.

1.2.4 Biological function of TMCO1

The biological process and function of the TMCO1 gene are still unknown, and there are few papers available to indicate the biological function of TMCO1.

TMCO1 may be involved in the lipid metabolism, since TMCO1 is down-regulated in liver and adipose tissues in response to a 3-day fast [Lkhagvadori, *et al.*, 2009]. The relationship between TMCO1 and cancers can be found in several

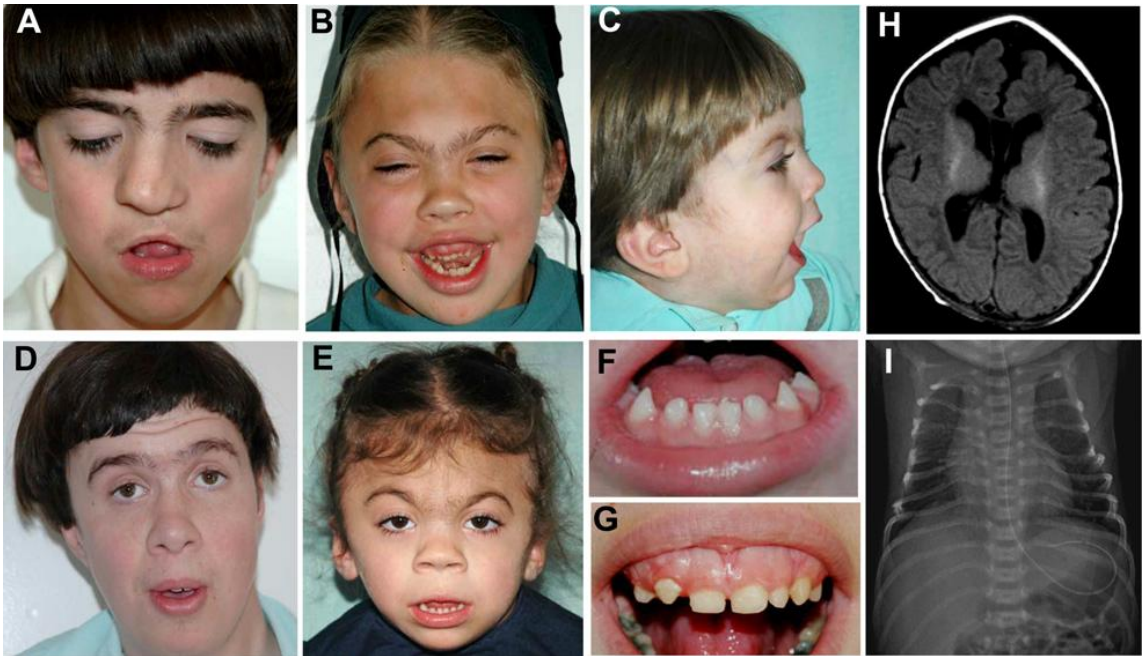


Figure 1.2.3 Clinical features of TMC01 defect syndrome [Xin, *et al.*, 2010]. (A-G) Facial characteristics of this syndrome; (H) Brain Magnetic resonance imaging (MRI) of a patient with TDS indicating prominence of cerebrospinal fluid space around the frontal lobes with extension into the anterior interhemispheric fissure; (I) Chest x-ray film of an affected individual showing multiple rib anomalies.

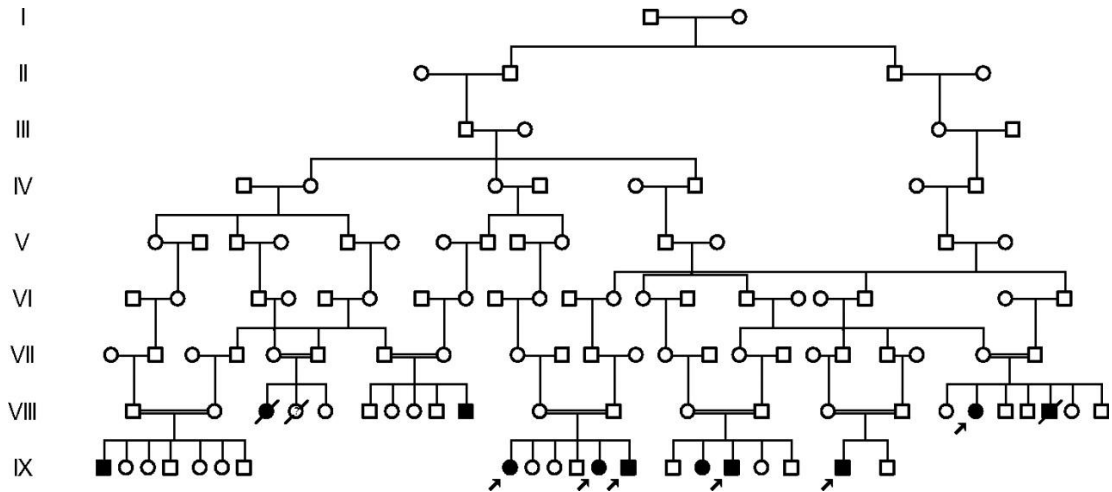


Figure 1.2.4 Partial pedigree chart of the family with TMCO1 defect syndrome [Xin, *et al.*, 2010]. ■, affected males; □, unaffected males; ●, affected females; ○, unaffected females; ==, consanguinity.

studies: meta-analysis of microarray data showed that TMCO1 is upregulated in breast cancer [Kondrakhin, *et al.*, 2008]; TMCO1 may be a potential pharmacogenomic predictor in phase II clinical trials of trastuzumab for breast cancer [Pusztai, *et al.*, 2007]; and in bladder cancer, the previous study indicates that lipolysis stimulated lipoprotein receptor (LSR) can be upregulated by P53, which may impair bladder cancer cells from gaining invasive properties. Affymetrix GeneChips experiment shows that siRNA knockdown of LSR leads to the down regulation of TMCO1 expression [Herbsleb, *et al.*, 2008]. BCL6 is a BTB/POZ domain transcription repressor that is required for normal germinal center development and is expressed by the majority of normal GC B cells and a subset of diffuse large B cell lymphomas [Polo, *et al.*, 2007]. The BCL6 targeting proteins are enriched in modulators of transcription, chromatin structure, protein ubiquitylation, cell cycle, and DNA damage responses. As one of BCL6 targeting genes, TMCO1's biological activities may be found among some of these events. Furthermore, TMCO1 is found to be associated with the onset of diabetes and renal function in a type II diabetes mouse model. In this study, the TMCO1 transcript ratios in liver, brain, islets, EDL, soleus muscle, and adipose between diabetes-susceptible DBA/2J mice and diabetes-resistant C57BL/6J mice were calculated [Dokmanovic-Chouinard, *et al.*, 2008]. TMCO1 may be involved in the regulation of renal water excretion through altered Aquaporin-2 (a molecular water channel). Altered Aquaporin-2 protein, which is abundant in the renal collecting duct, is the main factor responsible for water balance abnormalities associated with different clinical states. TMCO1 is one of Aquaporin-2's

transcriptional regulators and is expressed only in the medullary thick ascending limb cells and renal proximal tubule cells in native rats, but not in the renal collecting duct [Yu, *et al.*, 2009]. Most recently, other possible functions of TMCO1 may be outlined by Musashi 1 study. Musashi1 is a highly conserved RNA-binding protein with pivotal functions in stem cell maintenance, nervous system development, and tumorigenesis. TMCO1 is one of the Musashi1-associated mRNAs, which implicates that the TMCO1's biological function is related to at least one of Musashi 1's functions: 1) cell cycle, cell proliferation, cell differentiation, and apoptosis; 2) protein modification (including ubiquitination and ubiquitin cycle); and 3) tumor formation [De Sousa Abreu, *et al.*, 2009]. In summary, more work needs to be done to dig out the systematic functions of TMCO1.

1.2.5 References

- Aktas D, Utine EG, Mrasek K, Weise A, von Eggeling F, Yalaz K, Posorski N, Akarsu N, Alikasifoglu M, Liehr T and Tuncbilek E. Derivative chromosome 1 and GLUT1 deficiency syndrome in a sibling pair. *Mol Cytogenet*, 2010, 28;3(1):10-17
- Atkin NB. Chromosome 1 abberations in cancer. *Cancer Genet Cytogenet*, 1986, 15;21(4):279-285
- Battaglia A and Shaffer LG. 1p36 Deletion Syndrome. In: Pagon RA, Bird TC, Dolan CR, Stephens K, editors. *GeneReviews* [Internet]. Seattle (WA): University of Washington, Seattle; 2008:1993

- Caramazza D, Hussein K, Siragusa S, Pardanani A, Knudson RA, Ketterling RP and Tefferi A. Chromosome 1 abnormalities in myeloid malignancies: a literature survey and karyotype-phenotype associations. *Eur J Haematol*, 2010, 84(3):191-200
- Daub H, Olsen JV, Bairlein M, Gnad F, Oppermann FS, Körner R, Greff Z, Kéri G, Stemmann O and Mann M. Kinase-selective enrichment enables quantitative phosphoproteomics of the kinome across the cell cycle. *Mol Cell*, 2008, 31(3):438-448
- Dephoure N, Zhou C, Villén J, Beausoleil SA, Bakalarski CE, Elledge SJ and Gygi SP. A quantitative atlas of mitotic phosphorylation. *Proc Natl Acad Sci U S A*, 2008, 105(31):10762-10767
- De Sousa Abreu R, Sanchez-Diaz PC, Vogel C, Burns SC, Ko D, Burton TL, Vo DT, Chennasamudaram S, Le SY, Shapiro BA and Penalva LO. Genomic analyses of musashi1 downstream targets show a strong association with cancer-related processes. *J Biol Chem*, 2009, 284(18):12125-12135
- Dokmanovic-Chouinard M, Chung WK, Chevre JC, Watson E, Yonan J, Wiegand B, Bromberg Y, Wakae N, Wright CV, Overton J, Ghosh S, Sathe GM, Ammala CE, Brown KK, Ito R, LeDuc C, Solomon K, Fischer SG and Leibel RL. Positional cloning of "Lisch-Like", a candidate modifier of susceptibility to type 2 diabetes in mice. *PLoS Genet*, 2008, 4(7):e1000137
- Gregory SG, Barlow KF, McLay KE, Kaul R, Swarbreck D, Dunham A, Scott CE, Howe KL, Woodfine K, Spencer CC, Jones MC, Gillson C, Searle S, Zhou Y, Kokocinski F, McDonald L, Evans R, Phillips K, Atkinson A, Cooper R, Jones

C, Hall RE, Andrews TD, Lloyd C, Ainscough R, Almeida JP, Ambrose KD, Anderson F, Andrew RW, Ashwell RI, Aubin K, Babbage AK, Bagguley CL, Bailey J, Beasley H, Bethel G, Bird CP, Bray-Allen S, Brown JY, Brown AJ, Buckley D, Burton J, Bye J, Carder C, Chapman JC, Clark SY, Clarke G, Clee C, Cobley V, Collier RE, Corby N, Coville GJ, Davies J, Deadman R, Dunn M, Earthrowl M, Ellington AG, Errington H, Frankish A, Frankland J, French L, Garner P, Garnett J, Gay L, Ghori MR, Gibson R, Gilby LM, Gillett W, Glithero RJ, Grafham DV, Griffiths C, Griffiths-Jones S, Grocock R, Hammond S, Harrison ES, Hart E, Haugen E, Heath PD, Holmes S, Holt K, Howden PJ, Hunt AR, Hunt SE, Hunter G, Isherwood J, James R, Johnson C, Johnson D, Joy A, Kay M, Kershaw JK, Kibukawa M, Kimberley AM, King A, Knights AJ, Lad H, Laird G, Lawlor S, Leongamornlert DA, Lloyd DM, Loveland J, Lovell J, Lush MJ, Lyne R, Martin S, Mashreghi-Mohammadi M, Matthews L, Matthews NS, McLaren S, Milne S, Mistry S, Moore MJ, Nickerson T, O'Dell CN, Oliver K, Palmeiri A, Palmer SA, Parker A, Patel D, Pearce AV, Peck AI, Pelan S, Phelps K, Phillimore BJ, Plumb R, Rajan J, Raymond C, Rouse G, Saenphimmachak C, Sehra HK, Sheridan E, Shownkeen R, Sims S, Skuce CD, Smith M, Steward C, Subramanian S, Sycamore N, Tracey A, Tromans A, Van Helmond Z, Wall M, Wallis JM, White S, Whitehead SL, Wilkinson JE, Willey DL, Williams H, Wilming L, Wray PW, Wu Z, Coulson A, Vaudin M, Sulston JE, Durbin R, Hubbard T, Wooster R, Dunham I, Carter NP, McVean G, Ross MT, Harrow J, Olson MV, Beck S, Rogers J, Bentley DR, Banerjee R, Bryant SP, Burford DC, Burrill WD, Clegg SM, Dhami P, Dovey O, Faulkner

- LM, Gribble SM, Langford CF, Pandian RD, Porter KM and Prigmore E. The DNA sequence and biological annotation of human chromosome 1. *Nature*, 2006, 441(7091):315-321
- Herbsleb M, Birkenkamp-Demtroder K, Thykjaer T, Wiuf C, Hein AM, Orntoft TF and Dyrskjøt L. Increased cell motility and invasion upon knockdown of lipolysis stimulated lipoprotein receptor (LSR) in SW780 bladder cancer cells. *BMC Med Genomics*, 2008, 1:31-48
- Iwamuro S, Saeki M and Kato S. Multi-ubiquitination of a nascent membrane protein produced in a rabbit reticulocyte lysate. *J Biochem*, 1999, 126(1):48-53
- Kurimura A, Saeki M, Kato S and Iwamuro S. Analyses of intracellular localization and dynamic behaviors of human hydrophobic protein HP10122. *Zoo Sci*, 2002, 19: 1432
- Kondrakhin YV, Sharipov RN, Keld AE and Kolpakov FA. Identification of differentially expressed genes by meta-analysis of microarray data on breast cancer. *In Silico Biol*, 2008, 8(5-6):383-411
- Lkhagvadorj S, Qu L, Cai W, Couture OP, Barb CR, Hausman GJ, Nettleton D, Anderson LL, Dekkers JC and Tuggle CK. Microarray gene expression profiles of fasting induced changes in liver and adipose tissues of pigs expressing the melanocortin-4 receptor D298N variant. *Physiol Genomics*, 2009, 38(1):98-111

- Nousiainen M, Silljé HHW, Sauer G, Nigg EA and Körner R. Phosphoproteome analysis of the human mitotic spindle. *Proc Natl Acad Sci USA*, 2006, 103:5391–5396
- Ohya Y, Nakamoto M, Yamazato M and Sakima A. Congenic strain for chromosome 1 quantitative trait locus for blood pressure. *Nippon Rinsho*, 2006,64(Suppl 5):284-289
- Olsen JV, Blagoev B, Gnäd F, Macek B, Kumar C, Mortensen P and Mann M. Global, in vivo, and site-specific phosphorylation dynamics in signaling networks. *Cell*. 2006 Nov 3;127(3):635-648
- Polo JM, Juszczynski P, Monti S, Cerchiatti L, Ye K, Greally JM, Shipp M and Melnick A. Transcriptional signature with differential expression of BCL6 target genes accurately identifies BCL6-dependent diffuse large B cell lymphomas. *Proc Natl Acad Sci U S A*, 2007, 104(9):3207-3212
- Povey S and Parrington JM. Chromosome 1 in relation to human disease. *Gene mapping and medical genetics. J Med Genet*, 1986;23: 107-115
- Pusztai L, Anderson K and Hess KR. Pharmacogenomic predictor discovery in phase II clinical trials for breast cancer. *Clin Cancer Res*, 2007, 13(20):6080-6086
- Schwemmler C, Schulze B and Ptok M. Chromosome 1q syndrome and hearing loss: an unusual case. *Laryngorhinotologie*, 2006,85(4):279-282
- Wang B, Malik R, Nigg EA and Korner R. Evaluation of the low-specificity protease elastase for large-scale phosphoproteome analysis, *Anal Chem*, 2008, 80:9526-9533

- Xin B, Puffenberger EG, Turben S, Tan H, Zhou A and Wang H. Homozygous frameshift mutation in TMCO1 causes a syndrome with craniofacial dysmorphism, skeletal anomalies, and mental retardation. *Proc Natl Acad Sci U S A*, 2010, 107(1):258-263
- Yachie N, Saito R, Sugahara J, Tomita M and Ishihama Y. In silico analysis of phosphoproteome data suggests a rich-get-richer process of phosphosite accumulation over evolution. *Mol Cell Proteomics*, 2009, 8(5):1061-1071
- Yu MJ, Miller RL, Uawithya P, Rinschen MM, Khositseth S, Braucht DW, Chou CL, Pisitkun T, Nelson RD and Knepper MA. Systems-level analysis of cell-specific AQP2 gene expression in renal collecting duct. *Proc Natl Acad Sci U S A*, 2009, 106(7):2441-2446
- Zhang Z, Mo D, Cong P, He Z, Ling F, Li A, Niu Y, Zhao X, Zhou C and Chen Y. Molecular cloning, expression patterns and subcellular localization of porcine TMCO1 gene. *Mol Biol Rep*, 2009, 37(3):1611-1618

CHAPTER II

HUMAN PROSTATE CANCER CELL APOPTOSIS INDUCED BY

INTERFERON- γ AND DOUBLE-STRANDED RNA

2.1 Abstract

Interferons (IFNs) are a family of pleiotropic cytokines responsible for inducing innate and adaptive immunities against a wide-range of viruses and other microbial pathogens. IFNs also exert antitumor activities due to their anti-proliferative, immunomodulatory, and proapoptotic functions. In recent years, studies have revealed that a combination of IFNs with cytotoxic compounds, such as paclitaxel and thalidomide, augments the cytotoxicity for prostate cancer cells in an additive manner. Here we report that pretreatment of PC3 cells, a human prostate adenocarcinoma cell line, with IFNs sensitized these cells to dsRNAs-induced apoptosis. The enhancement effect of IFN treatment was dependent on IFN subtypes, particularly IFN- γ . In comparison with IFN- α or β , IFN- γ treatment remarkably augmented dsRNA-induced apoptosis in PC3 cells,

and by using mutant cell lines, we demonstrated that IFN-signaling is necessary for these effects. The silencing of dsRNA-dependent protein kinase R (PKR) and RNase L by siRNA did not have any significant impact on this event, suggesting that neither RNase L nor PKR is involved in this event. Further investigation of the apoptotic pathway revealed that Bak, a pro-apoptotic member of the Bcl-2 family, was up-regulated by IFN- γ and dsRNA. Our findings may lead to the design of novel therapeutic strategies for prostate cancer.

2.2 Introduction

Although prostate specific antigen (PSA) screening and digital rectal examination have been used widely for the early detection of prostate cancer, which bring a dramatic decrease in the mortality rate from prostate cancer, there are still a certain amount of patients who undergo disease progression after receiving primary treatment [Strief, *et al.*, 2007; Pienta, 2009; Bantis and Vasiliou, 2009; Bickers and Aukim-Hastie, 2009; Damber and Aus, 2008]. The choices of treatment for patients who are diagnosed with metastatic diseases are limited. The first line treatment for men with metastatic advanced prostate cancer is androgen ablation therapy using either luteinizing hormone releasing hormone (LRHR) agonists or surgical castration. Despite the early efficacy of hormone ablation therapy, the success of it is short-lived; almost all cases progress to an androgen insensitive state called hormone-refractory prostate cancer (HRPC) [Priolo, *et al.*, 2009]. Currently there is no cure for the disease at this stage.

The molecular biological characteristics of prostate cancer have been studied intensively, and many small-molecule inhibitors and recombinant humanized monoclonal antibodies have been tested in the preclinical setting. Although promising results have been achieved, many of them have not yielded clearly favorable results. Cytotoxic chemotherapy was thought to be the best choice in this situation, and recent studies have shown that docetaxel, a semi-synthetic analog of paclitaxel, can achieve a remarkable improvement on the survival of HRPC patients by inducing mitotic catastrophe and caspase-2 and -3-dependent apoptosis followed by freezing the entire microtubule network [Mediavilla-Varela, *et al.*, 2009; Fabbri, *et al.*, 2008]. Docetaxel has thus become the standard treatment for metastatic HRPC; however, lack of a response and development of resistance to docetaxel in a considerable number of patients limit its applications in prostate cancer therapy. Although the actions of other antitumor drugs in hormone-resistant prostate cancer were tested and examined, the efficacy of current therapy for hormone-refractory prostate cancer is still unsatisfactory [Fabbri, *et al.*, 2010]. Therefore, development and discovery of new drugs capable of prolonging survival have become an urgent clinical need.

IFNs are a family of cytokines expressed in eukaryotic cells as an early response to various stimuli, such as viruses, bacteria, parasites, double-stranded RNA, and immune inducers [Stark, *et al.*, 1998]. The use of IFNs in the treatment of cancer has been studied extensively, and during the recent decades the quantity of survivals and quality of lives for many cancer patients have been improved dramatically by IFN treatments [Damasio, *et al.*, 2000]. By reviewing

literature, a potent synthetic dsRNA IFN inducer, poly I:C, was found to be active against a number of transplanted tumors which can also inhibit the growth of a variety of human tumor cells in culture [Bart and Kopf, 1969; Zeleznick and Bhuyan, 1969; Lin, *et al.*, 1982; Hubbel, *et al.*, 1984]. However, there are few studies concerning the exact mechanism of how these effects are accomplished, and the effect of IFNs and dsRNA on prostate cancer cell apoptosis has not been reported. In the present study, we found that the pretreatment of PC3 cells with IFN- γ sensitized these cells to small amounts of dsRNA-induced apoptosis. Further, we demonstrated that IFN-signaling is necessary for these effects and Bak, a pro-apoptotic member of the Bcl-2 family, was up-regulated by IFN- γ /dsRNA. Our findings may be beneficial in the design of novel therapeutic strategies for prostate cancer.

2.3 Materials and methods

Reagents and antibodies

Poly I:C was from Sigma (St. Louis, MO). IFN α , IFN- β and IFN- γ were from R & D Systems (Minneapolis, MN). Antibodies to Bax, Bak, Bim, Caspase 3 and PKR were from Santa Cruz Biotechnology, Inc (Santa Cruz, CA). Anti- β -actin antibody was purchased from Chemicon (Temecula, CA).

Cell culture and treatments

PC3 cells, a human prostate cancer cell line (ATCC, Manassas, VA), were grown in RPMI-1640 medium (Media Lab of the Central Cell Service, Cleveland Clinic, Cleveland, OH) supplemented with streptomycin (100 μ g/mL), penicillin (100units/mL) and 10% cosmic calf serum (Hyclone, Logan, UT) in a humidified atmosphere of 5% CO₂ at 37 °C. Cells were grown to 90% confluence and incubated with 1000units/mL of IFN α , IFN- β or IFN- γ respectively for 18 h followed by transfection with or without 2 μ g/mL of poly I:C using lipofectomine (Invitrogen, Carlsbad, CA). Culture medium was added at 1 h after transfection. The effects of IFNs and dsRNA on the cell growth were also examined on DU145 cells, another prostate cancer cell line (ATCC, Manassas, VA).

Cell viability assay

Three days after treatments, the medium color of the cultured cells was recorded and the trypan blue dye exclusion assay was used to count viable cells. This assay is based on the principle that live cells possess intact cell membranes that exclude certain dyes, such as trypan blue, eosin, or propidium, whereas dead cells do not. In this test, a cell suspension is simply mixed with dye and then visually examined to determine whether cells take up or exclude dye. Cells were visualized under Olympus CKX31 at 100X magnification.

Annexin V assay

To determine whether the inhibiting effect of IFN- γ /dsRNA on PC3 cells' growth resulted from apoptosis, an Annexin V assay was performed. Phosphatidylserine (PS) is a type of phospholipid (Figure 2.3.1). Under normal conditions, PS is situated in the inner leaflet of the cell membrane, but at the early stage of apoptosis, PS is translocated to the outer leaflet of the cell membrane due to the loss of membrane asymmetry. Anenexin-V conjugated with flurochromes has very high affinity to PS, so the amount of cells undergoing early stage apoptosis can be quantified by measuring the florescence signals using flow cytometry. At the same time, the cells are stained with propidium iodine (PI) which is another kind of flurochrome. In the late stage of apoptosis the cell membrane is disintegrated, allowing PI to enter the cells and bind to the DNA. Thus, the cells undergoing later stage apoptosis can be evaluated by PI signals. Shown on the right part of Figure 2.3.1 is a typical Annexin-v assay result. The x-axis represents the number of cells undergoing early stage apoptosis and the y-axis represents the amount of cells undergoing later stages of apoptosis. The signals in the right upper area indicate the total amount of cells that undergo apoptosis.

In this study, Annexin V assay was performed using an Annexin V-FITC/propidium iodine apoptosis detection kit (BD Biosciences, San Jose, CA). Briefly, PC3 cells treated as described previously were collected and centrifuged at 2,000Xg for 5 min at 4°C. Then cells were washed with ice cold PBS and resuspended in 1X binding buffer provided by the manufacturer. FITC Annexin-V

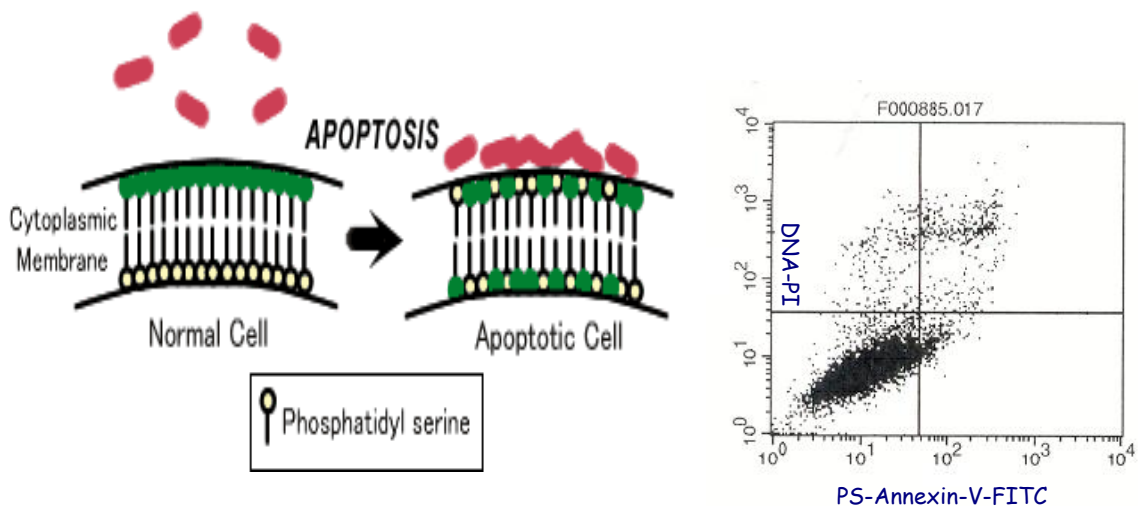


Figure 2.3.1 Principle of the Annexin-V assay

(http://www.biocat.com/bc/img/info_pix/PSAnnexin.gif) Phosphatidylserine

(PS) is a type of phospholipid. At the early stage of apoptosis, PS is retranslocated to the outer leaflet from the inner leaflet of the cell membrane and bound to Annexin-V, which is conjugated with fluorochromes. Apoptotic cells are sorted by the fluorescence signals using flow cytometry. Propidium iodide (PI), which is another type of fluorochrome, is able to penetrate the disintegrated cell membrane of apoptotic cells to bind to the DNA. Thus, the cells undergoing later stage apoptosis can be evaluated by PI staining.

(5 μ L) and propidium iodide (5 μ L) were added to cell suspension containing 1×10^5 cells for each assay. After incubation for 15 min in the dark at room temperature, 400 μ L of 1X binding buffer was added to the cell suspension and cells were analyzed by two-color cytometry using a FACScanTM (Becton Dickinson, Franklin Lake, NJ).

Determination of DNA fragmentation

DNA fragmentation represents a characteristic hallmark of apoptosis and the DNA fragmentation assay is another typical method used for evaluating cell apoptosis. During apoptosis, endonuclease is activated and subsequently degrades the DNA molecules in the region between the nucleosomes so that the consequent DNA fragments are essentially multiples of 200-base-pair lengths.

In this study, DNA in the IFNs/dsRNA treated cells was isolated using an apoptotic DNA ladder kit (Roche, South San Francisco, CA). Briefly, 200 μ L of cell suspensions in PBS was mixed with 200 μ L binding buffer (Roche, South San Francisco, CA). After incubation for 10 min at room temperature, 100 μ L of isopropanol (Mallinckrodt Baker, Phillipsburg, NJ) was added to the samples, followed by vortexing. DNA was then purified using glass fibers. DNA samples with ethidium bromide staining were separated on 2% agarose gel and visualized under UV light.

TUNEL assay

To further confirm whether IFN- γ combined with dsRNA induces PC3 cell apoptosis, we performed a terminal deoxynucleotidyl transferase dUTP nick end labeling (TUNEL) assay. Shown on Figure 2.3.2 is the working principle of a TUNEL assay. Basically terminal deoxynucleotidyl transferase (TdT) is used to transfer deoxyuridine triphosphates (dUTP) conjugated with a fluorochrome to these strand breaks of cleaved DNA and the total amount of strand breaks in the cleaved DNA is evaluated with fluorochrome, such as FITC, by flow cytometry.

The TUNEL assay was performed using an APO-BRDU kit (BD Biosciences, San Jose, CA). Briefly, IFNs/dsRNA treated PC3 cells were scraped, collected and fixed in 1% paraformaldehyde for 45 min followed by washing with PBS twice. Then cells were stored in 70% ethanol at -20°C until staining and analysis. DNA fragmentation was examined by incorporating Brdu and staining with a FITC-labeled anti-BrdU mAb. The total DNA breaks were determined with FITC and the labeled cells were sorted by flow cytometry in a FACS.

Caspase activity assay

Caspase 3 belongs to a family of cysteine proteases (caspases) that cleave proteins at aspartate residues [Strasser, *et al.*, 2000]. Caspase 3 is the executioner of cell death in the cell apoptotic pathway and it is worthwhile to examine the activity of caspase 3 to evaluate cell apoptosis. The activity of caspase 3 in the cells treated with IFN- γ and /or dsRNA was examined using CaspACE™ Assay system (Promega, Madison, WI) as instructed by

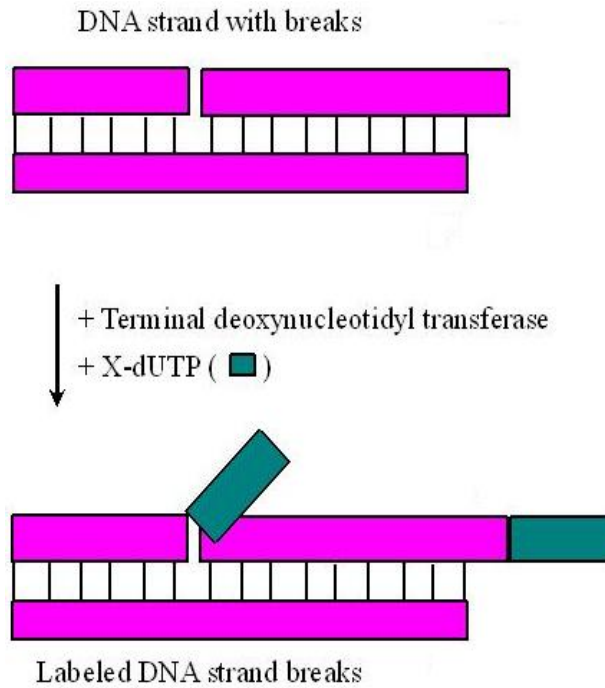


Figure 2.3.2 Working principle of TUNEL assay

(http://www.biocompare.com/images/bc/006/ArticleImages/RocheApplied_InSituCellDeathDetectionKit_slide030_img.jpg)

Terminal deoxynucleotidyl transferase (TdT) is used to transfer deoxyuridine triphosphates (dUTP) conjugated with a fluorochrome to these strand breaks of cleaved DNA and the total amount of strand breaks in the cleaved DNA is evaluated with fluorochrome, such as FITC, by flow cytometry.

manufacturer. This assay is based on caspase cleavage of chromophore p-nitroaniline (pNA) substrate linked with the tetrapeptide DEVD. Free pNA produces a yellow color that is monitored by spectrophotometer at 405 nm. In brief, cells were treated as described above and cytosolic extracts were prepared by cell lysis buffer provided by the manufacturer. After centrifugation at 15,000Xg for 20 min at 4 °C, cell extract containing 50 µg of proteins were transferred into a 96-well plate to mix with the CaspACE™ assay reagent. After incubation for 4 h at 37 °C, caspase activity was determined by absorbance at 405 nm using a LD400 AD/LD analysis spectrometer (Beckman Coulter, Brea, CA).

Western blot analysis

The expressions of several proteins in the apoptotic pathway were examined by western blot analysis. PC3 cells were harvested after being treated with IFNs and/or dsRNA. Cytoplasmic extracts were prepared by suspension of cell pellets in NP-40 lysis buffer [Zhou, *et al.*, 2005]. After centrifugation in a microcentrifuge at 4°C for 10 min, the supernatant was removed and stored at -80°C. Cellular extracts were fractionated on SDS-10% polyacrylamide gels and transferred to polyvinylidene difluoride membranes (Millipore, Billerica, MA). The membranes were blocked with 5% non-fat milk in PBS containing 0.02% sodium azide and 0.2% (v/v) Tween 20 and incubated with different primary antibodies overnight at 4°C. The membranes were then washed with PBS containing 0.2% (v/v) Tween 20 and incubated with corresponding secondary antibodies conjugated with HRP

(Cell Signaling Technology, Boston, MA) for 1 h at room temperature. After washing, these proteins were detected by a chemiluminescence method, according to the manufacturer's specification (Amersham, Piscataway, NJ).

Inhibition of the expression of dsRNA-dependent protein kinase R (PKR) in PC3 cells by small interference RNA (siRNA)

PC3 cells were transfected with a heterogeneous mixture of 21-23 bp PKR siRNA (New England Biolab, Ipswich, MA) using the transpass R2 transfection reagent (New England Biolab, Ipswich, MA) according to the manufacturer's instructions. Briefly, PC3 cells were grown to 50% confluence. PKR siRNA was incubated with the transfection reagent in serum-free medium for 20 min at room temperature. Subsequently, the mixture was evenly dispersed on the cells that had been washed with serum-free medium once. The final concentration of siRNAs was 12.5 nM. After being incubated for 3 h, the complete culture medium was added to the cells. At 30 h after transfection the cells were treated with IFNs and dsRNA as described previously. The apoptotic effects of these treatments on the PKR siRNA transfected PC3 cells were analyzed. Meanwhile, part of the transfected cells were lysed and western blotting analysis was performed to determine the expression of PKR in PC3 cells.

Inhibition of the expression of RNase L in PC3 cells by small interference RNA (siRNA)

A pool of 3 target-specific 20-25 nt RNase L siRNA designed to knock down the RNase L gene expression was purchased from Santa Cruz Biotechnology, Inc. (Santa Cruz, CA). PC3 cells were transfected with RNase L siRNA to knock down the expression of RNase L in PC3 cells using the Lipofectamine 2000 transfection reagent (Invitrogen, Carlsbad, CA) according to the manufacturer's instruction. Briefly, before transfection, PC3 cells were cultured with antibiotic-free medium in 60-mm plates overnight and the cells were ready for transfection when the cell confluence was around 50%. Ten μL of lipofectamine 2000 was added to 300 μL of serum free medium. After being incubated for 5 min at room temperature, another 300 μL serum free medium containing 8.3 μL of RNase L siRNAs was added to this mixture and incubated for 20 min at room temperature. Then the mixture was dispersed evenly to cells. The final concentration of RNase L siRNA was 26 nM. After 4 h, the medium was replaced with complete culture medium. At 30 h after transfection, part of the RNase L siRNA transfected cells were collected and pelleted for western blot assay to examine whether the expression of RNase L was knocked down and part of the RNase L siRNA transfected cells were treated with IFNs and/or dsRNA as indicated previously.

2.4 Results

IFN- γ and dsRNA synergistically decrease PC3 cells viability

The cytotoxicity of IFNs has limited its clinical application in the treatment of cancers; thus the combinations of IFNs with other cytotoxic agents have recently been the new direction for the use of IFNs in cancer treatments. To determine the direct effect of IFNs and dsRNA on prostate cancer cells, we treated the PC3 cells with IFNs and poly I:C. Three days after treatment, the medium color of the cells treated with IFN- γ /dsRNA remained pink while medium color of cells treated in other ways became yellow (Figure 2.4.1). When cells grow well, the medium color will change from pink to yellow due to a change in pH as a result of cell waste products; therefore the pink medium in the IFN- γ /dsRNA treated well indicated that most cells in this well were dead. Cell viability was analyzed by trypan blue exclusion assay; all treated cells exhibited a decrease in their viability, but IFN- γ /dsRNA showed a notably stronger ability to suppress PC3 cell growth when compared with other types of treatment as shown in Figure 2.4.2. Similar results were visualized under Olympus CKX31 at 100X magnification (Figure 2.4.3). To rule out the bias caused by prostate cancer cell lines, we conducted the same experiment on DU145 cells, another prostate carcinoma cell line, and similar results were obtained. Most of the IFN- γ /dsRNA treated DU145 cells died, while the cells treated in other ways showed normal morphology (Figure 2.4.4).

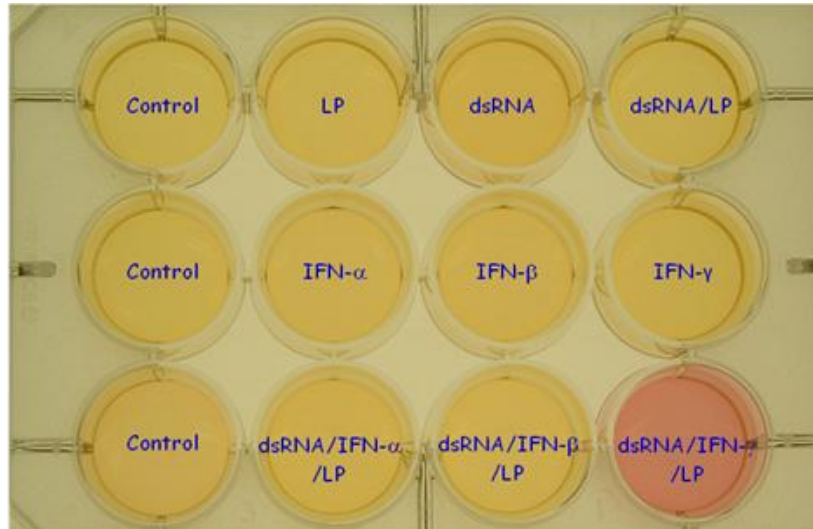


Figure 2.4.1 IFN- γ and dsRNA synergistically decrease PC3 cell viability.

PC3 cells were treated with 1,000 units/mL of IFN α , β or γ overnight, and then transfected with or without 2 μ g/mL of dsRNA using the lipofectomine reagent.

The picture was taken on day 3 of the post treatment.

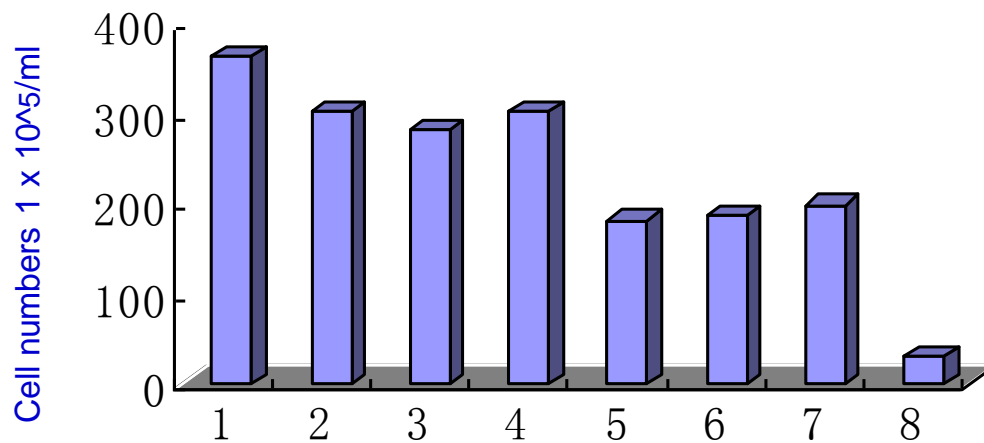


Figure 2.4.2 Growth of PC3 cells are inhibited significantly by the IFN- γ /dsRNA treatment. PC3 cells were treated with 1,000 units/mL of IFN α , β or γ overnight, and then transfected with or without 2 μ g/mL of dsRNA using lipofectomine. After 48 h, the cells' viability was analyzed by a trypan blue exclusion assay. 1, Control; 2, dsRNA alone; 3, IFN- α ; 4, IFN- β ; 5, IFN- γ ; 6, IFN- α /dsRNA; 7, IFN- β /dsRNA; 8. IFN- γ /dsRNA

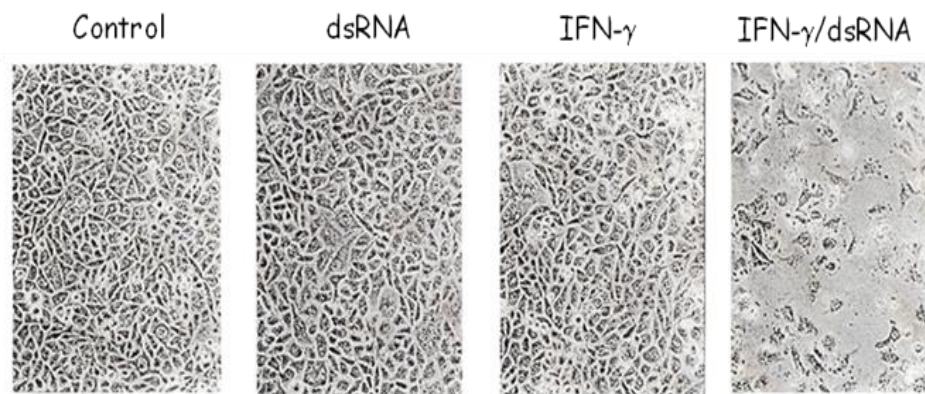


Figure 2.4.3 Morphology of PC3 cells treated with IFN- γ /dsRNA PC3 cells were treated with 1,000 units/mL of IFN α , β or γ overnight, and then transfected with or without 2 μ g/mL of dsRNA using lipofectomine. After 3 days, cells were visualized under Olympus CKX31 at 100 x magnification.

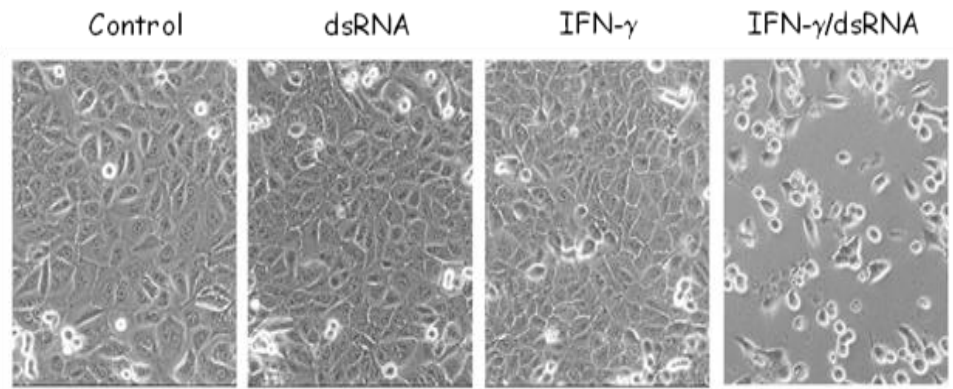


Figure 2.4.4 IFN- γ and dsRNA synergistically inhibit the growth of DU145 cells. DU145 cells were treated with 1,000 units/mL of IFN α , β or γ overnight, and then transfected with or without 2 μ g/mL of dsRNA using lipofectomine. After 3 days, cells were visualized under Olympus CKX31 at 100 x magnification.

IFN- γ /dsRNA induce apoptosis in PC3 cells

To determine whether the decreased PC3 cell viability was actually a result of IFN- γ /dsRNA-induced apoptosis, the translocation of membrane phospholipids phosphatidylserine (PS) from the inner to the outer leaflet of the plasma membrane was examined as an early event of cell apoptosis. Annexin V is a 35-36kD Ca²⁺ dependent, phospholipids-binding protein that has a high affinity for PS. Therefore, FITC-conjugated Annexin V is commonly used to identify apoptotic cells at an early stage. The Annexin-FITC staining showed that 21.4% of PC3 cells were positively labeled with Annexin V after being treated with IFN- γ /dsRNA, while 4.45% of cells were labeled when cells were treated with dsRNA only and in IFN- α /dsRNA- and IFN- β /dsRNA-treated wells there were 6.58% and 6.31% of cells labeled respectively. These results indicated that the combination of IFN- γ and dsRNA is a potent inducer of PC3 cell apoptosis (Figure 2.4.5). To further confirm that IFN- γ combined with dsRNA can induce PC3 cell apoptosis, we performed a TUNEL assay. In TUNEL assay, terminal deoxynucleotidyl transferase (TdT) is used to transfer Br-dUTP to the strand breaks of cleaved DNA. The total amount of strand breaks in the cleaved DNA was evaluated with Anti-Brdu antibody conjugated with FITC. As shown on Figure 2.4.6, the combination of IFN- γ and dsRNA induced 4 times more cells undergoing apoptosis than IFN- γ - or dsRNA-treatment did. We next evaluated apoptosis by DNA fragmentation assay. During apoptosis, endonuclease is activated and cuts the DNA molecules in the region between the nucleosomes and then the consequent DNA fragments are essentially multiples of 200-base-pair lengths. In

this experiment, only the IFN γ /dsRNA treated lane showed DNA fragments, suggesting that only IFN γ /dsRNA induced PC3 cell apoptosis (Figure 2.4.7).

IFN- γ /dsRNA activate caspase 3

To further characterize the IFN γ /dsRNA induced apoptosis in prostate cancer cells, we determined the activity of caspase 3 in IFN- γ and/or dsRNA treated PC3 cells. The activity of caspase 3 in the cells treated with IFN- γ and/or dsRNA was examined by CaspACETM Assay system (Promega, Madison, WI). IFN- γ /dsRNA induced the activity of caspase 3 in PC3 cells by 2.8-fold while IFN- γ or dsRNA increased the caspase 3 activity by 1.1- and 1.7-fold respectively (see figure 2.4.8).

IFN- γ /dsRNA enhance the expression of Bak

Apparently, IFN- γ combined with dsRNA was able to effectively induce PC3 cell apoptosis; the next question is what the molecular mechanism is by which IFN- γ /dsRNA activate the apoptotic pathway. In mammalian cells, there are two major apoptotic pathways, termed “extrinsic” and “intrinsic” [Elmore, 2007]. The extrinsic pathway, also termed as the Death Receptor Pathway, is activated by the binding of a “death” ligand to its receptor. Subsequently the adapter proteins FADD and caspase 8 are recruited to the intracellular portion of the receptor, resulting in the activation of caspase 8 and caspase 3--the executioner of cell apoptosis. Cellular stress initiates the intrinsic apoptotic pathway, also termed as the Mitochondrial Pathway, and involves the upregulation of BH3-only proteins

such as Bim, PUMA, and Bad. These proteins inhibit the activity of the anti-apoptotic Bcl-2 proteins, resulting in Bax dimerization and translocation to the mitochondria, subsequently triggering the release of cytochrome C. Then Cytochrome C combined with APAF-1 and caspase 9 forms apoptosome and further promotes caspase 3 cleavage and activation, leading to apoptosis (see Figure 2.4.9). To test how IFN- γ and dsRNA affect the apoptotic signaling pathways, several members of this pathway were examined using western blot analysis. Bak, a pro-apoptotic member of the Bcl-2 family, was upregulated by IFN- γ /dsRNA (see Figure 2.4.10). The full length of caspase 3 was significantly decreased in IFN- γ /dsRNA treated cells, suggesting that caspase 3 was cleaved and activated to trigger cell apoptosis. However, there was no significant difference in the expression of Bax, Bim and caspase 8 among different treatments.

JAK/SATA pathway is involved in IFN- γ /dsRNA induced PC3 cell apoptosis

It is believed that IFNs execute most of their functions through IFN's Jak-stat signaling pathway [Borden, *et al.*, 2007]. To examine the role of Jak-stat pathway in the IFN- γ /dsRNA-induced prostate cancer cell apoptosis, we determined two mutant cell lines: U3A and LNcap cells. The U3A cell is a stat1 null human fibrosarcoma cell line and the 2FTGH cell is its parental cell line, while the LNcap cell is a prostate cancer cell line with Jak1 deficiency. In these experiments, U3A and LNcap cells were treated as previously described and the cell viability was

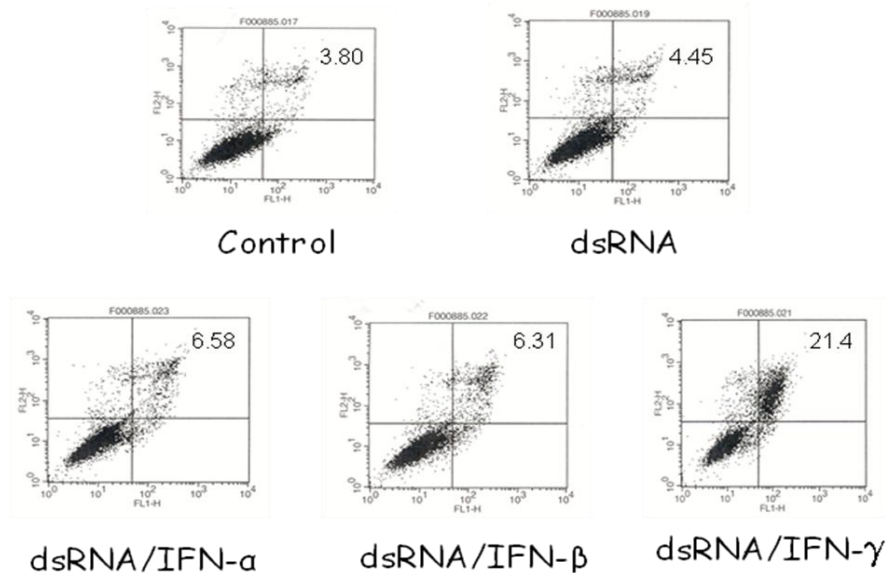


Figure 2.4.5 Determination of PC3 cell apoptosis by Annexin-V analysis
 PC3 cells were pretreated with 1,000 units/mL of IFN α , β or γ overnight and then treated with 2 μ g/mL of dsRNA and subjected to Anexin-V assay by flow cytometry after 20 h incubation.

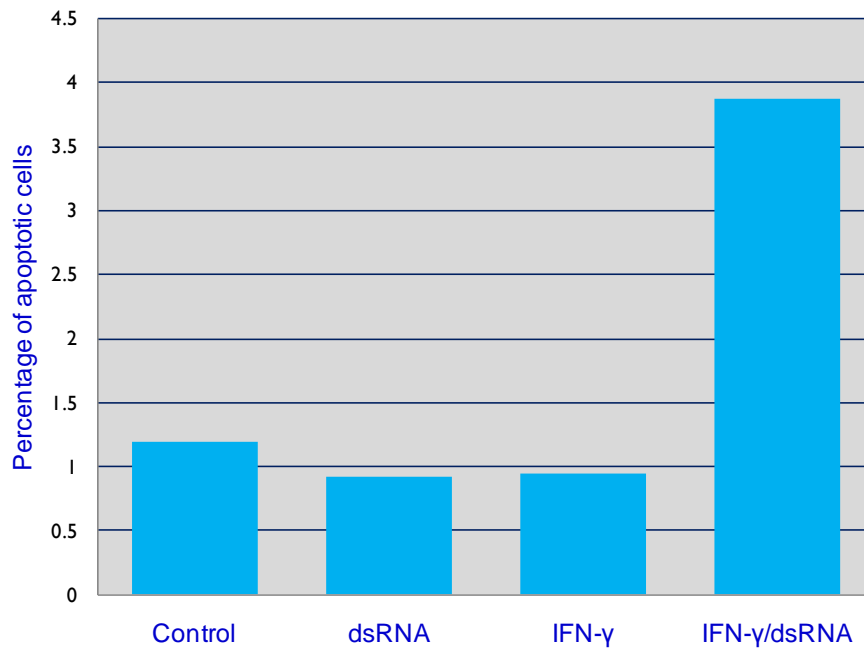


Figure 2.4.6 Determination of PC3 cell apoptosis by TUNEL assay PC3 cells were pretreated with 1,000 units/mL of IFN α , β or γ overnight and treated with 2 μ g/mL dsRNA. After 20 h, the cells were scraped, collected and fixed in 1% paraformaldehyde for 45 min, followed by washing with PBS twice. Then cells were stored in 70% ethanol at -20°C until staining and analysis. DNA fragmentation was examined by incorporating Brdu and staining with a FITC-labeled anti-BrdU mAb. The total DNA breaks were determined with FITC and the labeled cells were sorted by flow cytometry.

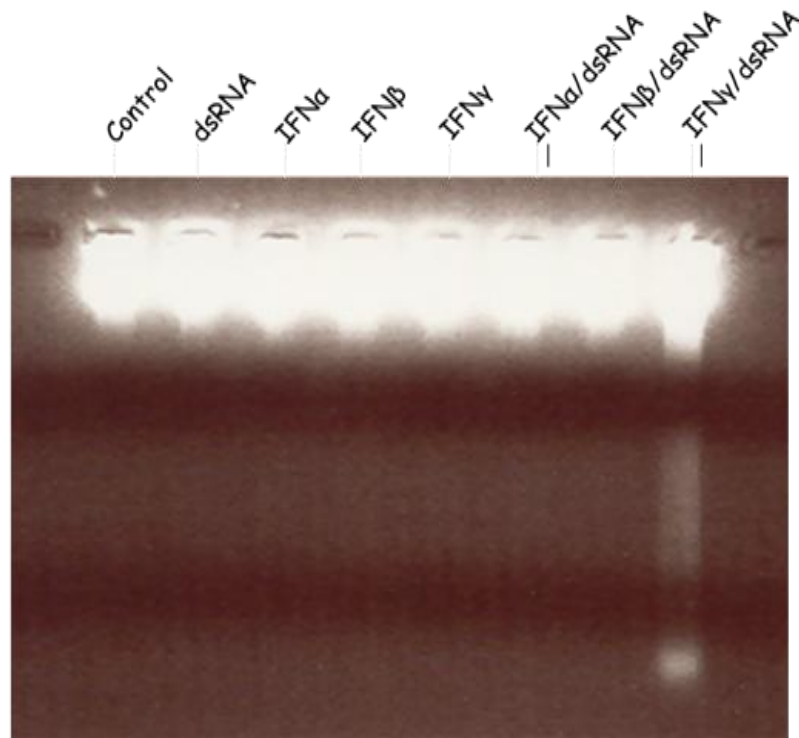


Figure 2.4.7 IFN- γ and dsRNA induce DNA fragmentation in PC3 cells DNA in the IFNs/dsRNA treated cells was isolated using an apoptotic DNA ladder kit (Roche, South San Francisco, CA), separated by agarose gel, stained with ethidium bromide and visualized under UV light.

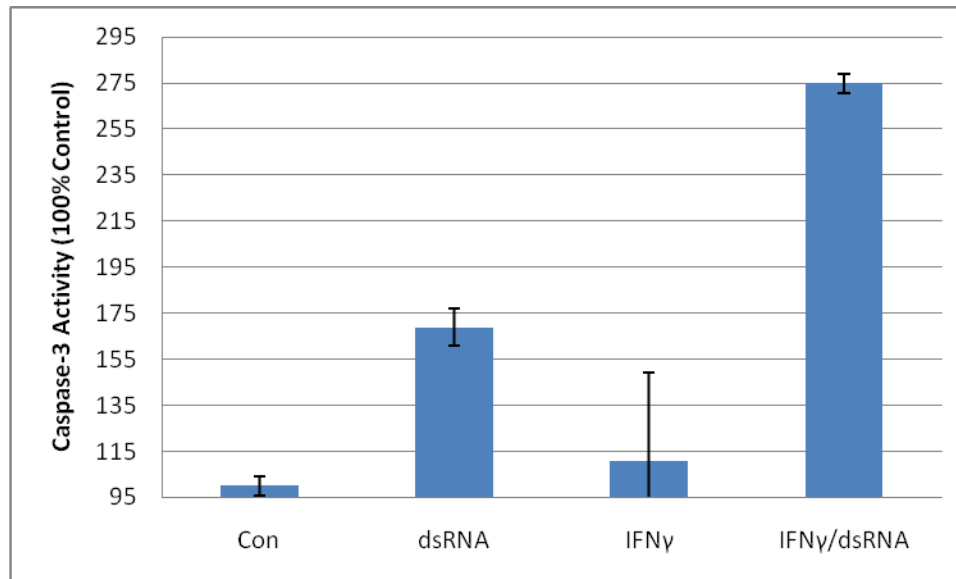


Figure 2.4.8 Caspase 3 activity assay The activity of caspase 3 in PC3 cells treated with IFN- γ and /or dsRNA for 10 h was examined using CaspACETM Assay system. Briefly, the treated cells were lysed and the cell extract containing 50 μ g of proteins was transferred into a 96-well plate to mix with the CaspACETM assay reagent. After incubation for 4 h at 37 $^{\circ}$ C, caspase activity was determined by absorbance at 405 nm using a LD400 AD/LD analysis spectrometer.

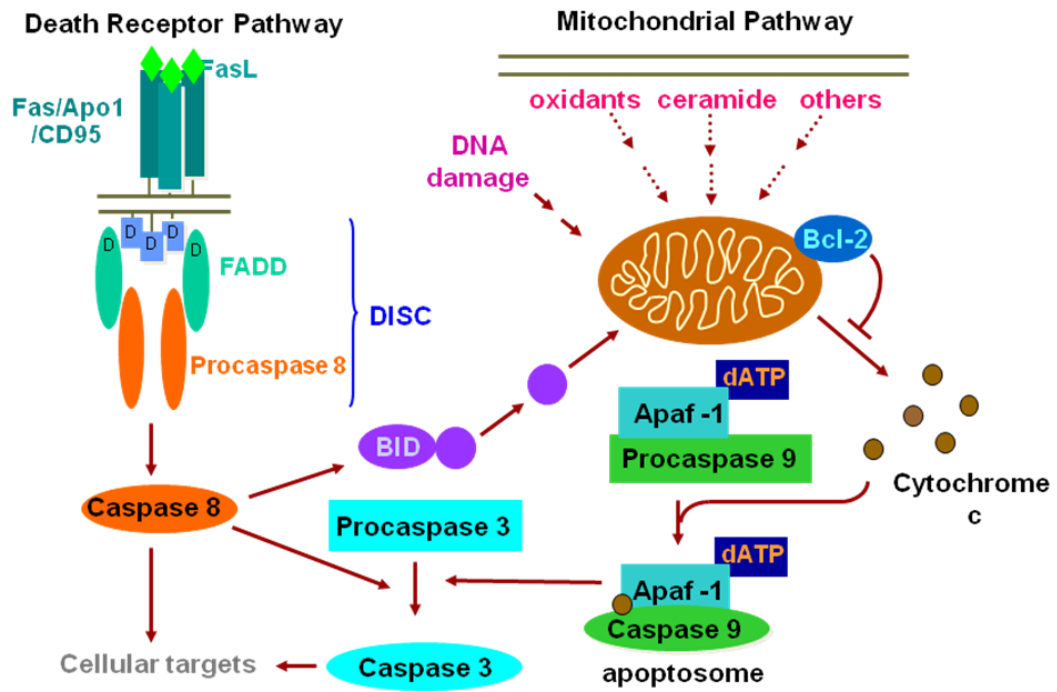


Figure 2.4.9 A scheme of major apoptotic pathways in mammalian cells
 (www.healthcare.uiowa.edu/research/sfrbm/papers/.../Tome-Apoptosis.ppt)

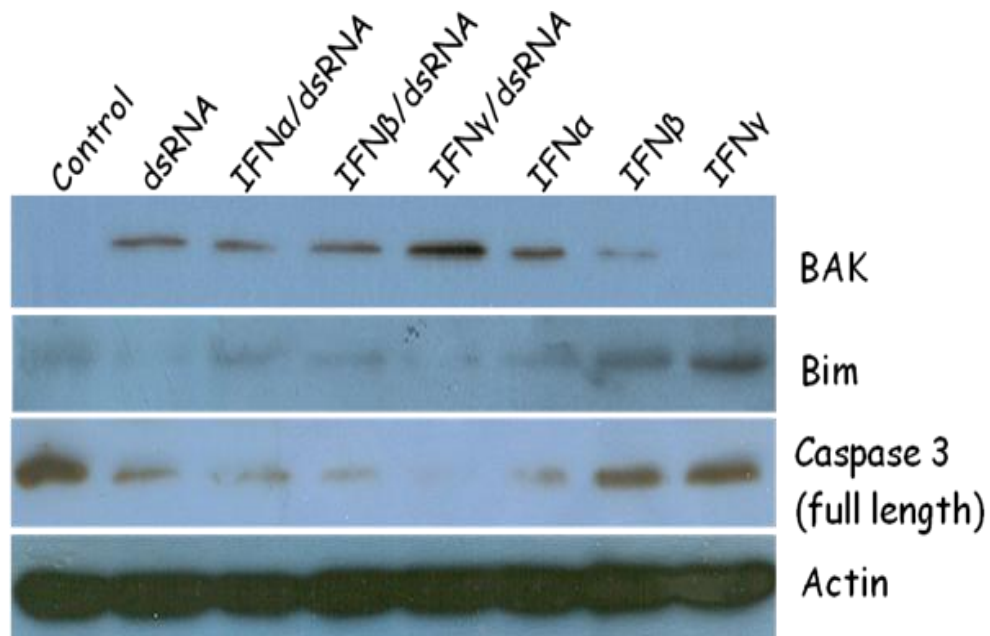


Figure 2.4.10 Effect of IFN- γ and dsRNA on the expression of apoptotic proteins PC3 cells were harvested after being treated with IFNs and/or dsRNA for 20 h. Cellular extracts were fractionated on 10% SDS-PAGE and transferred to PVDF membrane. The membranes were blocked with 5% no fat milk in PBS containing 0.02% sodium azide and 0.2% (v/v) Tween 20 and incubated with different primary antibodies overnight at 4°C. The membranes were then washed with PBS containing 0.2% (v/v) Tween 20 and incubated with corresponding secondary antibodies conjugated with HRP for 1 h at room temperature. After washing, these proteins were detected by a chemiluminescence method.

examined by trypan blue exclusion assay. As expected, both U3A and LNCap cells were not responded to the IFN- γ /dsRNA treatment (Figure 2.4.11, Figure 2.4.12, and Figure 2.4.13), suggesting that the Jak-stat signaling pathway is necessary for the IFN- γ /dsRNA-induced prostate cancer cell apoptosis.

PKR is not involved in the IFN- γ /dsRNA induced PC3 cell apoptosis

As mentioned previously, IFNs, in most cases, induce apoptosis through stimulating the expression of certain IFN-stimulated genes (ISGs). Here we checked the role of several ISGs in the IFN- γ /dsRNA-induced apoptosis. PKR is a proapoptotic protein. As shown in Figure 2.4.14 [Samuel, 2001], after being induced by IFNs, PKR is activated by dsRNA, commonly from viral infection (ssRNA forms some dsRNA segments in its secondary structure). The activated PKR phosphorylates the eukaryotic initiation factor 2 α and subsequently inhibits mRNA translation. As a result, viral replication and cell proliferation are inhibited. Previous studies have demonstrated that PKR can mediate cell apoptosis in various cell types [Jagus, *et al.*, 1999]. To test whether PKR is involved in IFN- γ /dsRNA-induced PC3 cell apoptosis, the expression of PKR in PC3 cells was knocked down by PKR siRNA, and then the cells were treated with IFNs/dsRNA as previously described. The results showed that IFN- γ combined with dsRNA had similar effects on the PKR knockdown PC3 cells as on normal PC3 cells (Figure 2.4.15). The expressing level of PKR in PC3 cells is very low and PKR does not respond to IFN- γ induction either. To prove that PKR siRNA can knock down the expression of PKR effectively, the siRNA trasfected cells were treated

with 1000 unites/mL of IFN- α and then western blot analysis was conducted to examine PKR protein expression. As shown in Figure 2.4.16, PKR siRNA effectively knocked down the expression of PKR in the cells. Thus, these results ruled out the involvement of PKR in IFN- γ /dsRNA-induced apoptosis in PC3 cells.

RNase L is not involved in the IFN- γ /dsRNA induced PC3 cell apoptosis

RNase L is another dsRNA related ISG. It is one of the key enzymes for the IFN's function against cell proliferation and viral infection. In this system, IFNs induce the expression of oligoadenylate synthetase (OAS), whose activity is regulated by dsRNA. OAS catalyzes the synthesis of oligoadenylates of the general structure pp(A₂'p)_n, commonly abbreviated as 2-5 A. As a latent endoribonuclease, RNase L is activated by the binding of 2-5A and leads to the degradation of viral and cellular RNA. As a result, viral replication is inhibited and cells undergo apoptosis (Figure 2.4.17) [Samuel, 2001]. To test whether RNase L contributes to IFN- γ /dsRNA induced PC3 cell apoptosis, the expression of RNase L in PC3 cells was knocked down by RNase L siRNA (Figure 2.4.18) and then the cells were treated as previously described. Our results showed that although the expression of RNase L was knocked down by RNase L siRNA, PC3 cells were still sensitive to the treatment of IFN- γ /dsRNA (Figure 2.4.19). The expression of RNase L in PC3 cells treated with different IFNs and/or dsRNA was also examined by a western blot assay (Figure 2.4.20). These results showed that IFN- γ /dsRNA treatment did not induce a significant difference in the expression of RNase L.

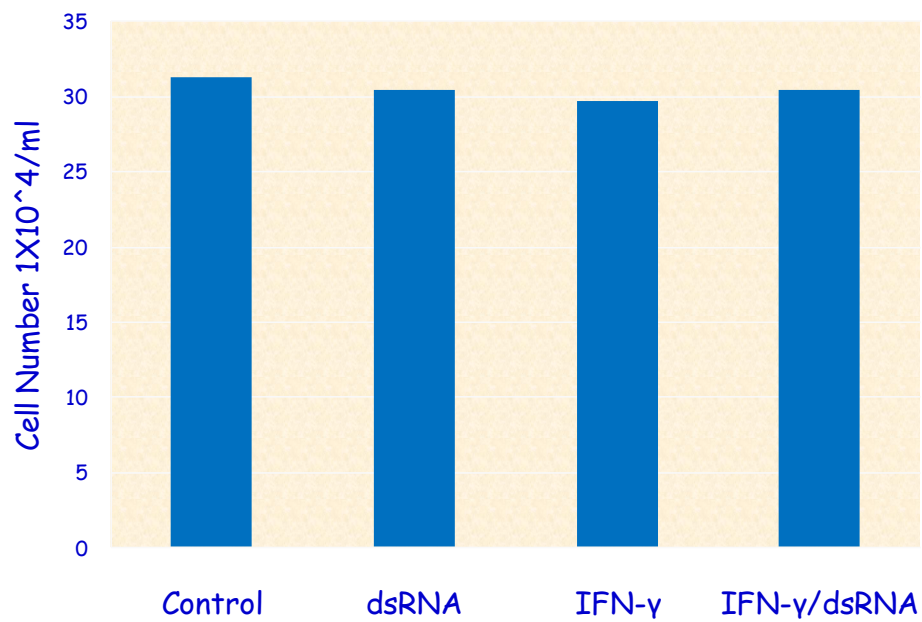


Figure 2.4.11 Effect of IFN-γ/dsRNA on the viability of LNCap cells LNCap cells were treated with IFN-γ and/or dsRNA for 72 h and the viability of the treated cells was analyzed by a trypan blue exclusion assay.

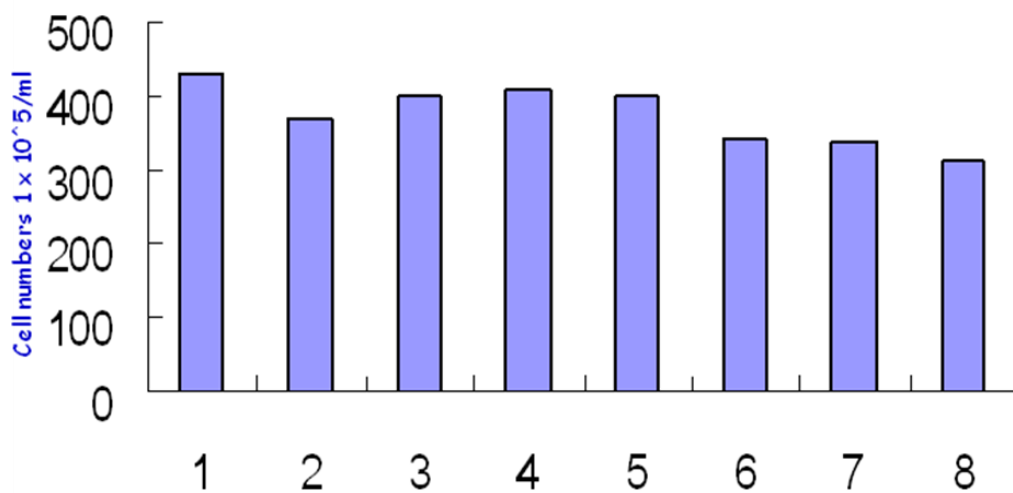


Figure 2.4.12 Effect of IFN- γ /dsRNA on the viability of U3A cells U3A cells were treated with IFNs and/or dsRNA. The viability of the treated cells was analyzed by a trypan blue exclusion assay. 1, Control; 2, dsRNA alone; 3, IFN- α ; 4, IFN- β ; 5, IFN- γ ; 6, IFN- α /dsRNA; 7, IFN- β /dsRNA; 8. IFN- γ /dsRNA

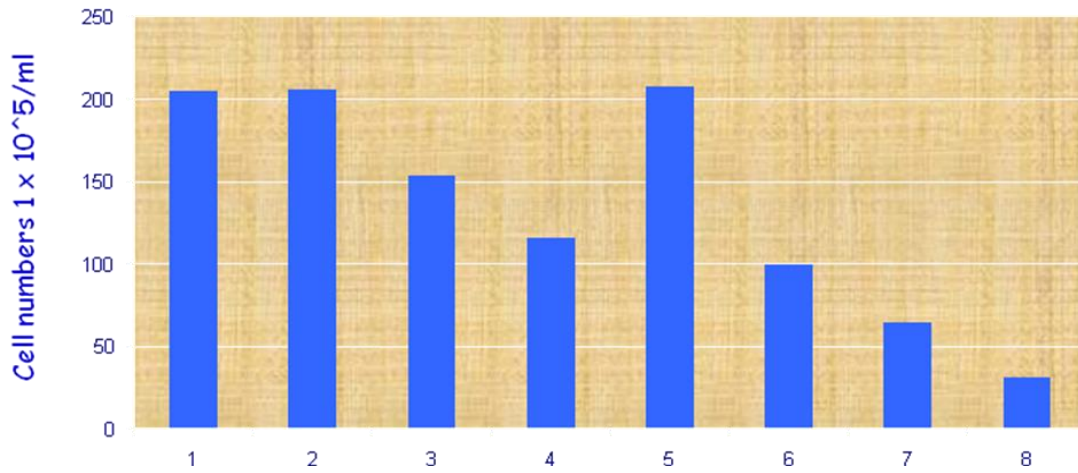


Figure 2.4.13 Effect of IFN- γ /dsRNA on the viability of 2FTGH cells. 2FTGH cells were treated with IFNs and/or dsRNA. The viability of the treated cells was analyzed by a trypan blue exclusion assay. 1, Control; 2, dsRNA alone; 3, IFN- α ; 4, IFN- β ; 5, IFN- γ ; 6, IFN- α /dsRNA; 7, IFN- β /dsRNA; 8, IFN- γ /dsRNA

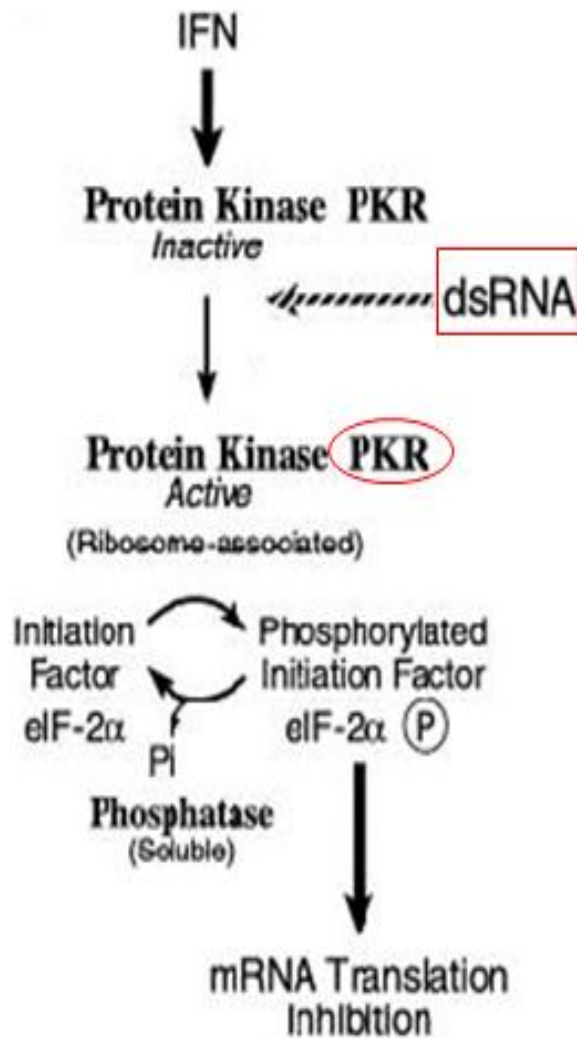


Figure 2.4.14 Role of PKR in IFNs' functions [Samuel, 2001]

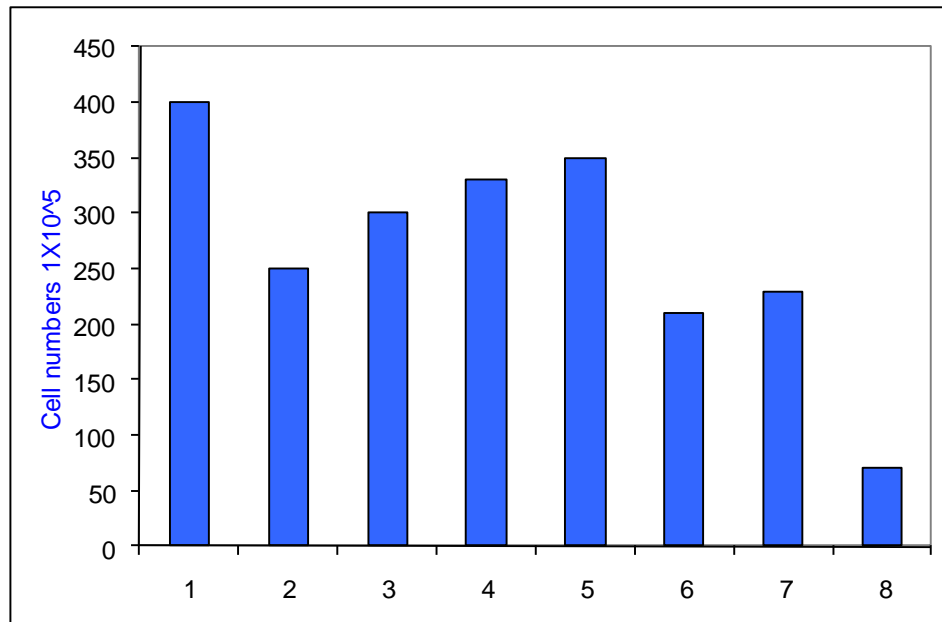


Figure 2.4.15 Role of PKR in IFNs/dsRNA-induced PC3 cell apoptosis PC3 cells were transfected with PKR siRNA. At 30 h after transfection, the cells were treated with IFNs and/or dsRNA. The apoptotic cells were analyzed by a trypan blue assay. 1, Control; 2, dsRNA alone; 3, IFN- α ; 4, IFN- β ; 5, IFN- γ ; 6, IFN- α /dsRNA; 7, IFN- β /dsRNA; 8, IFN- γ /dsRNA

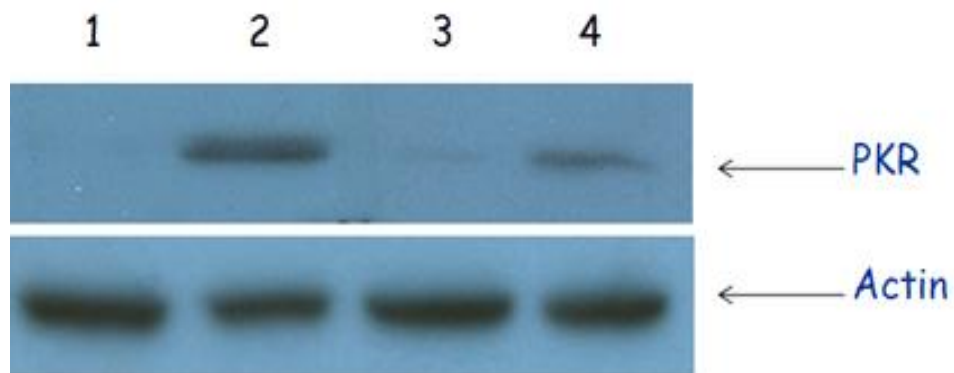


Figure 2.4.16 Knockdown of PKR by siRNA in PC3 cells PC3 cells were transfected with PKR siRNA and then were treated with 1000 unites/mL of IFN- α . The expression level of PKR in the cells was analyzed by a western blot analysis. 1, Control; 2, IFN- α ; 3, PKR siRNA; 4, PKR siRNA+IFN- α

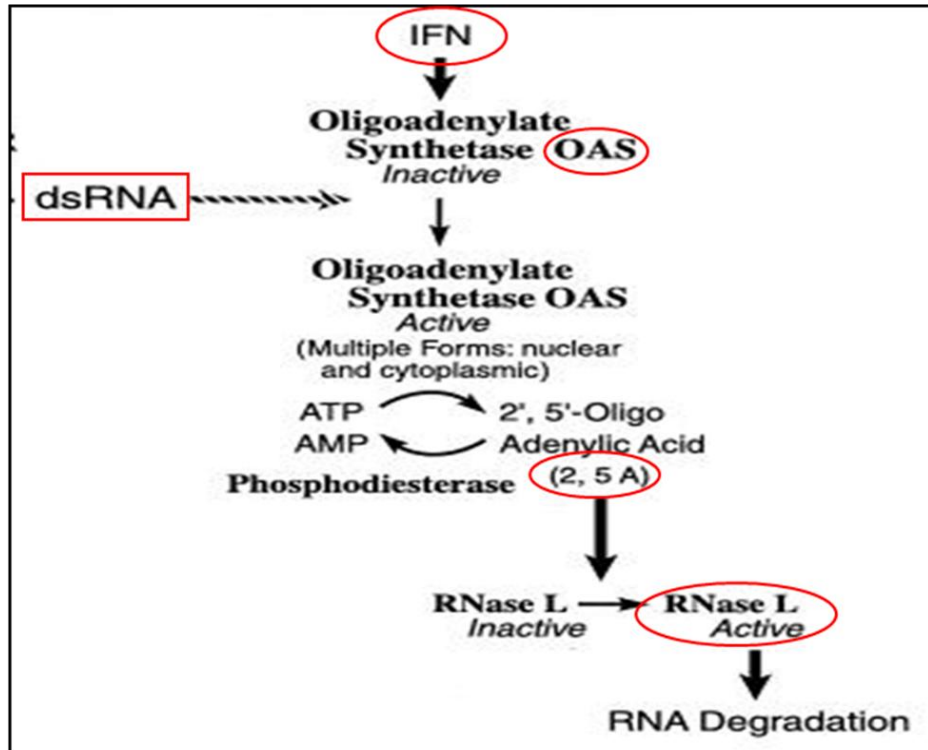


Figure 2.4.17 The 2-5 A system [Samuel, 2001]

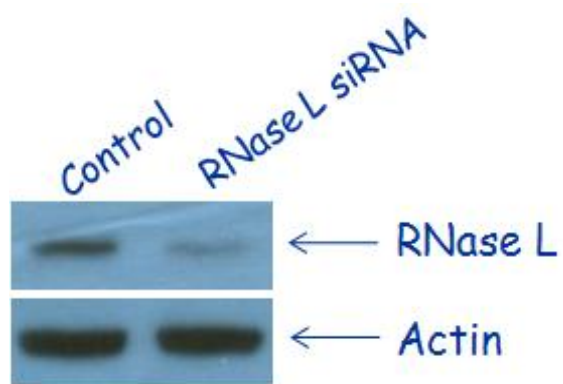


Figure 2.4.18 Knockdown of RNase L by siRNA in PC3 cells PC3 cells were transfected with RNase L siRNA using the Lipofectamine 2000 reagent. After 30 h incubation, the cells were collected, lysed and a western blot analysis was performed to evaluate the protein expression of RNase L.

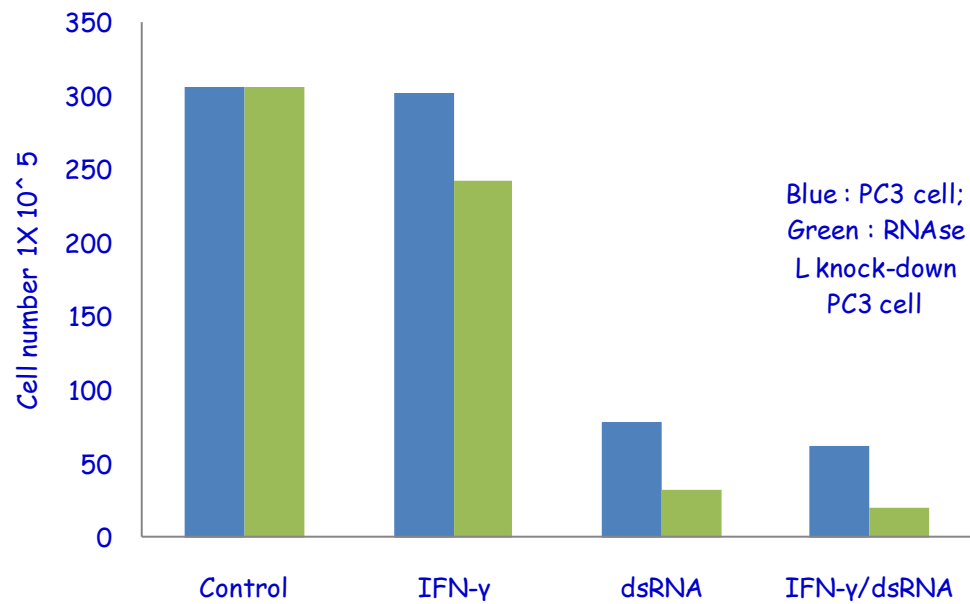


Figure 2.4.19 Role of RNase L in IFN- γ /dsRNA induced PC3 cell apoptosis

The RNase L knockdown cells were treated with IFN- γ and/or dsRNA and the viability of the treated cells was analyzed by a trypan blue exclusion assay.

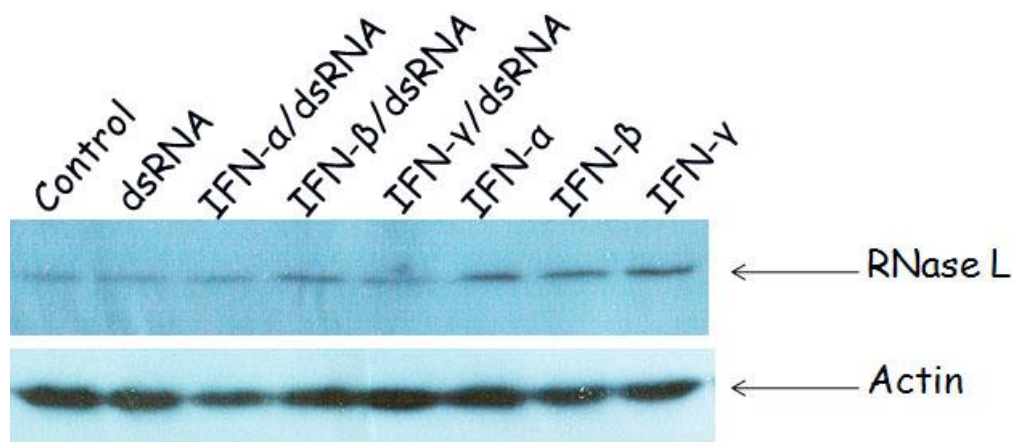


Figure 2.4.20 Expression of RNase L in IFNs/dsRNA treated PC3 cells A western blot analysis was conducted to evaluate the protein expression of RNase L in PC3 cells treated with IFNs and/or dsRNA.

INF- γ has no effect on the expression of death associate protein 3 (DAP3) and 5 (DAP5)

Death associated proteins (DAPs) are uniquely induced by IFN- γ , and the role of DAPs in mediating IFN- γ induced apoptosis in certain cell types has been well established in recent years [Kissil, *et al.*, 1995; Hirota, *et al.*, 2004]. To determine whether DAPs are responsible for IFN- γ /dsRNA-induced PC3 cell apoptosis, DAP3 and DAP5 were examined by Western blot analysis. The results showed that there was no difference in the expression of DAP3 and DAP5 between the control and IFN- γ treated PC3 cells (Figure 2.4.21). This suggests that DAP3 and DAP5 were not responsible for this event.

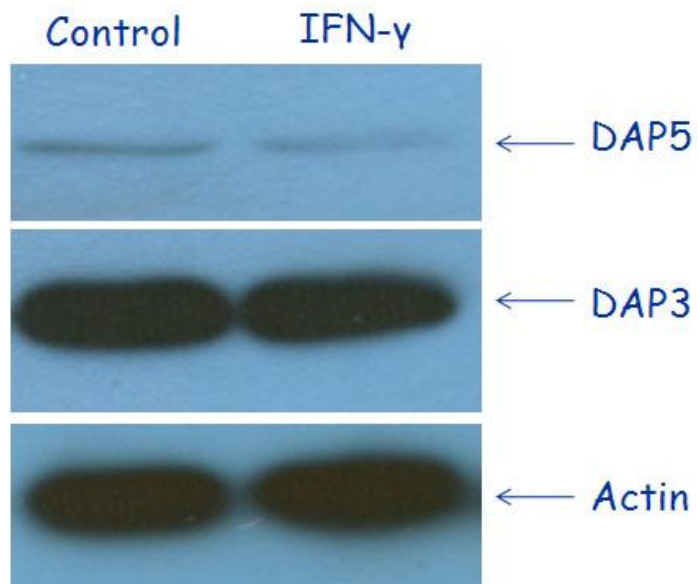


Figure 2.4.21 Expression of DAPs in IFN- γ treated PC3 cells PC3 cells were treated with 1000 unit/mL of IFN- γ and the expression of death associated proteins (DAPs) was analyzed by a western blot assay.

2.5 Discussion

In this study, we examined the effect of dsRNA and IFNs on the apoptosis of PC3 cells and discovered that pretreatment of human PC3 prostate cancer cells with IFNs, especially IFN- γ , significantly enhances the vulnerability of these cells to dsRNA-induced apoptosis. Similar results were obtained on DU145 cells which are another type of prostate cancer cell line, while other types of cancer cells displayed a dramatic difference in response to the stimulation with the subtypes of IFN.

RNase L and PKR are two IFN-inducible proteins which are very important in many IFN regulated events. Previous studies showed that increased expression of 2-5A synthases was observed in both HeLa cells and mouse L-cells treated with IFN- β and dsRNA [Nilsen *et al.*, 1981; Goswami and Sharma, 1984]. Furthermore, INF- γ is able to induce the expression of 2-5A synthetase in human colon carcinoma cell line BE, but there is no synergistic effect observed in the combination of IFN- γ and dsRNA [Chapekar and Glazer, 1986]. These results are consistent with our finding that RNase L-deficient PC3 cells are still sensitive to the treatment of IFN- γ and dsRNA. In addition, there was no overt difference in the RNase L expression in the cells treated with or without the dsRNA/IFN- γ . All of these suggest that RNase L may not be involved IFN- γ /dsRNA-induced apoptosis in PC3 cells. Magnusson *et al.* [2006] reported that arthritis triggered by dsRNA is not dependent on PKR. In the present study, after the expression of PKR was knocked down by siRNA, the PC3 cells were still sensitive to the

treatment of IFN- γ /dsRNA, suggesting again that PKR does not participate in the event.

The JAK/STAT pathway has been well established during the studies on the IFNs' function. It has been observed that Stat1 is required for IFN-inducible responsiveness to the extracellular dsRNA [Elco and Sen, 2007]. Arthritis triggered by dsRNA is associated with the ability to produce type I IFN and is critically dependent on type I IFN receptor signaling [Magusson *et al.*, 2006]. U3A cells, which lack STAT1, were not sensitive to IFN- γ /dsRNA. However, IFN- γ /dsRNA are able to synergistically induce apoptosis in 2ftgh, the parental cells of U3A, implicating that the JAK/STAT pathway is necessary for this event. Furthermore, LNcap cells, which are deficient in Jak1, were resistant to the IFN- γ /dsRNA treatment. Taken together, these data indicate the JAK/STAT pathway is indispensable for the apoptosis induced by IFN- γ /dsRNA in PC3 cells.

Either dsRNA or IFN- γ is able to induce a broad range of gene expressions [Potten and Wilson, 2004]. In the global profiling of dsRNA and IFN- γ -induced genes in rat pancreatic beta cells, one of the BCL-2 family members, Bax, is highly inducible [Rasschaert, *et al.*, 2003]. Noxa is another protein induced by the cells exposed to dsRNA, interferon, and virus [Sun and Leaman, 2005]. To determine whether any of the Bcl-2 family members is involved in PC3 cell apoptosis induced by IFN- γ /dsRNA, we examined the expression of several Bcl-2 family proteins and found that Bak was upregulated by IFN- γ /dsRNA, implying that apoptosis in PC3 cells induced by IFN- γ /dsRNA depends on the participation of mitochondria.

2.6 References

- Bantis A and Vasiliou O. Prostate cancer incidence, mortality, total and free prostate specific antigen. *Hell J Nucl Med*, 2009,12(2):106-109
- Bart RS and Kopf AW. Inhibition of the growth of murine malignant melanoma with synthetic double-stranded ribonucleic acid. *Nature*, 1969, 224:3-12
- Bickers B and Aukim-Hastie C. New molecular biomarkers for the prognosis and management of prostate cancer--the post PSA era. *Anticancer Res*, 2009, 29(8):3289-3298
- Borden EC, Sen GC, Uze G, Silverman RH, Ransohoff RM, Foster GR, Stark GR. et al. Interferons at age 50: past, current and future impact on biomedicine. *Nat Rev Drug Discov*, 2007, 6:975-990
- Chapekar MS and Glazer RI. Potentiation of the cytotoxic effect of human immune interferon by different synthetic double-stranded RNAs in the refractory human colon carcinoma cell line BE. *Cancer Res*, 1986, 46:1698-1702
- Damber JE and Aus G. Prostate cancer. *Lancet*, 2008,371(9625):1710-1721
- Damasio EE, Clavio M, Masoudi B, Isaza A, Spriano M, Rossi E, Casciaro S, Cerri R, Risso M, Nati S, Siccardi M, Truini M, Gobbi M. Alpha-interferon as induction and maintenance therapy in hairy cell leukemia: a long-term follow-up analysis. *Eur J Haematol*, 2000, 64(1):47-52
- Elco CP and Sen GC. Stat1 required for interferon-inducible but not constitutive responsiveness to extracellular dsRNA. *J Interferon Cytokine Res*, 2007, 27(5):411-424

- Elmore S. Apoptosis: A Review of Programmed Cell Death. *Toxicol Pathol*, 2007, 35(4): 495–516
- Fabbri F, Amadori D, Carloni S, Briigliadori G, Tesei A, Ulivi P, Rosetti M, Vannini I, Arienti C, Zoli W and Silvestrini R. Mitotic catastrophe and apoptosis induced by docetaxel in hormone-refractory prostate cancer cells. *J cell physiol*, 2008, 217(2):494-501
- Fabbri F, Briigliadori G, Carloni S, Ulivi P, Tesei A, Silvestrini R, Amadori D and Zoli W. Docetaxel-ST1481 sequence exerts a potent cytotoxic activity on hormone-resistant prostate cancer cells by reducing drug resistance-related gene expression. *Prostate*, 2010, 70(2):219-227
- Goswami BB and Sharma OK. Degradation of rRNA in interferon-treated vaccinia virus infected cell. *J Biol Chem*, 1984, 259:1371-1374
- Hirota T, Obara K, Matsuda A, Akahoshi M, Nakashima K, Hasegawa K, Takahashi N, Shimizu M, Sekiguchi H, Kokubo M, Doi S, Fujiwara H, Miyatake A, Fujita K, Enomoto T, Kishi F, Suzuki Y, Saito H, Nakamura Y, Shirakawa T, Tamari M. Association between genetic variation in the gene for death-associated protein-3 (DAP3) and adult asthma. *J Hum Genet*, 2004, 49(7):370-5
- Hubbel HR, Liu RS and Maxwell BL. Independent sensitivity of human tumor cell lines to interferon and double-stranded RNA. *Cancer Res*, 1984, 44:3252-3257
- Jagus R, Joshi B and Barber GN. PKR, apoptosis and cancer. *Int J Biochem Cell Biol*. 1999, 31(1):123-138

- Kissil JL, Deiss LP, Bayewitch M, Raveh T, Khaspekov G, Kimchi. A. Isolation of DAP3, a novel mediator of interferon-gamma-induced cell death. *J Biol Chem*, 1995, 270:27932–27936
- Lin SL, Greene JJ, Ts'o POP and Carter WA. Sensitivity and resistance of human tumor cells to interferon and $rl_n \cdot rC_n$. *Nature*, 1982,297:417-419
- Liu D, Cardozo AK, Darville MI, Eizirik DL. Double-stranded RNA cooperated with interferon-gamma and IL-1 beta to induce both chemokine expression and nuclear factor-kappa B dependent apoptosis in pancreatic beta-cells: potential mechanisms for viral-induced insulinitis and beta-cell death in type 1 diabetes mellitus. *Endocrinology*, 2002,143(4): 1225-1234
- Magnusson M, Zare F, Tarkowski A. Requirement of type I interferon signaling for arthritis triggered by double-stranded RNA. *Arthritis Rheum*, 2006, 54(1)148-157
- Mediavilla-Varela M, Pacheco FJ, Almaguel F, Perez J, Sahakian E, Daniels TR, Leoh LS, Padilla A, Wall NR, Lilly MB, De Leon M and Casiano CA. Docetaxel-induced prostate cancer cell death involves concomitant activation of caspase and lysosomal pathways and is attenuated by LEDGF/p75. *Mol Cancer*, 2009,28(8):68-82
- Nilsen TW, Maroney PA and Baglioni C. Double-stranded RNA causes synthesis of 2',5'-oligo(A) and degradation of messenger RNA in interferon-treated cells. *J Biol Chem*, 1981, 256:7806-7811
- Pienta KJ. Critical appraisal of prostate-specific antigen in prostate cancer screening: 20 years later. *Urology*, 2009, 73(5 Suppl):S11-20

- Potten C and Wilson J. Apoptosis: the life and death of cells. Cambridge University Press, New York, USA, 2004, pp38-43
- Priolo C, Oh WK and Loda M. Novel therapeutic strategies in prostate cancer: establishing a stratification system for patient selection in targeted trials. *IDrugs*, 2009,12(3):165-168
- Rasschaert J, Liu D, Kutlu B, Cardozo AK, Kruhøffer M, ØRntoft TF, Eizirik DL. Global profiling of double stranded RNA- and IFN- γ -induced genes in rat pancreatic beta cells. *Diabetologia*, 2003,46:1641-1657
- Samuel CE. Antiviral action of interferons. *Clin Microbiol Rev*, 2001, 14(4):778-809.
- Stark GR, Kerr IM, Williams BR, Silverman RH and Schreiber RD. How cells respond to interferons. *Annu Rev Biochem*, 1998, 67:227-264
- Strasser A, O'Connor L and Dixit VM. Apoptosis signaling. *Annu Rev Biochem*, 2000,69:217-245
- Strief DM. An overview of prostate cancer: diagnosis and treatment. *Urol Nurs*, 2007, 27(6):475-479
- Sun Y and Leaman DW. Involvement of Noxa in cellular apoptotic responses to interferon, double-stranded RNA, and virus infection. *J Biol Chem*, 2005,280(16): 15561-15568
- Zeleznick LD and Bhuyan RK. Treatment of leukemia (L1210) mice with double-stranded polyribonucleotides. *Proc Soc Exp Biol Med*, 1969, 130:126-128
- Zhou Y, Chase BI, Whitmore M, et al. Double-strand RNA-dependent protein kinase is downregulated by phorbol ester. *FEBS J*, 2005, 272:1568-1576

CHAPTER III
**STUDIES ON THE BIOLOGICAL ROLES OF TRANSMEMBRANE AND COILED-
COIL DOMAINS 1**

3.1 Abstract

Transmembrane and coiled-coil domains 1 (TMCO1) is a membrane-associated protein and belongs to the DUF841 superfamily of several eukaryotic proteins with unknown functions. The human TMCO1 gene is located on chromosome 1q22-q25. A homozygous frame shift mutation in the TMCO1 gene, c.139_140delAG, has been identified in patients with TMCO1 defect syndrome (TDS). TDS is characterized by distinctive craniofacial dysmorphism, skeletal anomalies, and mental retardation. To further investigate the biological functions of TMCO1, we first attempted to generate an antibody against TMCO1 protein. In this study, human TMCO1 was expressed in both bacteria and mammalian cells. The recombinant TMCO1 expressed in bacteria was purified in preparation for a workable antibody. Subcellular localization using the immune-fluorescent staining

technique revealed that TMCO1 may be mainly expressed in the mitochondria of cells. Interestingly, the lymphocytes isolated from the peripheral blood of the patients with TDS grew significantly faster than those from healthy individuals, suggesting that TMCO1 may be involved in the regulation of cell proliferation. In addition, we have generated a TMCO1 knockdown cell line, which can be used for further the study of the molecular basis underlying TDS.

3.2 Introduction

TMCO1 is a plasma membrane-associated protein located in the long arm of the 1st chromosome. Recently, it was found that the homozygous mutation in TMCO1 caused a syndrome with craniofacial dysmorphism, skeletal anomalies and mental retardation, named TMCO1 defect syndrome (TDS) [Xin, *et al.*, 2010]. TDS is an autosomal recessive condition in Old Order Amish of Northeastern Ohio, and a homozygous 2-base pair deletion within exon 2 of the TMCO1 gene was identified. Though the function of this gene is still unclear, distribution analyses revealed that TMCO1 is universally expressed in all human tissues and is highly conserved among multiple species. The ubiquitous expression pattern in human adult and fetal tissues and the high sequence conservation may suggest that TMCO1 plays important biological roles. Structural analysis indicates that the TMCO1 gene consists of one coiled-coil domain and two transmembrane domains, and there are 3 phosphoserine residues identified, which may participate in signaling transduction. Currently, the study concerning the function of TMCO1 is largely lacking, although some reports show that the

TMCO1 gene is regulated by different events--for instance, fast, cancer, and diabetes. [Lkhagvadorj, *et al.*, 2009; Kondrakhin, *et al.* 2008; Dokmanovic-Chouinard *et al.*, 2008; Yu, *et al.*, 2009]. In this study, we subcloned the TMCO1 gene into several mammalian cell expression vectors and an ectopic expression of the gene in different cell types. By using these cell lines we determined the localization of TMCO1 and examined the effect of TMCO1 on cell functions. We also generated an effective antibody against human TMCO1. Based on the results obtained from lymphocyte cells derived from TDS patients and TMCO1 knockdown cell lines, TMCO1 may play an important role in cell proliferation.

3.3 Materials and methods

Materials and reagents

Human TMCO1 cDNA was purchased from ATCC (Manassas, VA). pET-21d vector was from Novagen (Brookfield, WI). pIRESHyg vector was purchased from Clontech (Brookfield, WI). Choice-Taq™ DNA Polymerase was from Denville Scientific INC. (Metuchen, NJ). All digestion enzymes and the T4 DNA ligase kit were obtained from New England Biolab (Ipswich, MA). The QIAEXii gel extraction and QIAprep Spin Miniprep kits were purchase from Qiagen (Valencia, CA). SOC medium and ultrapure agarose were from Invitrogen (Carlsbad, CA). XL10-gold ultracompetent cell was from Stratagen (Kirkland, WA).

Subcloning of TMCO1 to pET-21d

To express TMCO1 in *E. coli*, TMCO1 cDNA was subcloned to pET-21d vector with a His-tag (Figure 3.3.1). The TMCO1 cDNA was amplified by polymerase chain reaction (PCR) from pOTB7 vector in a reaction mixture (50 μ L) containing 10 mM Tris-HCl (pH 8.3), 10 mM KCl, 1.5 mM MgCl₂, 8mM (NH₄)₂SO₄, 0.05% NP-40, 200 mM each deoxynucleoside triphosphate, 1.0 U of *Taq* polymerase, and 0.5 μ g of a pair of primers. The first denature step was done at 94°C for 3 min. The PCR amplification was carried out for 30 cycles consisting of template denaturation (1 min at 94°C), primer annealing (45 sec at 55°C), and polymerization (1 min at 72°C). The final extension step was 1 cycle of 72°C for 8 min. The forward primer used was 5'GGT GCG ACC ATG GGC ACT ATG TT3' and the reverse primer was 5'AGA ACT CCT CGA GAG AGA ACT TCC3'. Both PCR products and pET-21d vector were digested with restriction enzymes XhoI and NcoI. The digestion reaction mixture (50 μ L) included 5 μ L of PCR product or pET-21d vector DNA, 5 μ L of buffer 2 and 3 μ L of XhoI and ddH₂O. The mixture was incubated at 37°C for 1 h followed by adding additional 3 μ L of NCOI and 2 μ L of NaCl (0.1 M) then incubated for another 1 h. Both the PCR product digestion mixture and pET-21d vector digested mixture were separated by 1% agarose gel and undergone gel purification using the QIAEXii gel extraction kit. A T4 DNA ligase kit was used to ligate the DNAs. The ligation buffer contained 5 μ L of pET-21d digestion mixture, 4 μ L of PCR product digestion mixture, 2 μ L of 10X T4 buffer, 1 μ L of T4 ligase, and distilled-deionized water (ddH₂O) to 20 μ L in total. The ligation reaction was

done at room temperature for 2 h, followed by transformation. Briefly, the mixture of 10 μ L of ligation solution and 50 μ L of XL10-gold ultracompetent cell (good for big size cloning) was left on ice for 30 min, 40^oC water bath for 90 sec, and ice for 2 min. Then 300 μ L of SOC medium was added to the mixture and the tube was shaken at 37^oC for 1 h. Three hundred μ L of the mixture was applied to a LB agarose plate with ampicillin (100 μ g/mL) and incubated overnight at 37^oC. In the next morning, 12 single clones were picked up and grown in LB medium. TMCO1/pET-21d plasmid DNA was extracted using the QIAprep Spin Miniprep kit and transformed to *E. coli* BL21 (DE3) competent cells (Sigma, St. Louis, MO) for protein expression. The authenticity of the clones was confirmed by DNA sequencing.

Subcloning of TMCO1 to pIRESHyg

In order to express the TMCO1 gene in mammalian cells, TMCO1 cDNA was cloned to a pIRESHyg vector. TMCO1 was amplified by PCR from the plasmid pOTB7 as previously described. The primers used for this PCR were 5' CTA CGG ATC CCG TTT TCG CTT C3' (forward) and 5' GGC TCT GGA TCC AAA ACA GTT G3 (reverse). Both PCR product and pIRESHyg vector (Figure 3.3.2) were digested with BamH1. After digestion, the DNAs were treated with alkaline phosphatase calf intestine (CIP) at 37^oC for 30 min, followed by gel purification. The purified DNAs were ligated, and then transformed as described above. Purified TMCO1/ pIRESHyg plasmid DNA was kept for the transfection.

Other subclonings

Several other constructs were generated. (1) TMCO1-pFLAG-CMV-2 (Figure 3.3.3): primers used were 5'CGG CCG CGA ATT CGA GCA CTA TGT TC3' (forward) and 5'GGC TAC CTA TGG CTC TTG CT3' (reverse). EcoR1 and XbaI were used to digest the DNAs. (2) TMCO1-pCMV-Myc (Figure 3.3.4): the primers were the same as used for cloning TMCO1 to pFLAG-CMV-2, but restriction enzymes were EcoR1 and XhoI. (3) TMCO1-pCMV-HA (Figure 3.3.5): the primers were 5'AGG TGC GAA TTC AGA CTA TGT TCG C3' (forward) and 5'GAA AGA GGC TCG AGT AGT AAG GCT A3' (reverse). EcoR1 and XhoI were used to digest the DNAs.

Immunofluorescence staining

Human U87 cells were human glioblastoma-astrocytoma cells (ATCC, Manassas, VA). Cells were grown in RPMI-1640 medium (Media Lab of the Central Cell Service, Cleveland Clinic, Cleveland, OH) supplemented with streptomycin (100 µg/mL), penicillin (100 unites/mL) and 10% cosmic calf serum (Hyclone, Logan, UT) in a humidified atmosphere of 5% CO₂ at 37 °C. U87Cells were seeded on BD Falcon™ CultureSlides (BD Biosciences, Bedford, MA) and transfected with the pFlag-CMV-2 vector or pFlag-CMV-2/TMCO1 plasmid DNA using lipofectomine 2000 reagents (Invitrogen, Carlsbad, CA). After 30 h, transfected cells were incubated with growth medium containing 0.5 µM MitoTracker Red CMXRos (Invitrogen, Carlsbad, CA) for 15 min at 37°C and immunofluorescence was performed following standard protocols. In brief, after

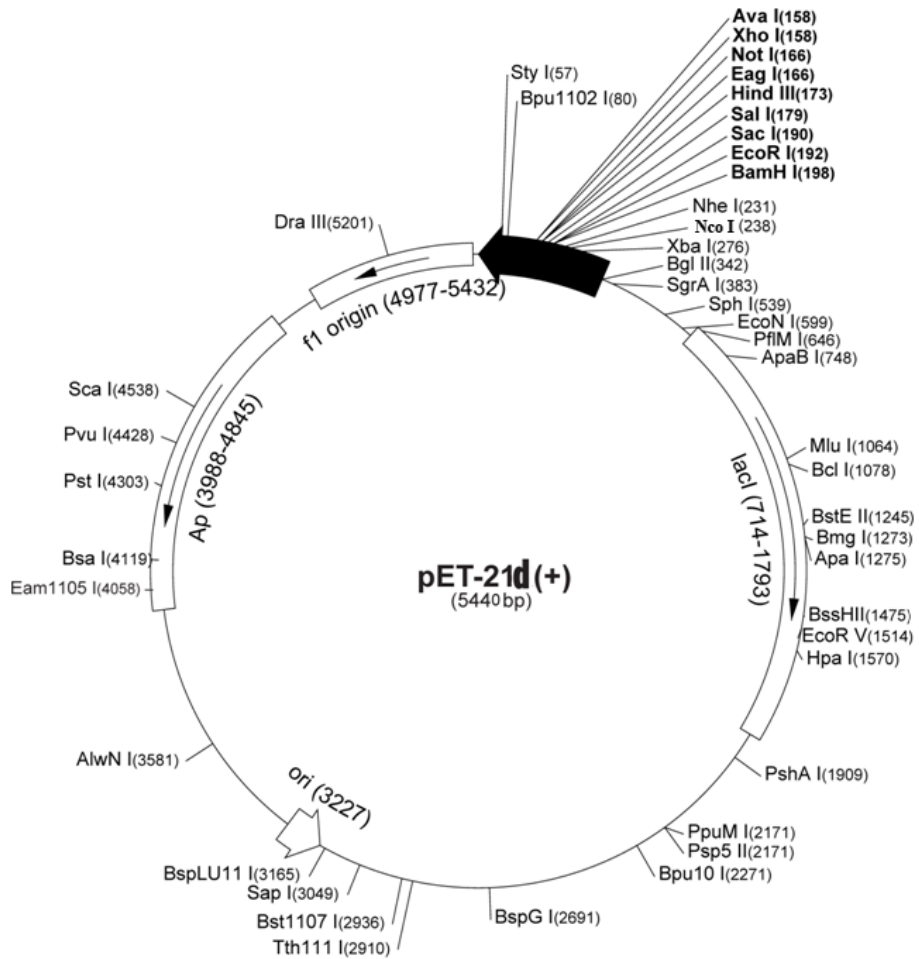


Figure 3.3.1 pET-21d vector map (Novagen, Brookfield, WI)

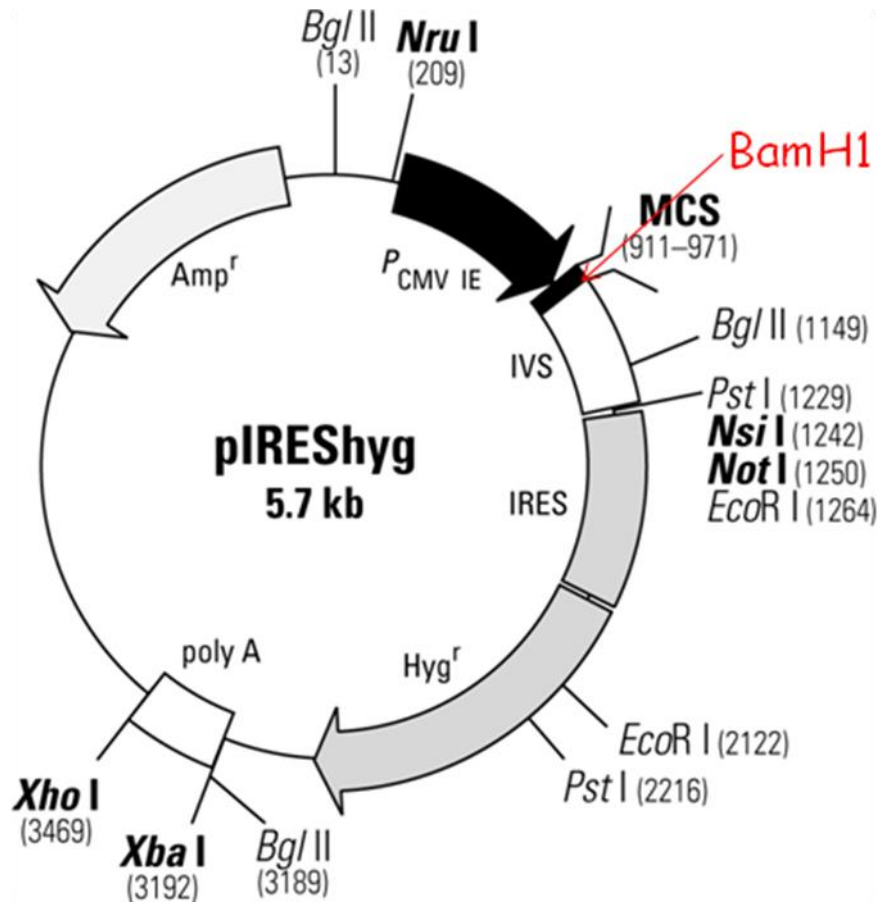
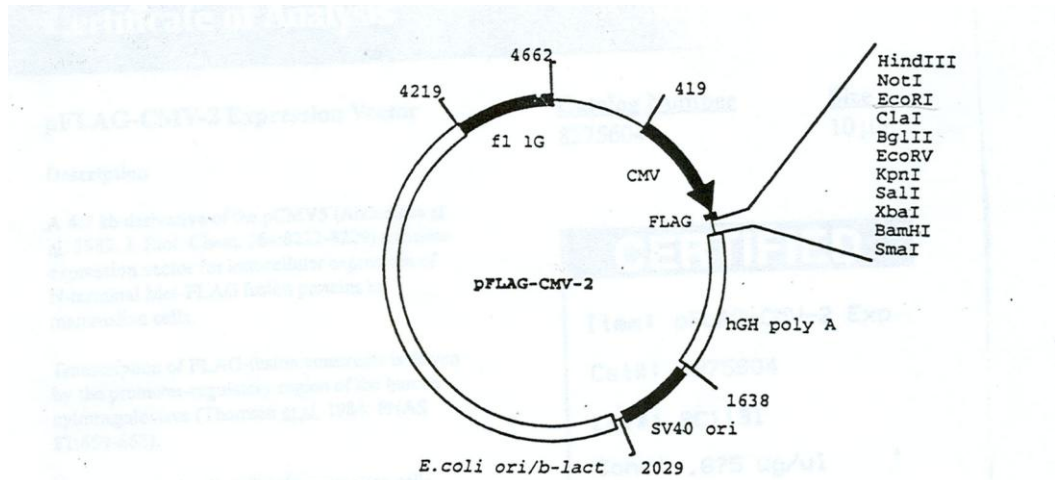


Figure 3.3.2 pERESHyg^r vector information (Clontech, Brookfield, WI)



Nucleotide Sequence of the Multiple Cloning Region of the pFLAG-CMV-2 Expression Vector

Sequence Range: 922 to 1015

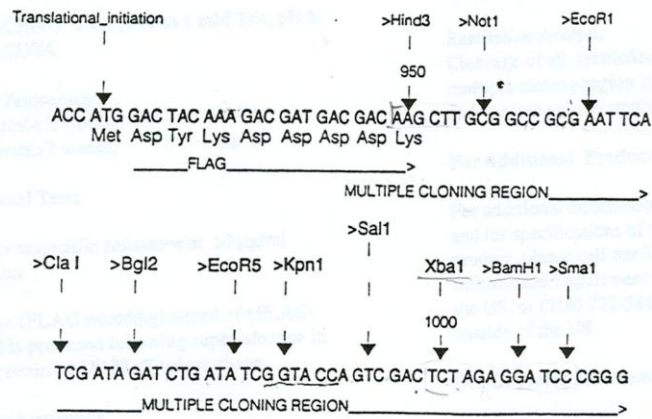
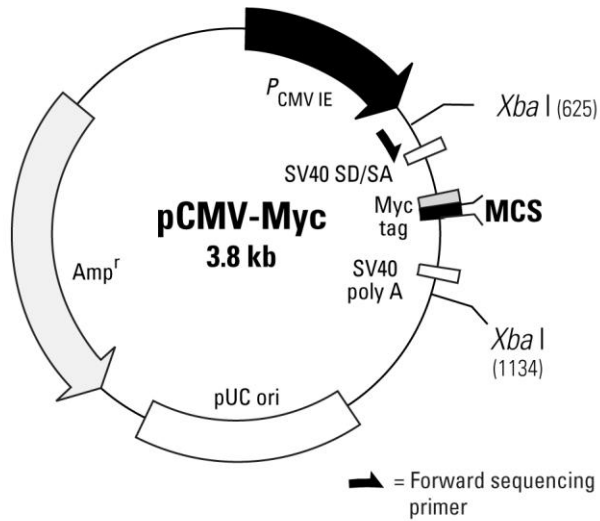


Figure 3.3.3 pFLAG-CMV-2 vector information (Eastman Kodak Company, New Haven, CT)



```

      830      840      850      860      870
C ACC ATG GCA TCA ATG CAG AAG CTG ATC TCA GAG GAG GAC CTG CTT
      Myc tag

      880      890      900      910      920
ATG GCC ATG GAG GCC CGA ATT CGG TCG ACC GAG ATC TCT CGA GGT ACC GCG GCC GC
      Sfi IA,B   EcoR I   Sal IB   Bgl II   Xho IA Kpn I   Not I

```

Figure 3.3.4 pCMV-Myc vector information (BD Biosciences, Palo Alto, CA)

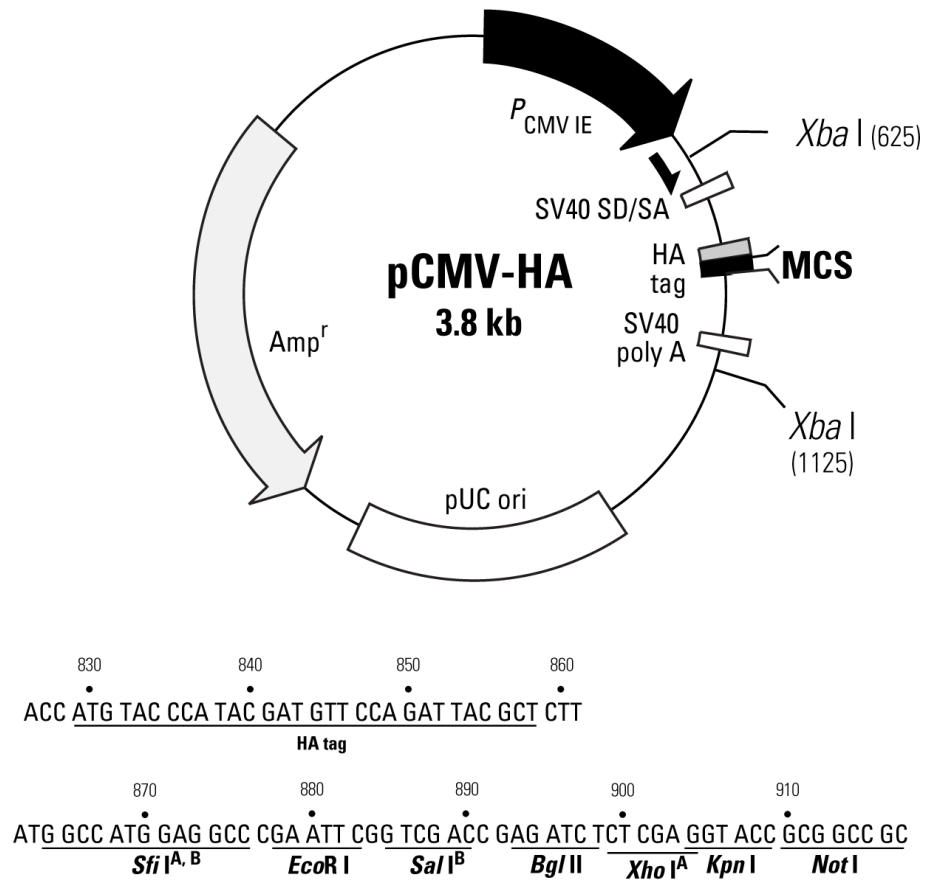


Figure 3.3.5 pCMV-HA vector map and MCS (BD Biosciences, Palo Alto, CA)

being rinsed with 1XPBS (Media Lab of the Central Cell Service, Cleveland Clinic, Cleveland, OH), the cells were fixed with 3% formaldehyde (Sigma, St. Louis, MO) for 15 min at room temperature, followed by 3 times of washing with PBS. The cells were then permeabilized with ice-cold methanol (Pharmco-AAPER, Shelbyville, KY) for 10 min at -20°C and blocked with block buffer (2.5 mL of 10XPBS, 1.25 mL of normal goat serum, 75 μL of Triton X-100 and dH_2O to 25 mL) for 60 min at room temperature, followed by incubation in primary antibody, a mouse monoclonal anti-Flag M5 antibody (Sigma-Aldrich, St. Louis, MO) overnight at 4°C . Then the cells were rinsed with 1XPBS for 3 times and incubated with the secondary antibody: Dylight TM 488 conjugated Anti-mouse IgG (Cell signaling, Boston, MA), for 1.5 h at room temperature in dark. After 5 times of washing with high salt PBS (0.4 M NaCl, 1XPBS), the walls of culture slides were removed, and the nuclei were counterstained with DAPI (Invitrogen, Carlsbad, CA). Then the slides were mounted with Prolong Gold Antifade Reagent (Invitrogen, Carlsbad, CA) and the edges of cover slips were sealed with nail polish. The slides were examined using a Delta Vision RT microscope.

TMCO1 protein expression in *E. coli* BL21 cells

E. coli BL21 cells bearing TMCO1/pET-21d construct were grown in LB medium supplemented with ampicillin (100 $\mu\text{g}/\text{mL}$) to an O.D. value of 0.5 at 600 nm and the expression of TMCO1 was induced by adding isopropyl thiogalactoside (IPTG) to a final concentration of 1 mM. After being shaken at

30°C for 6 h, bacterial cells were harvested by centrifugation (1750 Xg at 4°C for 30 min). The cell pellets were frozen at -80°C.

Purification of TMCO1

The cell pellets were thawed and resuspended in lysis buffer (50 mM phosphate buffer with 800 mM NaCl, pH 8.0, 0.1% Triton X-100) on ice, followed by sonication and centrifugation to sediment cell debris. The supernatant was diluted with 6 M guanidine HCl in 1:1 volume ratio to a final concentration of 25 mM phosphate, 400 mM NaCl and 3 M guanidine HCl (pH 8.0). Then the diluted supernatant was mixed with a nickel-chelating histidine-binding resin (Qiagen, Valencia, CA) for 1 h and loaded into an empty column. After washed with PBS buffer containing 20 mM imidazole and 3 M guanidine HCl, the TMCO1 protein was eluted with PBS buffer containing 100 mM imidazole and 3 M guanidine HCl (pH 8.0). Fractions containing TMCO1 were pooled and dialyzed against 4 L Tris-buffered saline (1 mM EDTA, 1 mM benzamidine and pH 7.4) at 4°C. The dialyzed sample was stored at -80°C until use.

Production of polyclonal anti-TMCO1 antibody

The amino acid sequence of TMCO1 was “MSTMFADTLLIVFISVCTALLAEG ITWVLVYRTDKYKRLKAEVEKQSKKLEKKKETITESAGRQQKKKIERQEEKLKN NNRDLSMVRMKSMFAIGFCFTALMGMFNSIFDGRVVAKLPFTPLSYIQGLSHRN LLGDDTTDCSFILYILCTMSIRQNIQKILGLAPSRAATKQAGGFLGPPPPSGKFS ,” which was submitted to GenSript Company (Piscataway, NJ) together with Hek

293 cell lysate as a positive control for peptide polyclonal anti-TMCO1 antibody production. The antigen peptide designed and synthesized by GeneScript company was “CKIERQEEKLKNNNR.” To gain an effective immunization effect, the peptide was conjugated with a big molecule Keyhole limpet hemocyanin (KLH). Then the conjugated peptide antigen was used to immunize 6 rabbits. Affinity purification was used to purify the TMCO1 antibody from the serum of immunized rabbits.

RNA isolation and RT-PCR

The lymphocytes from normal, carrier (one copy of TMCO1 gene was mutated), and affected (both copies of TMCO1 gene were mutated) individuals were pelleted in 15 mL centrifuge tubes and washed with PBS twice. The total RNA was isolated using Trizol (Invitrogen, Carlsbad, CA) according to the manufacturer's instructions. Briefly, 3 mL of Trizol reagent was added to the tube. After a brief vortex, 0.8 mL of chloroform was added followed by vigorous vortex for 1 min. Samples were centrifuged at 10,000 x g for 30 min at 4°C and the colorless upper aqueous phase was moved to a new 15 mL centrifuge tube. After added equal amount of isopropyl alcohol and inverted for several times, the sample sat at room temperature for 10 min followed by centrifugation at 10,000 x g for 20 min at 4°C. Then the RNA precipitate formed a gel-like pellet on the side and bottom of the tube. The supernatant was discarded and 1mL of 80% ethanol (pre-cooled at -20°C) was used to suspend RNA. The RNA suspension was transferred to a new 1.5 mL microcentrifuge tube and centrifuged at 7,000 x g for

5 min at 4°C. Then the alcohol was removed as much as possible and the RNA was dissolved in 100 µL of diethyl pyrocarbonate (DEPC) (Sigma-Aldrich, St. Louis, MO)-treated RNase-free H₂O by passing several times through a pipette tip.

One-step RT-PCR was performed using a SuperScript™ One-Step RT-PCR with Platinum Taq Kit (Invitrogen, Carlsbad, CA) according to the manufacturer's instructions. First strand cDNA synthesis and pre-denaturation steps were done at 45°C for 30 min and 94°C for 2 min and were followed immediately by PCR amplification. PCR amplification conditions were as follows: 35 cycles of denaturation at 94°C for 1 min, annealing at 55°C for 45 sec, and extension at 72°C for 1 min 30 sec. Finally, 1 cycle of final extension was set at 72°C for 8 min.

Western blot analysis

Lymphocytes were harvested from normal, carrier, or affected individuals. Cytoplasmic extracts were prepared by suspension of cell pellets in NP-40 lysis buffer. After centrifugation in a microcentrifuge at 4°C for 10 min, the supernatant was removed. Cellular extracts were fractionated on SDS-12% polyacrylamide gels and transferred to polyvinylidene difluoride membranes (Millipore, Billerica, MA). The membranes were blocked with 5% non-fat milk in PBS containing 0.02% sodium azide and 0.2% (v/v) Tween 20 and incubated with TMCO1 antibody (Genescript, NJ) overnight at 4°C. The membranes were then washed with PBS containing 0.2% (v/v) Tween 20 and incubated with anti-rabbit IgG secondary antibody conjugated with HRP (Cell Signaling Technology, Boston,

MA) for 1 h at room temperature. After the washing step, these proteins were detected by a chemiluminescence method, according to the manufacturer's specification (Amersham, Piscataway, NJ). The expression of TMCO1 in different cell lines was examined.

Knockdown of TMCO1's expression

Oligonucleotides coding for short hairpin RNA (shRNA) specifically against TMCO1 were cloned into pSilence 4.1-CMV neo (Ambion, Austin, TX). The following target regions of TMCO1 were chosen: (1) GCCAUAGGUAGCCUUACUA; (2) GCAAGUUGGCUGUCUAUGA and (3) CAAGGAGAGAUCUGUUUCA. Stably transfected clones were established by selection with G418 (Calbiochem, Brookfield, WI). The TMCO1 expression in each picked clone was examined by western blot assay.

Growth rate of lymphocytes from patients with TMCO1 defect

To check the effect of TMCO1 on the growth of lymphocytes, 6.27×10^5 of lymphocytes from normal, carrier, or affected individuals were seeded to each flask respectively. Cells were counted using trypan blue dye exclusion assay after 6 days and the medium color of each flask was recorded.

3.4 Results

TMCO1 was subcloned to the pET-21d and pIRESHyg vectors

In order to explore the function of TMCO1, we attempted to prepare an anti-TMCO1 antibody by using a purified recombinant TMCO1 protein. TMCO1 cDNA was subcloned into the pET-21d vector, which was fused with a His tag, using XhoI and NcoI. Several clones were identified as the right clones and the constructs were further confirmed by DNA sequencing (Figure 3.4.1 and Figure 3.4.2). In addition, TMCO1 was inserted into pIRESHyg using Bam HI and the constructs were confirmed by DNA sequencing as well (see Figure 3.4.3).

Purification of the recombinant TMCO1 protein

The purification of recombinant TMCO1 was achieved by using metal chelation affinity chromatography. As shown in Figure 3.4.4, after induction, the expressed TMCO1 protein in the cell lysate was passed through an affinity column packed with Ni²⁺ saturated beads and the bound recombinant TMCO1 protein was eluted with 100 mM imidazole after the column was washed with 20 mM imidazole. The insolubility of a recombinant protein expressed in bacteria is a common problem. To increase the yield, 6 mM guanidine hydrochloride (GnCl) was added to the cell lysate to promote the solubility of the recombinant TMCO1 protein during the purification process. After purification, GnCl was removed by dialysis. The purified protein was analyzed by SDS-PAGE (Figure 3.4.5). However, although the purity of the purified recombinant TMCO1

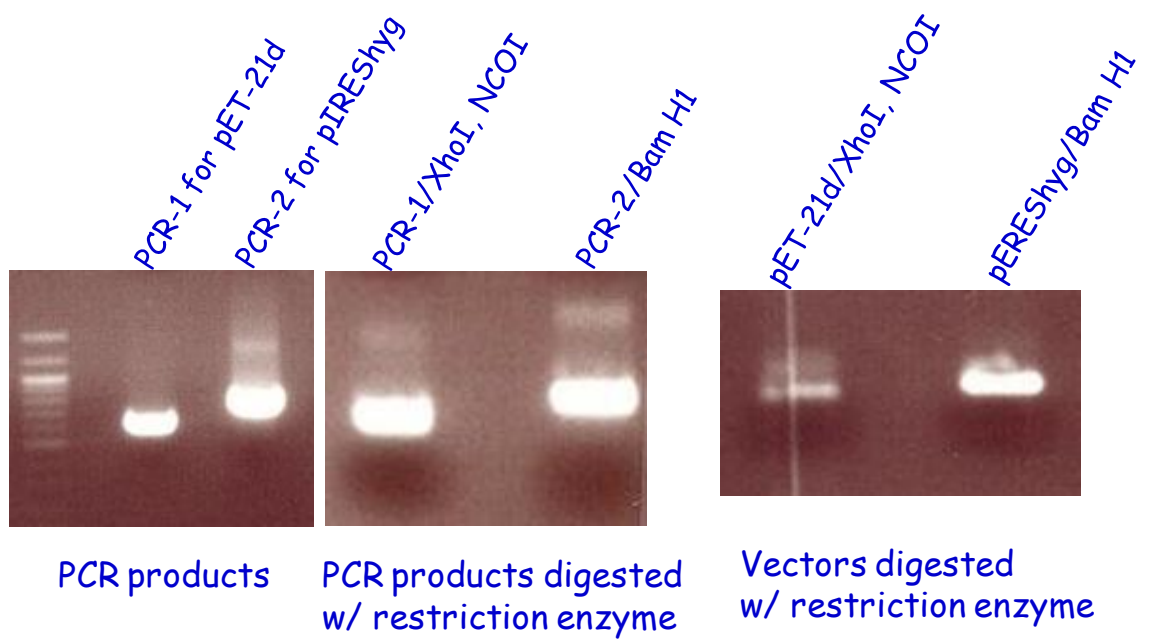


Figure 3.4.1 Digestion of PCR products and vectors TMCO1 cDNA was amplified by PCR and both PCR products and vectors were digested with corresponding restriction enzymes.

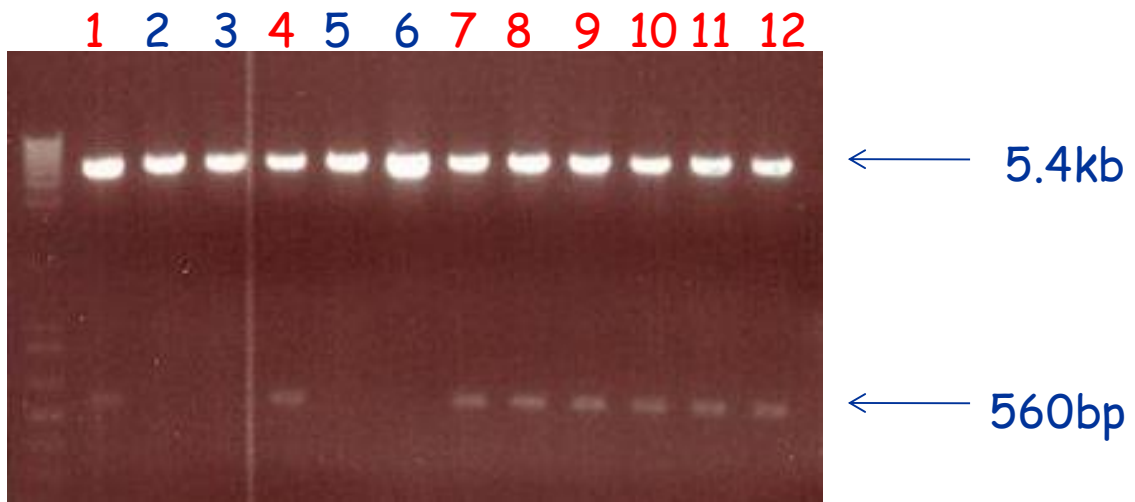


Figure 3.4.2 TMC01/pET-21d clone selection After subcloning, 12 clones were picked up and cultured in LB medium. Plasmid DNA was purified from each clone and digested by XhoI and NcoI.

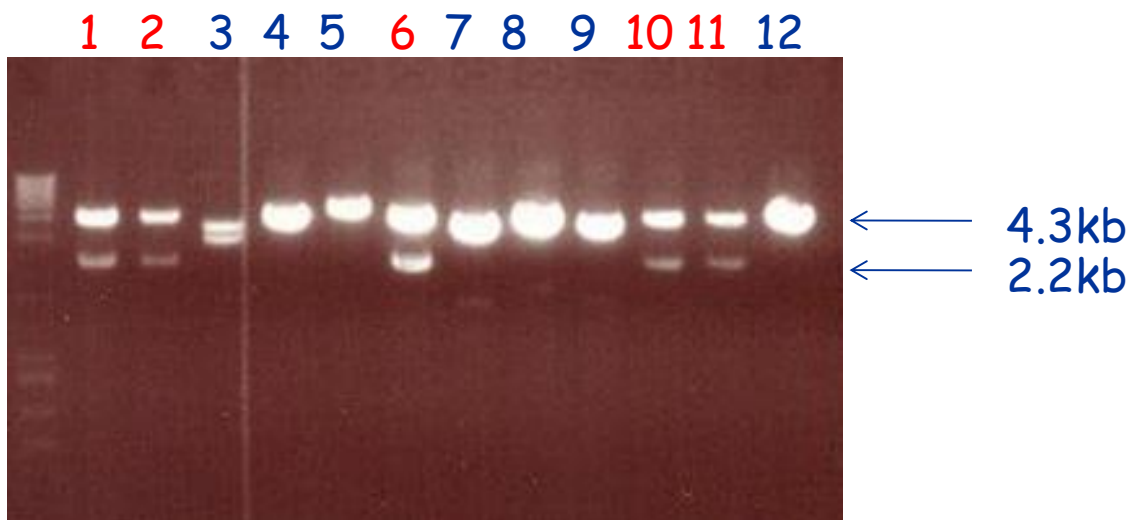


Figure 3.4.3 TMCO1/pIRESHyg clone selection After subcloning, 12 clones were picked up and cultured in LB medium. Plasmid DNA was purified from each clone and digested by XbaI.

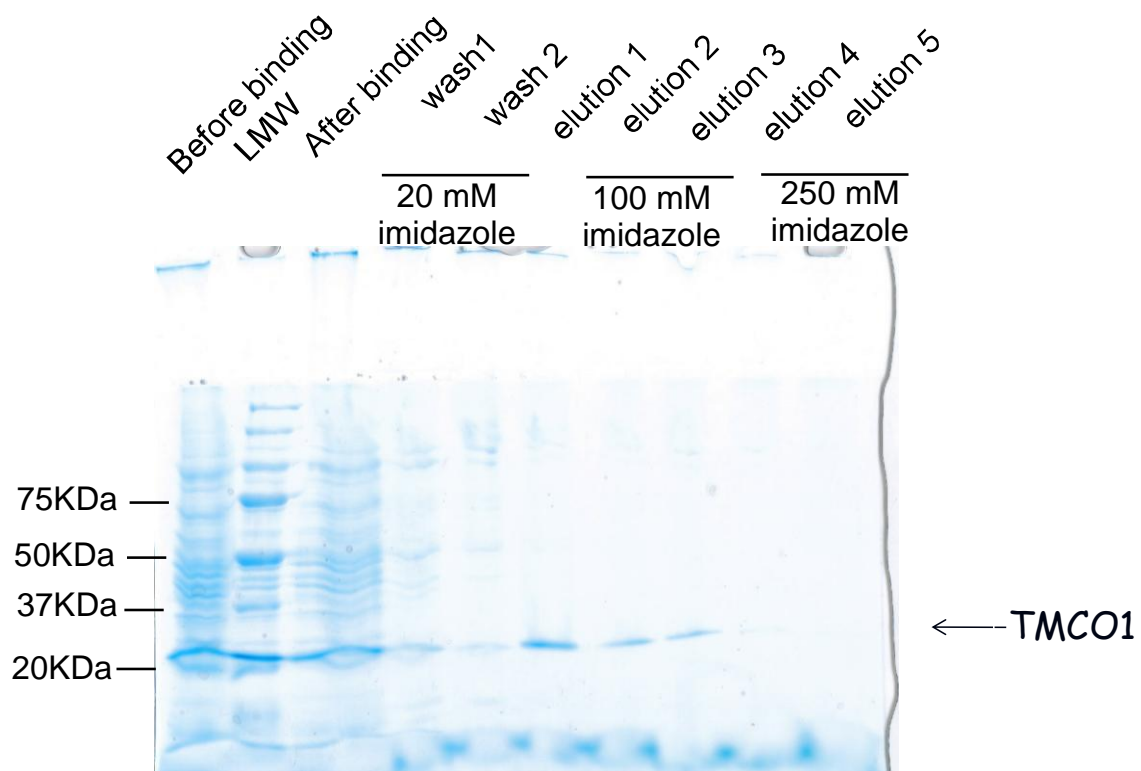


Figure 3.4.4 Purification of TMCO1 protein by nickel affinity chromatography E.coli BL21 cells bearing TMCO1/pET21-d construct were grown in LB medium supplemented with ampicillin (100 $\mu\text{g}/\text{mL}$) to an OD value of 0.5 at 600 nm and the expression of TMCO1 as induced by adding IPTG to a final concentration of 1mM. After being shaken at 30°C for 6 h, bacteria cells were pelleted, lysed, and mixed with nickel charged beads. The impurities were washed away by 20 mM imidazole and most TMCO1 protein was eluted by 100 mM imidazole. The collection from each step was separated by SDS-PAGE and stained by Coomassie brilliant blue.

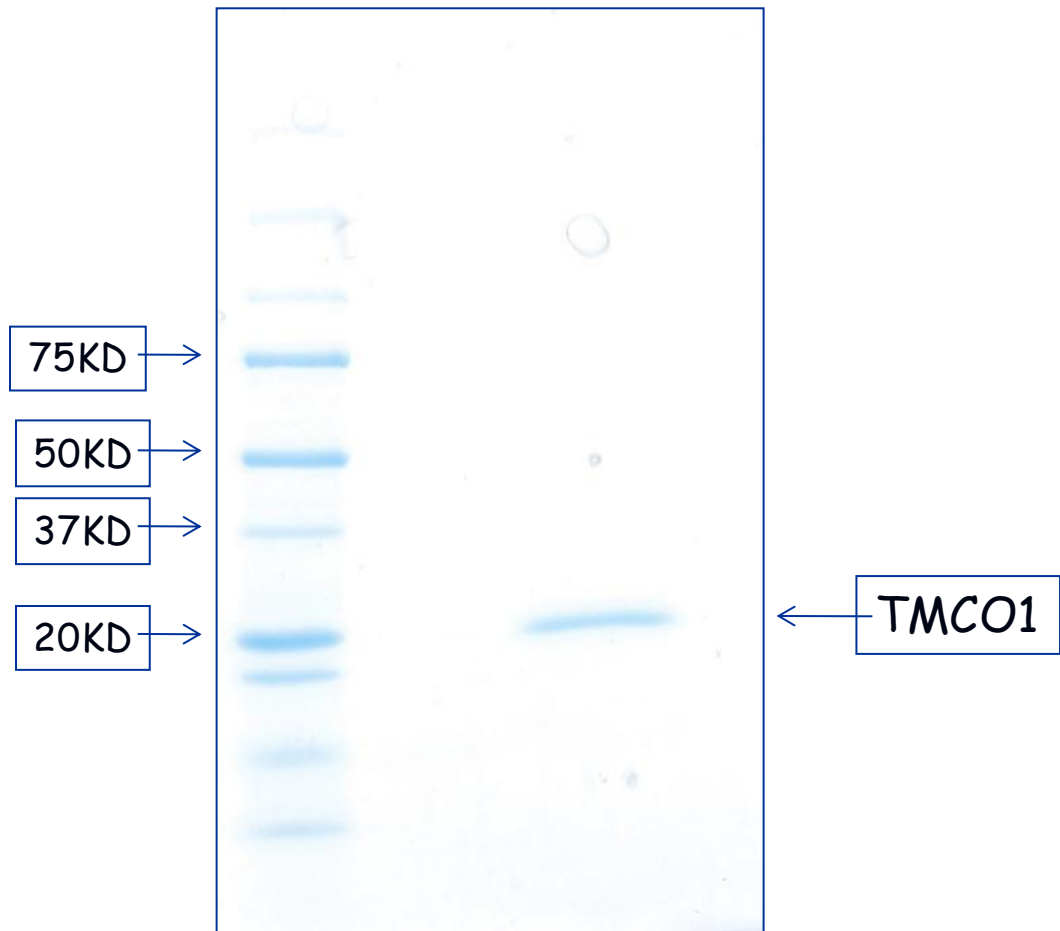


Figure 3.4.5 Purified TMCO1 protein

protein was very good, it was difficult to prepare a sufficient amount of protein to immunize an animal. Thus, we lately made an anti-TMCO1 antibody by using synthesized peptides.

Localization of TMCO1

To determine the subcellular localization of TMCO1, U87 cells were transfected with either TMCO1- pFLAG-CMV-2 or TMCO1- pCMV-HA. After 48 h, the cells were labeled with antibodies against FLAG or HA, respectively, and then stained with Dylight™ 488 conjugated Anti-mouse IgG. As shown in Figure 3.4.6, TMCO1 was localized in mitochondria of U87 cells. However, the result needs to be further confirmed.

TMCO1 mRNA, but not the protein, is expressed in the lymphocytes of patients with TMCO1 defect syndrome

To investigate the expression of TMCO1 at the transcriptional level in the lymphocytes of patients with TDS, the total RNA was extracted from the cells isolated from normal, carrier and affected individuals, and the mRNA expression levels of TMCO1 were examined by RT-PCR (Figure 3.4.7). GAPDH was examined as a control. Apparently, there was no significant difference at the level of TMCO1 mRNA between the normal individuals and patients with TDS. To determine the expression of TMCO1 at its protein level, cell lysate obtained from the cells of normal and carrier individuals as well as patients with TDS, were subjected to a western blot analysis. As expected, there was not a full length of

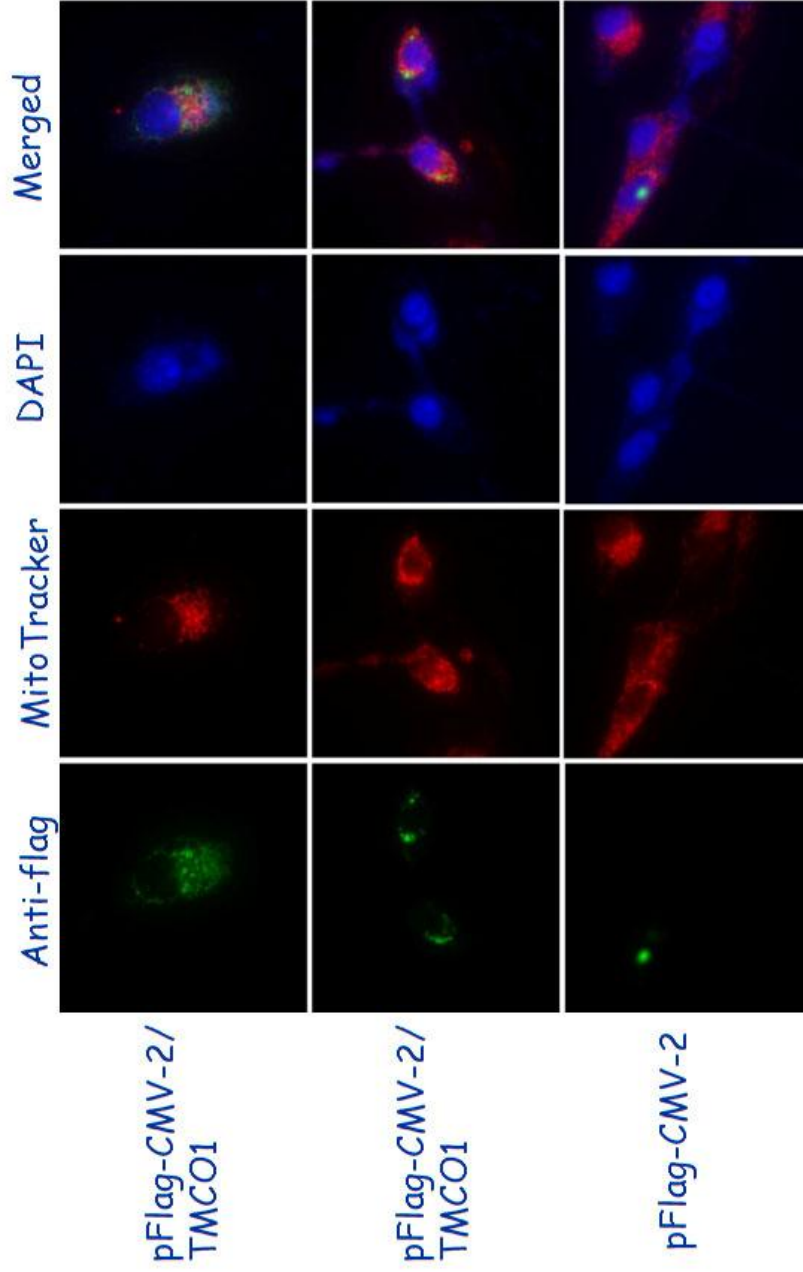


Figure 3.4.6 Subcellular localization of pFlag-CMV-2 conjugated TMCO1 in U87 cells U87 cells were transfected with the pFlag-CMV-2 vector or pFlag-CMV-2/TMCO1 using the lipofectomine 2000 reagent. After 30 h, the cells were incubated with growth medium containing the mitochondrial marker for 15 min at 37°C and immunofluorescence was performed using an anti-Flag primary antibodies and a Dylight™ 488 conjugated second antibody. DNA was counterstained with DAPI. The cells were analyzed using a Delta Vision RT microscope.

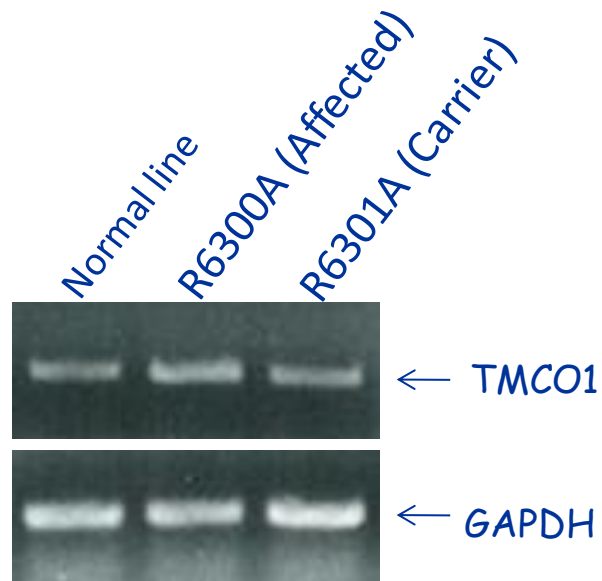


Figure 3.4.7 TMCO1 mRNA expression in human lymphocytes The total RNA of the lymphocytes from normal, carrier, and affected individuals was isolated using the Trizol reagent and the mRNA expression was evaluated by One-step RT-PCR.

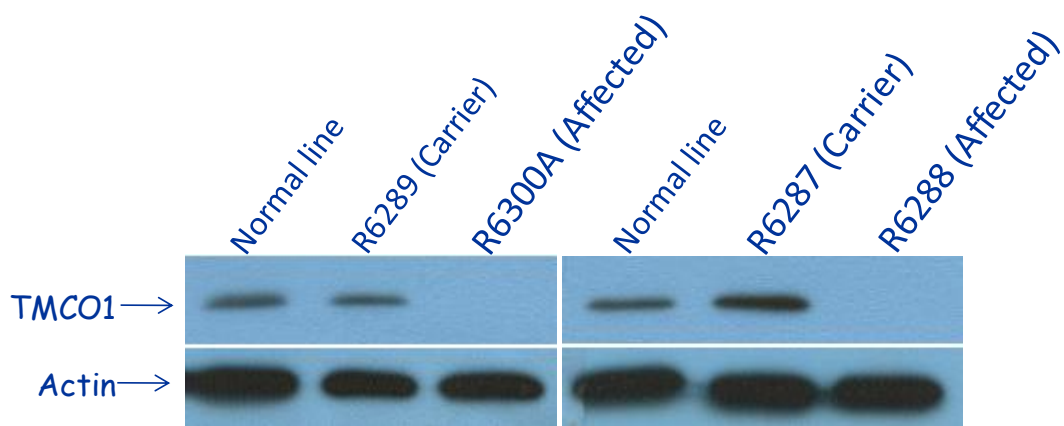


Figure 3.4.8 TMCO1 protein expression in human lymphocytes Cell extracts of lymphocytes from normal, carrier and affected individuals were separated by 12% SDS-PAGE. A western blot assay was conducted using an anti-TMCO1 primary antibody.

TMCO1 protein detected in the cell extract from patients with TDS, which supports the conclusion drawn previously based on the observation of the patients' phenotypes (Figure 3.4.8).

TMCO1 is ubiquitously expressed in all cells examined

In order to examine the differential distributions of TMCO1 in human cells, the relative protein expression levels of TMCO1 were evaluated by a western blot analysis in prostate cancer cell lines (PC3 and LNCap), brain cancer cell line (U87), ovarian cancer cell line (Hey1B), liver cancer cell lines (HEPG2, HEP3B, A549, H292 and H522), neuroblastoma cell line (N1E115), fibrosarcoma cell line (HT1080), and embryonic kidney cell line (Hek 293). Although TMCO1 is ubiquitously expressed in all cells examined, its expression was relatively higher in PC3 cells, LNCap cells, Hey 1B cells, HEOG2 cells, HEP3B cells and H522 cells (Figure 3.4.9).

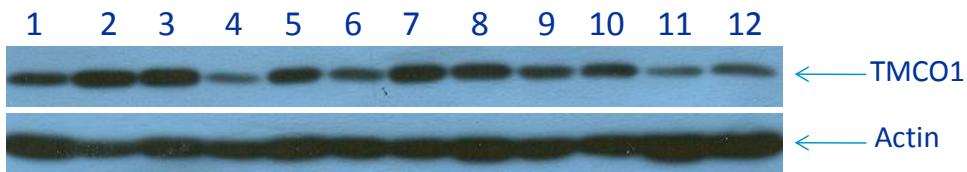
TMCO1 is knocked down by TMCO1 shRNA in U87 cells

To investigate the biological role of TMCO1, we knocked down TMCO1 in U87 cells. The cells were transfected with TMCO1 shRNA pSilence4.1-CMVneo, and selected in medium containing 400 ug/mL of G418. Four groups of constructs, one scrambled shRNA and three different TMCO1 shRNAs, were used to transfect the cells. Twelve clones from each group were examined by western blot analysis using a polyclonal antibody to human TMCO1. As shown in

Figure 3.4.10 and Figure 3.4.11, the expression of TMCO1 was significantly knocked down in the clones: B2, B5, and C7.

TMCO1 may be involved in the regulation of cell proliferation

Since one of the phenotypes in patients with TDS was abnormally growing, we determined the effect of TMCO1 on cell proliferation. Interestingly, we found that the lymphocytes from the affected patients grew much faster than the cells from normal and carried individuals (Figure 3.4.11). The doubling time of the lymphocytes from the patients was 36 h, whereas the cells from the healthy individuals needed 48 h to reach the cell numbers. This observation was confirmed by the medium color in the cell seeded with the same number of lymphocytes. Overtly, lymphocytes from the patients consumed nutrients much faster (Figure 3.4.12). Furthermore, TMCO1 knocked down cells such as B2, B5 and C7 also grew 1.5-fold faster than control cells. These results suggest that TMCO1 may play an important role in cell proliferation.



- | | |
|-------------------------------|------------------------|
| 1. PC3 (prostate cancer) | 7. HEPG2(liver cancer) |
| 2. LNCap (prostate cancer) | 8. HEP3B(liver cancer) |
| 3. U87 (brain cancer) | 9. A549 (lung cancer) |
| 4. Hek293 (embryonic kidney) | 10. H292 (lung cancer) |
| 5. Hey1B (ovarian cancer) | 11. H522(lung cancer) |
| 6. N1E115 (neuroblastoma) | 12. HT1080 (sarcoma) |

Figure 3.4.9 TMCO1 expression in different cell lines Cell extracts were obtained from different cell lines as indicated and the expression of TMCO1 protein was determined by a western blot analysis using anti-TMCO1 antibody.

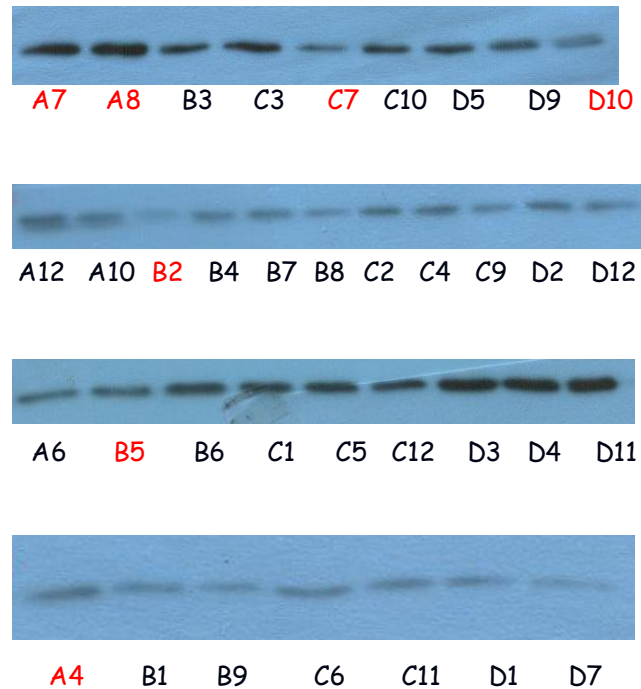


Figure 3.4.10 TMCO1 knockdown clone selection U87 cells were stably transfected with TMCO1 shRNA construct using lipofectomine 2000 and the clones were selected by 400 µg/mL of G418. The expression of TMCO1 in the selected clones was determined by a western blot analysis using an anti-TMCO1 antibody. A, mock (control); B, C and D, TMCO1 shRNA

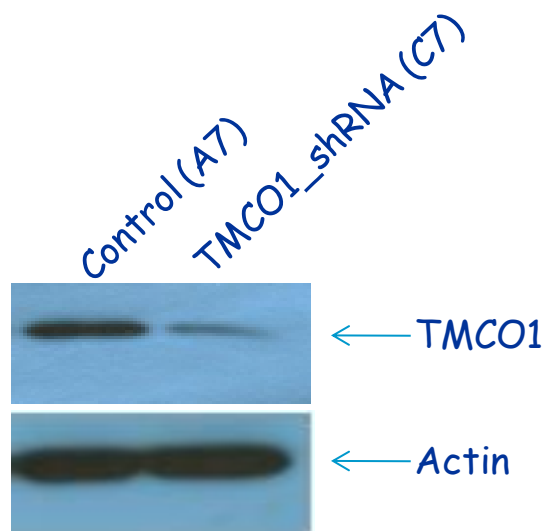


Figure 3.4.11 TMCO1 is knocked down by TMCO1 shRNA

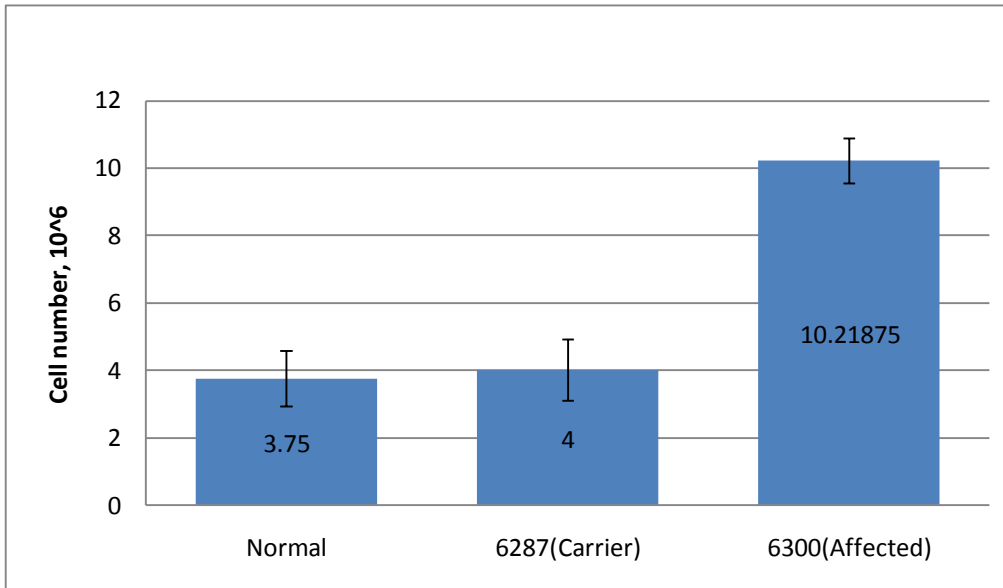


Figure 3.4.12 Effect of TMCO1 on the growth of human lymphocytes

Lymphocytes from normal, carrier, and affected individuals were seeded at 6.27×10^5 cells in each flask and the cells were counted by a trypan blue dye exclusion assays after 6 days.

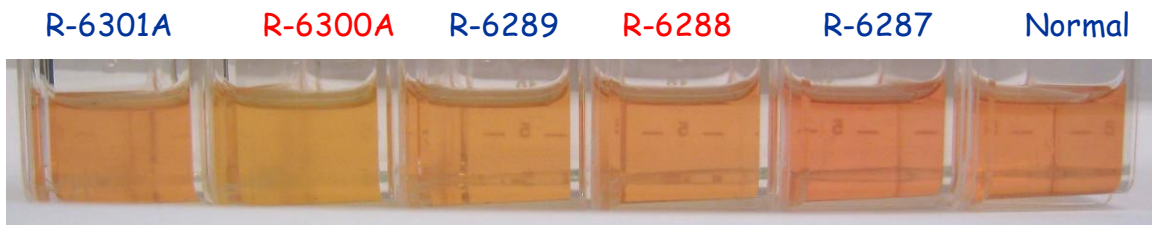


Figure 3.4.13 Medium color changes related to the growth of human lymphocytes Lymphocytes from normal, carrier, and affected individuals were seeded at 6.27×10^5 cells in each flask and the medium color in the flasks was recorded on day 6. Carrier: R-6287, R-6289 and R-6301A; Affected: R-6288 and R-6300A

3.5 Discussion

TMCO1 is a transmembrane protein with one coiled coil domain. The coiled coil is a structural motif in proteins in which 2-7 alpha-helices are coiled together like the strands of a rope. It has been found that approximately 10% of all protein sequences have coiled coil motifs which are extremely stable and responsible for the oligomerization of proteins in a highly specific manner [McFarlane, *et al.*, 2009]. The functions of coiled coil type proteins are diverse and are involved in different important biological processes including cytokinesis (Lee, *et al.*, 2008), gene transcription (Landschulz, *et al.*, 1988) and regulation (Nooren, *et al.*, 1999), membrane fusion (Deng, *et al.*, 2006), molecular motors (Yun, *et al.*, 2003), muscle fibres (Strelkov, *et al.*, 2002), apoptotic cleavage site (Lin, *et al.*, 2007), multidrug resistance (Higgins, *et al.*, 2004), and the potential delivery systems either in the development of novel vaccines (Schroeder, *et al.*, 2009) or for the treatment of cancer (Eriksson, *et al.*, 2009). The universal expression of TMCO1 in all tissues examined [Xin, *et al.*, 2010; Zhang, *et al.*, 2010; Iwamuro, *et al.*, 1999] and the highly evolutionary conservation in large animals implicate a critical role of TMCO1. Our result showed that TMCO1 may be located in the mitochondria of U87 cells, which is consistent with previous findings that TMCO1 is located in the mitochondria of PK-15 cells (pig kidney cells). As an energy plant in the body, one of the main mitochondrial functions is to produce cellular ATP which is essential for eukaryotic cells. There are many nuclear encoded proteins which are imported into the intermembrane space of mitochondria where they adopt a coiled coil fold and can perform either oxidoreductase or

metallochaperon function [Banci, *et al.*, 2009]. These characteristics of TMCO1 may give a hint about its biological function in cells.

TDS is a unique autosomal recessive condition with significant clinical phenotypes including generalized dimorphism disorders with craniofacial, skeletal, and CNS features such as brachycephaly and mental retardation. The molecular mechanism by which TMCO1 defect causes these clinical features is of great interest. One striking characteristic in several TSD patients is tall stature [Xin, *et al.*, 2010]. It is possible that TMCO1 controls the elongation of the bones and dysmorphic proportion [Scotos and Argente, 2008]. Tall stature can be seen in several other syndromes. For instance, estrogen, as a factor to arrest growth, is deficient in aromatas deficiency, estrogen receptor deficiency, and hypogonadism which result in the tall stature. FBN1, TGFBR2, FBN2, and cystathionine β -synthase are essential for inhibiting elongation of the bones and dysmorphic proportion, the defect of these genes leads to Marfan syndrome I, Marfan syndrome II, Beads syndrome, and homocystinuria type 1 respectively [Argente, *et al.*, 2000]. Our results showed that the lymphocytes from patients with TDS grew significantly faster than that from normal individuals, suggesting that TMCO1 may be involved in cell proliferation, cell cycle, cell growth, and tumor suppression. Further investigation needs to be done to elucidate how TMCO1 contributes to the cell proliferation.

3.6 References

- Argente J, Pe´rez-Jurado LA and Sotos JF. Molecular bases of pathological growth. *J Endocr Genet*, 2000,1(4):179–210
- Banci L, Bertini I, Ciofi-Baffoni S and Tokatlidis K. The coiled coil-helix-coiled coil-helix proteins may be redox proteins. *FEBS Lett*, 2009, 583(11):1699-1702
- Deng Y, Liu J, Zheng Q, Yong W and Lu M. Structures and polymorphic interactions of two heptad-repeat regions of the SARS virus S2 protein. *Structure*, 2006, 14: 889–899
- Dokmanovic-Chouinard M, Chung WK, Chevre JC, Watson E, Yonan J, Wiegand B, Bromberg Y, Wakae N, Wright CV, Overton J, Ghosh S, Sathe GM, Ammala CE, Brown KK, Ito R, LeDuc C, Solomon K, Fischer SG, Leibel RL. Positional cloning of "Lisch-Like", a candidate modifier of susceptibility to type 2 diabetes in mice. *PLoS Genet*, 2008, 4(7):e1000137
- Eriksson M, Hassan S, Larsson R, Linder S, Ramqvist T, Lövborg H, Vikinge T, Figgemeier E, Müller J, Stetefeld J, Dalianis T and Özbek S. Utilization of a right-handed coiled-coil protein from archaebacteria *Staphylothermus marinus* as a carrier for cisplatin. *Anticancer Res*, 2009, 29: 11–18
- Higgins MK, Bokma E, Koronakis E, Hughes C and Koronakis V. Structure of the periplasmic component of a bacterial drug efflux pump. *Proc Natl Acad Sci USA*. 2004,101: 9994–9999

- Kondrakhin YV, Sharipov RN, Keld AE, Kolpakov FA. Identification of differentially expressed genes by meta-analysis of microarray data on breast cancer. *In Silico Biol*, 2008, 8(5-6):383-411
- Iwamuro S, Saeki M, Kato S. Multi-ubiquitination of a nascent membrane protein produced in a rabbit reticulocyte lysate. *J Biochem*, 1999, 126(1):48-53
- Landschulz WH, Johnson PF and McKnight SL. The leucine zipper: a hypothetical structure common to a new class of DNA binding proteins. *Science*, 1988, 240: 1759–1764.
- Lee HH, Elia N, Ghirlando R, Lippincott-Schwartz J and Hurley JH. Midbody targeting of the ESCRT machinery by a noncanonical coiled coil in CEP55. *Science*, 2008, 322: 576–580
- Lin HH, Hsu HL and Yeh NH. Apoptotic cleavage of NuMA at the C-terminal end is related to nuclear disruption and death amplification. *J Biomed Sci*, 2007, 14(5):681-694
- Lkhagvadorj S, Qu L, Cai W, Couture OP, Barb CR, Hausman GJ, Nettleton D, Anderson LL, Dekkers JC and Tuggle CK. Microarray gene expression profiles of fasting induced changes in liver and adipose tissues of pigs expressing the melanocortin-4 receptor D298N variant. *Physiol Genomics*, 2009, 38(1):98-111
- Lupas A and Gruber M. The structure of alpha-helical coiled coils. *Adv Protein Chem*. 2005, 70,37-78
- McFarlane AA, Orriss GL and Stetefeld J. The use of coiled-coil proteins in drug delivery systems. *Eur J Pharmacol*, 2009,625(1-3):101-107

- Nooren IMA, Kaptein R, Sauer RT and Boelens R. The tetramerization domain of the Mnt repressor consists of two right-handed coiled coils. *Nat Struct Biol*, 1999, 6: 755–759
- Schroeder U, Graff A, Buchmeier S, Rigler P, Silvan U, Tropel D, Jockusch BM, Aebi U, Burkhard P and Schoenenberger CA. Peptide nanoparticles serve as a powerful platform for the immunogenic display of poorly antigenic actin determinants. *J Mol Biol*, 2009, 386:1368–1381
- Sotos JF and Argente J. Overgrowth disorders associated with tall stature. *Adv Pediatr*, 2008;55:213-254
- Strelkov S, Herrmann H, Geisler N, Wedig T, Zimbelmann R, Aebi U, Burkhard P. Conserved segments 1A and 2B of the intermediate filament dimer: their atomic structures and role in filament assembly. *EMBO J*. 2002, 21: 1255–1266
- Xin B, Puffenberger EG, Turben S, Tan H, Zhou A, Wang H. Homozygous frameshift mutation in *TMCO1* causes a syndrome with craniofacial dysmorphism, skeletal anomalies, and mental retardation. *Proc Natl Acad Sci U S A*, 2010, 107(1):258-263
- Yu MJ, Miller RL, Uawithya P, Rinschen MM, Khositseth S, Braucht DW, Chou CL, Pisitkun T, Nelson RD, Knepper MA. Systems-level analysis of cell-specific *AQP2* gene expression in renal collecting duct. *Proc Natl Acad Sci U S A*, 2009, 106(7):2441-2446

Yun M, Bronner CE, Park CG, Cha SS, Park HW and Endow SA. Rotation of the stalk/neck and one head in a new crystal structure of the kinesin motor protein, Ncd. EMBO J, 2003, 22: 1–8

Zhang Z, Mo D, Cong P, He Z, Ling F, Li A, Niu Y, Zhao X, Zhou C, Chen Y. Molecular cloning, expression patterns and subcellular localization of porcine TMCO1 gene. Mol Biol Rep, 2009, 37(3):1611-1618